ISSN 2095-8137 CN 53-1229/Q

Volume **36** Issue **3**
18 May **2015**

ZR

动物学研究

ZOOLOGICAL RESEARCH

KUNMING INSTITUTE OF ZOOLOGY, CAS

CHINA ZOOLOGICAL SOCIETY

Science Press

CODEN: DOYADI

www.zoores.ac.cn

ZOOLOGICAL RESEARCH

Volume 36, Issue 3   18 May 2015

CONTENTS

Zoological Research Website: http://www.zoores.ac.cn/

A reflection on the significant findings published in *Zoological Research* over the past 35 years

Since its founding in 1980 by a group of first generation biologists after the reform and opening of China, *Zoological Research* (*ZR*) has followed a rather long and difficult 35-year journey. However, through the excellent guidance of our former and current editors-in-chief, the extraordinary members of the editorial board and reviewers, and most importantly, with the strong support of our diligent and enthusiastic authors and readers, we have never deviated from our original goals, despite setbacks and frustrations, such as financial difficulties. Through all the trials and tribulations, we have retained our leading position as a respectable and quality academic journal.

During the past 35 years, *ZR* has steadfastly placed a premium on the academic values and quality of the manuscripts it publishes. The many significant findings reported in *ZR* have not only aroused extensive discussions from both the academic and industrial fields, but also brought profound social effects.

Hosted by the Kunming Institute of Zoology of the Chinese Academy of Sciences and the China Zoological Society, *ZR* has provided an avenue for significant studies on animal biodiversity and taxonomy, including newly discovered species, which is imperative given the unique geography of the Yunnan Province, one of the world's 25 featured biodiversity regions. For example, the discovery and naming (Ma et al, 1990), as well as karyotype detection, of the Gongshan muntjac (*Muntiacus gongshanensis*) (Shi & Ma, 1988), an endangered species inhabiting the Gongshan Mountains in northwestern Yunnan, southeast Tibet and northern Myanmar, were originally published in *ZR*.

Another major area of coverage in *ZR* has been the study of non-human primates. From 1981-2010, many high quality articles were published regarding various aspects of primatology, including taxonomy, distribution, ecology, conservation, behavior and physiology in diversified primate species, such as the rhesus monkey (*Macaca mulatta*), Assam macaque (*Macaca assamensis*), Tibetan macaque (*Macaca thibetana*), Yunnan black-and-white snub-nosed monkey (*Rhinopithecus bieti*), black-crested gibbon (*Hylobates concolor jingdongensis*), hoolock gibbon (*Hoolock hoolock*), western black crested gibbon (*Nomascus concolor*), Francois' leaf monkey (*Trachypithecus francoisi*) and Phayre's leaf monkey (*Trachypithecus phayrei*). Publication of these important studies plays a crucial role in directing and promoting the development of primate research. Today, we continue to publish some of the very best research on primates, including the fields of primate conservation, behavior and brain sciences and their applications in the biomedical field, as featured by our special issues in recent years.

Moreover, *ZR* is also recognized by its featured publications on genetics and evolution and utilization of rich bioresources, i.e., studies on DNA polymorphism, *Bombina maxima* skin secretion proteomes and trefoil factors. The special issues released on November 1981 (Volume 2) and December 1987 (Volume 8) on the biochemical characteristics and physiological effects of snake venom represented pioneering studies of this field in China, and promoted transitions of these academic findings into clinical and industrial applications. Numerous relevant studies were later awarded with provincial and national honors.

Attributed to the outstanding work of our authors and readers, *ZR* has earned its position and shown its influence as a prosperous journal. Citations of *ZR* publications are impressive, and have been increasing since 2002. Up to April 30, 2015, a total of 1 384 articles have been cited 5 051 times, with the average citation per item being 3.65 (statistical data from January 1, 2002, to April 30, 2015, were obtained from Web of Science).

Due to the limited space here, we are unable to list all the many wonderful and deserved papers previously published in ZR. We hope this brief reflection can help our young readers and authors to better know the outstanding contributions of the earlier scientists and the path they paved. The dedication and endless support of our predecessors, by contributing their best research to *ZR*, has helped shape our reputation. We believe that following the strategies of our predecessors, we will have an enduring and substantial impact on *ZR* into the future. By working together, *ZR* will continue to publish the best research.

Sincerely yours,

Yong-Gang YAO, Editor-in-Chief
Kunming Institute of Zoology, *Chinese Academy of Sciences*
Kunming 650223, *China*

Yun ZHANG, Executive Editor-in-Chief
Kunming Institute of Zoology, Chinese Academy of Sciences
Kunming 650223*, China*

Appendix: 20 representative publications of *Zoological Research* from 1980-2015

1	Shi LM, Ma CX. 1988. A new karyotype of muntjac (*Muntiacus sp.*) from Gongshan County in China. *Zoological Research*, **9**(4): 343-347.
2	Ma SL, Wang YX, Shi LM. 1990. A new species of the genus muntiacus from Yunnan, China. *Zoological Research*, **11**(1): 47-53.
3	Jiang XL, Wang YX, Ma SL. 1991. Taxonomic revision and distribution of subspecies of rhesus monkey (*Macaca mulatta*) in China. *Zoological Research*, **12**(3): 241-247.
4	Lin ZH, Ji X. 1998. The effects of thermal and hydric environments on incubating eggs and hatchlings of the grass lizard, *Takydromus septentrionalis*. *Zoological Research*, 19(6): 439-445.
5	Zhang YP, Shi LM, 1992. Mitochondrial DNA polymorphisms in animals: a review. *Zoological Research,* **13**(3): 289-298.
6	Zhang YP, Wang W, Su B, Oliver AR, Fang ZY, Zhang HM. 1995. Microsatellite DNAs and kinship identification of the giant panda. *Zoological Research*, **16**(4): 301-306.
7	Zhang YP. 1996. DNA sequence and species tree. *Zoological Research*, **17**(3): 247-252
8	Yao YG, Zhang YP. 2000. Mitochondrial DNA and human evolution. *Zoological Research*, 21(5): 392-406.
9	Chen SH, Ding P, Fan ZY, Zheng GM. 2002. Selectivity of birds to urban woodlots. *Zoological Research*, **23**(1): 31-38.
10	Zheng ZM, Jiang GF. 2002. One new genus and seven new species of Tetrigoidea from southern region of Guangxi. *Zoological Research*, **23**(5): 409-416.
11	Chen B, Kang L. 2003. Supercooling point shift of pea leafminer pupae with latitude and its implication for the population dispersion. *Zoological Research*, **24**(3): 168-172.
12	Zhou Q, Wang W. 2004. Detecting natural selection at the DNA level. *Zoological Research*, **25**(1): 73-80.
13	Wang YQ, Fang SH. 2005. Taxonomic and molecular phylogenetic studies of amphioxus: a review and prospective evaluation. *Zoological Research*, **26**(6): 666-672.
14	Zhu XC, Liu HJ, Sun XW, Xue LL, Mao LJ. 2006. Assessment of homozygosity in gynogenetic diploid using microsatellite markers in Japanese Flounder (*Paralichthys olivaceus*). *Zoological Research*, **27**(1): 63-67.
15	Zhang Y. 2006. Amphibian skin secretions and bio-adaptive significance-implications from *Bombina maxima* skin secretion proteome. *Zoological Research*, **27**(1): 101-112.
16	Zhang ZW, Cao ZM, Yang H, Wang JL, Cao JL, Han YP, Wu TT. 2006. Microsatellites analysis on genetic variation between wild and cultured populations of *Ctenopharyngodon idella*. *Zoological Research*, **27**(2): 189-196.
17	Wang J, Zhou QX, Tian M, Yang YX, Xu L. 2011. Tree shrew models: a chronic social defeat model of depression and a one-trial captive conditioning model of learning and memory. *Zoological Research*, **32**(1): 24-30.
18	Wang XC, Sun XY, Sun QQ, Zhang DX, Hu J, Yang Q, Hao JS. 2011. Complete mitochondrial genome of the laced fritillary *Argyreus hyperbius* (Lepidoptera: Nymphalidae). *Zoological Research*, **32**(5): 465-475.
19	Xu L, Zhang Y, Liang B, LÜ LB, Chen CS, Chen YB, Zhou JM, Yao YG. 2013. Tree shrews under the spot light: emerging model of human diseases. *Zoological Research*, **34**(2): 59-69.
20	Irwin DM. 2015. Genomic organization and evolution of ruminant lysozyme *c* genes. *Zoological Research*, **36**(1): 1-17

ZOOLOGICAL RESEARCH

New observations - with older ones reviewed - on mass migrations in millipedes based on a recent outbreak on Hachijojima (Izu Islands) of the polydesmid diplopod (*Chamberlinius hualienensis*, Wang 1956): Nothing appears to make much sense

Victor Benno MEYER-ROCHOW[1,2,*]

[1] *Research Institute of Luminous Organisms*, *Hachijo*, 2749 *Nakanogo* (*Hachijojima*), *Tokyo*, 100-1623, *Japan*
[2] *Department of Biology* (*Eläinmuseo*), *University of Oulu*, *SF-90014 Oulu, P.O. Box 3000*, *Finland*

ABSTRACT

Mass aggregations and migrations of millipedes despite numerous attempts to find causes for their occurrences are still an enigma. They have been reported from both southern and northern hemisphere countries, from highlands and lowlands of both tropical and temperate regions and they can involve species belonging to the orders Julida and Spirobolida, Polydesmida and Glomerida. According to the main suggestions put forward in the past, mass occurrences in Diplopoda occur: (1) because of a lack of food and a population increase beyond sustainable levels; (2) for the purpose of reproduction and in order to locate suitable oviposition sites; (3) to find overwintering or aestivation sites; (4) because of habitat disruption and changes in the local environment; (5) as a consequence of weather conditions the year (or winter and spring) before. A recent outbreak (November 2014) of a mass migration of the polydesmid *Chamberlinius hualienensis* Wang 1956 on the Japanese Izu Island of Hachijojima 300 km to the south of Tokyo gave this author an opportunity to review the existing literature on millipede mass migrations and to carry out additional observations on the phenomenon in the field as well as the laboratory. Hitherto unreported heavy infestations with phoretic deutonymphs of the mite *Histiostoma* sp. as well as dense populations of internal rhabditid nematodes (*Oscheius* cf. *necromena* and an unidentified species of the genus *Fictor*), suggest that infestations of this kind could be necromenic and either have been a contributing factor for the mass migration or been a consequence of so many individuals occurring together at close proximity. It is concluded that mass migrations and aggregations in millipedes do not have one common cause, but represent phenomena that often are seasonally recurring events and appear identical in their outcome, but which have evolved as responses to different causes in different millipede taxa and therefore need to be examined on a case-to-case basis.

Keywords: Myriapoda; Spawning migration; Aggregation behaviour; Diplopod commensals and parasites

INTRODUCTION

Mass aggregations of millipedes are not a recent phenomenon (Hopkin & Read, 1992). They have in fact been reported as far back as 1878 (Tömösváry, 1878 cited in Voigtländer, 2005; Paszlavszky 1879) and possibly even earlier (Verhulst, 1845 cited in Zimmermann, 2013). They are known from countries of the southern hemisphere (Australia: Baker, 1978; Anonymous, 2013; Brazil: Boccardo et al, 1997, 2002; Fontanetti et al, 2010; South Africa: Lawrence, 1952; Robinson, 2005; Madagascar: Wesener & Schütte, 2010) and have been reported from numerous countries in the northern hemisphere, e.g., the USA (Brooks, 1919; Cook, 1924; Morse, 1903; Viosca, 1925), the UK (Chater, 2004; Ormerod, 1890; Scott, 1958a, b), France (Sahli, 1996;Verhoeff, 1900), Germany (reviewed by Voigtländer, 2005), Poland (reviewed by Kania & Tracz, 2005), Austria (Anonymous, 2006; Thaler, 1989; Zimmermann, 2013), Hungary (Korsós, 1998; Paszlavszky, 1879), Romania

Received: 20 January 2015; Accepted: 15 March 2015
*Corresponding Author, E-mail: vbmeyrow@gmail.com

(Tömösváry, 1878; Ceuca, 1984, cited in Voigtländer, 2005), Northern Yugoslavia (Ćurić & Makarov, 1995), Latvia (Becker, 1929), Norway (Meidell & Simonsen, 1985), Sweden (Lindgren, 1942) and Japan (Esaki, 1934; Niijima, 1998; Niijima & Shinohara, 1988).

Outbreaks have occurred in tropical climates like those of India (Mitra, 1976) and Brazil (Fontanetti et al, 2010), as well as in temperate and even Nordic climes, e.g. Norway (Meidell & Simonsen, 1985) and Sweden (Lindgren, 1942). Millipede mass aggregations are known from low altitude regions (Ehrnsberger, 2002), but equally so from mountainous or hilly areas, e.g., Japan (Hagiwara & Kuwabara, 2008; Niijima & Shinohara, 1988), Switzerland (Anonymous, 2011) and Austria (see first paragraph). Although in most of the above-mentioned cases certain species, e.g., *Ommatoiulus sabulosus* in Europe and the *Parafontaria laminata* group in Japan were over-represented, numerous other species were sometimes found to be involved and a list of millipedes in relation to their geographic distribution demonstrates the spread of taxa in connection with the phenomenon of mass migrations.

Juliformia and spirobolid species are the most important and common ones in connection with millipede mass aggregations. Voigtländer (2005) lists *Ommatoiulus sabulosus* (L), *Cylindroiulus caeruleocinctus* (Wood), *Julus scandinavius* (Latzel), *J. scanicus* (Lohmander) and *Ophyiulus pilosus* (Newport) as species known from mass occurrences in Germany and in addition *Megaphyllum projectum kochi* (Verhoeff), *M. unilineatum* (C.L. Koch), *J. terrestris* (Porat), *Tachypodoiulus niger* (Leach), *Unciger foetidus* (C.L. Koch) and *Cylindroiulus londinensis* (Leach) as species elsewhere in Europe linked to mass aggregations.

The spirobolid *Strongylosoma stigmatosum* (Eichwald) has been reported by Ceuca (1984) from Romania, while *Parajulus pennsylvanicus* was reported from New England by Morse (1903). *Streptogonopus phipsoni* (Pockcok) and *Gymnostreptus pyrrhocephalus* (C.L. Koch) are mentioned by Bellairs et al (1967) and Lawrence (1952) in connection with mass aggregations in India and South Africa, respectively. The Iberian species *Ommatoiulus moreleti* (Lucas) has been known to swarm in South and West Australia (Anonymous, 2013; McKillup et al, 1988), while *Urostreptus atrobrunneus* (Pierozzi & Fontanetti) is known from Brazilian aggregations (Fontanetti et al, 2010), *Spirostreptus* sp. from outbreaks in New Mexico (Cook, 1924; Thuringer, 1924) and *Spirobolus marginatus* (Say) from a mass occurrence in the New Orleans area near Lake Ponchartrain (Viosca, 1925).

Certain species belonging to the polydesmid group of millipedes are also known to swarm and to form mass aggregations, e.g., according to Esaki (1934) *Brachydesmus superus* (Latzel) in England, *Fontaria virginiensis* (Gray) and *F. brunnea* (Bollman) in the USA. Robinson (2005) furthermore mentions *Pseudopolydesmus serratus* (Say) from Ohio and Bellairs et al (1967) report swarming in *Streptogonopus phipsoni* (Pocock), while in Central Japan according to Niijima and Shinohara (1988) various subspecies of the *Parafontaria laminata* group have repeatedly been involved. The Taiwanese polydesmid *Chamberlinius hualienensis* (Wang, 1956) is not known to swarm in Taiwan, but in some places of Japan, notably the island of Hachijojima (Fujiyama et al, 2012 and this paper) this invasive species does and it then forms huge clusters of several thousands of individuals.

Glomerids are the last group of the Diplopoda known to possess species with a propensity to migrate and to form mass aggregations. From Poland mass occurrences of *Glomeris hexasticha* (Brandt) and from Madagascar those of *Zoosphaerium neptunus* (Butler) have been reported by Kania & Tracz (2005) and Wesener & Schütte (2010), respectively. One Australian bristle millipede, the polyxenid *Unixenus mjoebergi* (Verhoeff) is credited by Robinson (2005), who, however, uses the incorrect name *U. nijobergi*, to migrate after rainfall according to Koch (1985).

Numerous attempts have been made to find an explanation, i.e., causes and reasons, for the various mass migrations and aggregations amongst millipedes. And the most common suggestions, here briefly summarized on the basis of the works of Brade-Birks (1922), Cloudsley-Thompson (1949) and the publications mentioned above, are (a) population increases that lead to a lack of and consequently search for food; (b) migrations linked to reproduction and attempts to find oviposition sites; (c) the search of animals to locate suitable places to spend the winter or to aestivate during the summer; (d) a need to find wetter or drier habitats, in other words responses to adverse environmental conditions; (e) past weather conditions like mild previous winters in combination with warm springs. Attempts to correlate mass migrations with habitat changes, communal protection against predation, soil conditions and dominating plant communities have also been made.

However, as will be shown point by point in the Discussion, there is not a single suggestion, which is applicable to all of the observed mass migrations and aggregations amongst millipedes. In some instances the phenomenon occurs in predictable cycles and at identical seasons year after year, but in others there is no apparent repetitiveness at all and the phenomenon may occur in areas it has never been seen before and is never seen thereafter again. Given this state of affairs, the recent mass migration of the polydesmid *Chamberlinius hualienensis* on the island of Hachijojima provided an opportunity to test some of the suggestions that had earlier been offered as likely explanations for millipede mass occurrences.

The polydesmid *Chamberlinius hualinenensis* is a herbivorous species native to Taiwan (Wang, 1956). In Japan it was first noticed in the autumn of 1983 on the island of Okinawa. From there it reached the major Japanese island of Kyushu in 1999 and soon thereafter Honshu, causing minor outbreaks of mass swarming in the years 2009 and 2012 (Fujiyama et al, 2012). The exact date that the species arrived on the small Izu Island of Hachijojima, 300 km to the south of Tokyo, is not known, but the year 2002 is often mentioned by the locals as the first time they noticed this millipede.

As an invasive and alien species on the subtropical island of

Hachijojima with its lack of predators, populations of the species increased rapidly and the locals noticed year after year greater and greater numbers of this millipede and increasingly more substantial mass migrations principally between the months of October to early December. In the autumn of 2014 the largest mass occurrence of *Chamberlinius hualienensis* to date was seen on the island. It is that event which formed the basis for the investigations reported in this paper.

MATERIAL AND METHODS

On two sites, located at approx. N33°05' and E139°47' on the West Coast of the southern half of the Izu island Hachijojima 300 km to the South of Tokyo in the Pacific (Figure 1), mass aggregations of the introduced herbivorous Taiwanese polydesmid millipede *Chamberlinius hualienensis* Wang 1956 were observed and studied between 15-11-2014 and 24-12-2014.

Facing west to southwest, Site I consisted of a curved approx. 4 m high vertical wall made of concrete with rough surface texture and some parts painted dark brownred and others left cream-colored. The wall marked the entrance to a covered freeway viaduct. Parts of the viaduct support structure facing north and east and painted entirely brownred were also monitored, but not designated as separate sites on account of their close proximities to one another.

Site II, ca. 800 m to the south of Site I and facing north, consisted of an approx. 8 m high vertical cream-coloured concrete, 5.5 m×4.5 m wide support pylon with rough surface texture, on which the motorway rested. The two sites were accessible on foot via an old disused and overgrown narrow road that ran in a north-south direction more or less parallel to the freeway which was opened to traffic in the year 2000. Alongside the small road, there was a steep drop towards the oceanside to the West and a steep rise towards the island's interior mountains on the East. The slopes on either side of the road were thickly covered by green vegetation that consisted of a rich variety of mixed shrubs, bamboo, native and introduced trees, vines and weeds. Decaying leaf and other plant matter was plentiful and present all over the ground, the latter being basically volcanic in origin.

Daily climatic conditions for the period of observation with information on precipitation, temperatures and humidity were available from the website of the Japanese Meteorological Agency (2014, http: //www.data.jma.go.jp). To check the genders of the individuals in the aggregations or in the migrating swarms, specimens were collected in the field during the day (ca. 1400h) and at night (ca. 2000h) and examined under a binocular microscope at ×20 magnification in the lab. Mites and nematodes, collected from male as well as female specimens, were preserved in 70% ethanol and sent to labs outside Hachijojima (see acknowledgments) for further processing. Observations on biorhythmicity and photoreception were carried out in temperature and humidity controlled climate chambers of the institute set at 20 °C and 75% relative humidity.

RESULTS

Weather conditions immediately prior to and during the outbreak

The weather pattern for the month of November prior to when the mass occurrence of *Chamberlinius hualienensis* was first noticed on November 15th did not exhibit any unusual or extreme feature except for a very heavy downpour on the 5th with 104 mm recorded for that day alone. However, heavy showers are not rare on Hachijojima, which has an annual precipitation in access of 3 000 mm. On the 11th of November rainfall also exceeded 35 mm, but did not reach the level of November 5th. Nighttime temperature on the two days before the November 5th downpour had dropped from the more usual 18 °C to 15.8 °C on November 3rd and 13.8 °C on November 4th. Thereafter nighttime temperatures averaged again 17.8 °C until November 13th, when they dropped to 13.4 °C and remained around 12-13 °C for the next 10 days after which they climbed again to an average of 15 °C until December 1st. Then, however, day and nighttime temperatures fell rapidly reaching a minimum of 6.2 °C and 4.1 °C on December 18th. Towards December 24th, however, the day all observations ended, temperatures rose again by 3-5 °C. Heavy rainfall in December occurred only on days 1, 4 and 11.

Average relative humidity throughout the 2-week period prior to the start of the recognition of the outbreak on November 15th was always at least 70% and following rainy days even higher than 90%. A sudden drop to 58% occurred during the sunny spell from November 13th to November 16th. The remainder of November exhibited no unusual features with an average relative humidity of 80%, plenty of scattered rain, some sunny periods and gradually lower day and nighttime temperatures, which by early December reached 12 °C and 7 °C, respectively. The weather remained like this until virtually all millipedes, except for a handful of five or six isolated, but still living, stragglers had disappeared from the walls by December 24th.

Prior to November 13th between November 4th - 6th and 11th - 13th there had been very strong winds from the north, east and south with gusts in excess of 10 m/sec. The two weeks thereafter winds eased and, averaging 4 m/sec over this period, first changed to blow from the west for a week and thereafter mostly from the southeast and occasionally from the northern but not western directions. Westerly winds occurred again on December 1st and continued to be dominant for the entire month of December.

Migratory activities and densities of *Chamberlinius hualienensis* individuals

Irrespective as to whether they were exposed to bright sunshine (Site I) or were in the shade almost all day (Site II), dense clusters of individuals were present on all of the walls monitored (Figure 2-4). It made apparently not much of a difference whether the walls were facing the west, southwest, east or north and whether they were lighter or darker in colour. At the height of the mass occurrence between November 15th–18th it was estimated that at Site I, there would be up to approx. 15 000 individuals/m^2 (on the basis of counts of 400-600

individuals/20 cm^2) on the cream-coloured wall facing west as well as the brownred wall facing east. The area occupied by clusters of millipedes on these walls reached from the ground to more than 3 m above and horizontally to between 3 and 4 m.

A rough estimate of the total number of millipedes gathered together just on the walls alone was 100 000. An equal or even larger number is thought to have perished, forming a layer on the ground several cm thick (Figure 5) and emitting a smell described by some pedestrians as that of burning plastic. Adding the number of individuals of Site II (see next paragraph) and considering the new daily arrivals at both sites, the total number of millipedes that had come together at both sites could easily have been a million or more.

Site II, covered by the bridge overhead and mostly shadowed, also possessed an appreciable number of individuals, but distributed over a larger area they did not quite reach the densities seen at Site I. During the week in which winds from the west were absent (November 17th-25th) densities on the wall of Site I facing north increased significantly at the expense of the areas facing east, west and southwest. At the same time clusters at Site II thinned, but had re-grouped about 6 m above the ground. The snails present on these walls prior to the arrival of the millipedes stayed and apparently neither disturbed the millipedes nor suffered any harm from them.

It was obvious that the millipedes were able to ascend the vertical walls at any place, but that they preferentially used cracks or lines were slabs of concrete had been joined together. Small depressions, holes and crevices in the concrete seemed particularly attractive to them. Although many individuals in these clusters of animals that were moving around and climbed over others that were resting, were frequently paired (Figure 6) or even occurring as triplets with three individuals on top of each other (Figure 7), the majority were seemingly intent on being passive. At night, however, the situation was different. Approximately 15 minutes after sunset almost all of the animals, whether paired or not, became active. The huge aggregations broke up with smaller ones remaining, but the majority of the animals crawling around on the vertical wall did so apparently in no particular direction. At dawn the familiar aggregations of thousands of individuals were present again.

What was noticeable almost exclusively at night, were individuals that crawled from the surrounding bush along the old disused and overgrown road towards the aggregation Sites I and II. As if pulled by a magnet those as far away as approx. 400 m to the south of Site I approached that latter site and migrated upward in a northerly direction, but those further away and within 400 m of Site II migrated southward and down the sloping road toward their specific aggregation site. At night the road was teeming with crawling millipedes, seemingly single-mindedly heading into one direction only (either north or south) and following a route leading them to their respective aggregation sites.

Mechanically removed from their path by a metre or so, the displaced millipede returned to where their conspecifics were crawling. Using only one side of the road they did not swerve or take a detour when they encountered an obstacle in the form of a shallow puddle left over from a recent shower, but proceeded to crawl across it, even if in the process some drowned. In times of heavy rain, however, no migrations at all occurred. Illumination at night did not stop them, but some individuals did sometimes hesitate before continuing to crawl and some even tried to go around an approx 15 cm wide patch illuminated by the bright white light of a handheld torch.

The path to Site II was particularly intriguing, because in order to reach that site the millipedes first had to crawl downward for about 100 m from the somewhat brighter area into the darkness of the underside of the freeway viaduct and then upward again for the remaining 50 m in order to reach the concrete support pylon which they ascended to form clusters, even at a height of 6 m. Following the road to the pylon, the millipedes first had to head south, then for a few metres turn west and then approach their goal in a southwesterly to southern direction.

Speeds of around 1.6 cm/sec were recorded, which suggests that these millipedes can travel approx. 1 km per night. In case they hadn't reached their destination by dawn, they sought shelter under stones along the roadside. When there were cockroaches under the stones, the millipedes frequently caused the latter to abandon their shelter or to aggregate in corners the millipedes could not or did not want to reach.

An unexpected "two-way-traffic", resembling that which is often seen in ants, with slightly more millipedes heading downward and away from the aggregation Site I than towards it and thereby passing the new arrivals, was observed after a small rise in nighttime temperatures from an earlier 12 °C to around 15 °C on the nights of November 23rd – 26th (Figure 8). On which day these "return migrations" ceased was not recorded, but on November 27th only a small number of animals were still arriving, and both Sites I and II were far less populated with few individuals still clinging to the wall and its crevices. None were seen any longer heading in the opposite direction despite a relatively warm nighttime temperature of 14 °C. Given the huge number of animals that over at least 2 weeks had formed the massive aggregations described above, the total number of individuals that had headed back can only have been a trickle. The vast majority of the millipedes that had come together at Sites I and II perished there. And yet, that over several nights some animals returned at all is remarkable and so far has not been reported from any other millipede species.

From November 29th and during the first week of December with prevailing westerly winds of approx 7 m/sec streams of millipedes, mostly from the northern wall of Site I, where there was still a very substantial cluster, were heading to the opposite side of the freeway. They got there by first crawling up to the ceiling of the covered viaduct and then, upside down, crossing the freeway along 4 m above the traffic with some falling down onto the road, but most reaching the other side. On the other side of the freeway they again formed aggregations, but preferentially on the northern side of a pylon (Figure 9).

In early December furthermore smaller clusters of around 600-1 000 individuals became established approximately 500 m to the North of Site I along the banister on the opposite side of the freeway above concrete support pylons 14 m off the ground. On December 6th walls of Site I facing west, southwest and east

were nearly deserted with just a few isolated clusters of around 50 or so individuals hanging on, but a considerable number still present on the northern side and its flat horizontal top. Wall areas vacated by the millipedes once again became a habitat for geckos that hadn't been seen there during the times of millipede mass aggregation, but were present there on December 11th and 18th.

Since hardly any millipedes were seen to migrate from Site I to the new clusters that had formed along the freeway's banister ca. 400 m away and since the new clusters developed only on the banister above support pylons and inside holes and depressions nearby (Figures 10,11), the most likely way the millipedes could have got there was by ascending the 14 m high concrete support pylons on which the freeway rested at that point. A height like this climbed by millipedes would represent a new record.

Sizes and gender distributions

A total of 1, 645 adult *C. hualienensis* were sexed on 6 separate days in November. When samples taken during the day from Site I aggregations above 1 m were compared with those taken below 1 m the ratios between females and males were 240:205 and 148:137 on November 16th. For Site II the corresponding figures obtained on November 20th were 158:135 and 171:107. Under wet and drizzly conditions on November 22nd the female/male ratio at night of animals approaching Site II was 20: 4 with many individuals (not sexed) lying immobile and presumed dead in puddles.

The ratio between females and males migrating at night on November 26th to Sites I and II were 59:46 and 63:58, respectively. On the same day in bright sunshine at a temperature of 23 °C and moderately strong southerly wind (4.3 m/sec) some millipedes were seen to migrate towards the northern wall of Site I. The female/male ratio in these individuals was 17 : 18.

On November 23rd when millipedes at night were moving away from their aggregation sites passing others that were still arriving, female/male ratios of the departing and arriving animals at Site I were 14:10 and 9:4, respectively. At Site II only individuals still arriving and none leaving were seen and their female/male ratio was 11:11.

Total length measurements were carried out on 20 adult males and females pooled from both sites and killed by freezing. Length measurements on individuals preserved in this way are likely to deviate slightly from measurements of live and crawling individuals, which is why statistical analyses with standard deviations were considered meaningless in connection with the data. Unrolling the thawed and curled up corpses yielded average lengths of males and females of 35.6 mm (range 34-41 mm) and 36 mm (range 35-41 mm). Males were found to be slimmer, often softer and more frequently less opaque due to an empty digestive tube than the females.

Biorhythmicity and responses to light

There were always some individual *C. hualienensis* that were not at rest, but moving around on the aggregations that had formed on the walls of Sites I and II, even if exposed to bright midday sunshine. However, individuals migrating to or away from the aggregation sites were almost exclusively seen at night. Individuals hiding motionlessly under a stone or log during the day immediately became active as their shelters were taken away, while those that were on the move at night would sometimes stop or even deviate from the direction they were heading into when struck by the beam of some bright white torchlight.

When 40 individuals collected during the day at 1430h were divided into two groups of 20 and at 1500h individuals of one were put into a rectangular transparent plastic terrarium measuring 13 cm×15 cm×20 cm that contained shelters for the millipedes, while those of the other group were put into an identical terrarium at the same time, but in a darkroom with temperature and humidity as in the first group, individuals of the first group immediately found and rested in the hiding places, not appearing again until 15 minutes after sunset. They were then dispersing and freely crawling around the terrarium until dawn.

The animals that were placed into the darkroom, however, were active and moving around when briefly checked at 1600h and 1700h. The next morning at 0900h some 5 or 6 were still out in the open and crawling around, while the remainder were resting. Over the next three days the darkroom group settled to a biorhythm that saw them resting for most of the day, but starting their activity earlier than group one, which waited until sunset and it was getting dark. When they were then illuminated during the night they speedily sought shelters and waited in them motionlessly until the light was switched off again. Ten minutes later they were then crawling around again in the open as before.

Observations on interactions with other species of animals

When live *C. hualienensis* male as well as female individuals were placed in mild soapy water, hundreds of tiny nematodes, no longer than maximally 0.75 mm long and 0.01 mm thick appeared. Almost certainly residing inside (and not on) the millipedes, the nematodes were identified as members of the Rhabditida group. Light (Figure 12) and scanning electron micrographs (Figure 13) were taken of individuals that were sent in 70% ethanol to Prof. T. Hariyama's lab of Hamamatsu Medical University and then further processed by Dr. Takaku according to a method recently described (Takaku et al, 2013). Specimens were also sent to Dr. Lynn Carta of the USDA-ARS Nematology Laboratory in the U.S., who confirmed that the nematodes were rhabditids and on the basis of ribosomal DNA markers could be identified as two species, namely *Oscheius* cf. *necromena* and a member of the genus *Fictor*. Their presence suggests that infestations of this kind could be necromenic and either have been an additional cause for the mass migration or been a consequence of so many individuals occurring together at close proximity. When and how they could have colonized individuals of *C. hualienensis* and to what extent they affected their host's behaviour is not known, but members of the Rhabditida are known from other arthropods and also occur in decaying matter, where they feed on bacteria and other microorganisms.

Figure 1 Area of mass outbreak (Seen from the west with freeway viaduct in the centre and mountains on the far side (to the east) of the road; the tunnel entrance is to the left**)**

Figure 2 Masses of the polydesmid millipede *C. hualienensis* on their way to aggregation Site 1

Figure 3 Clusters of *C. hualienensis* indiviuduals on the north-facing side of a wall, apparently making use of cracks and slight depressions between the blocks of concrete

Figure 4 Up to approximately 15 000 individuals/m^2 were assembled at the aggregation sites

Figure 5 Thousands more on the ground are forming many centimetre-thick layers of exhausted and dying individuals

Figure 6 Paired individuals were a common sight during the aggregation phase

Figure 7 Sometimes triplet individuals were seen amongst the clustered animals

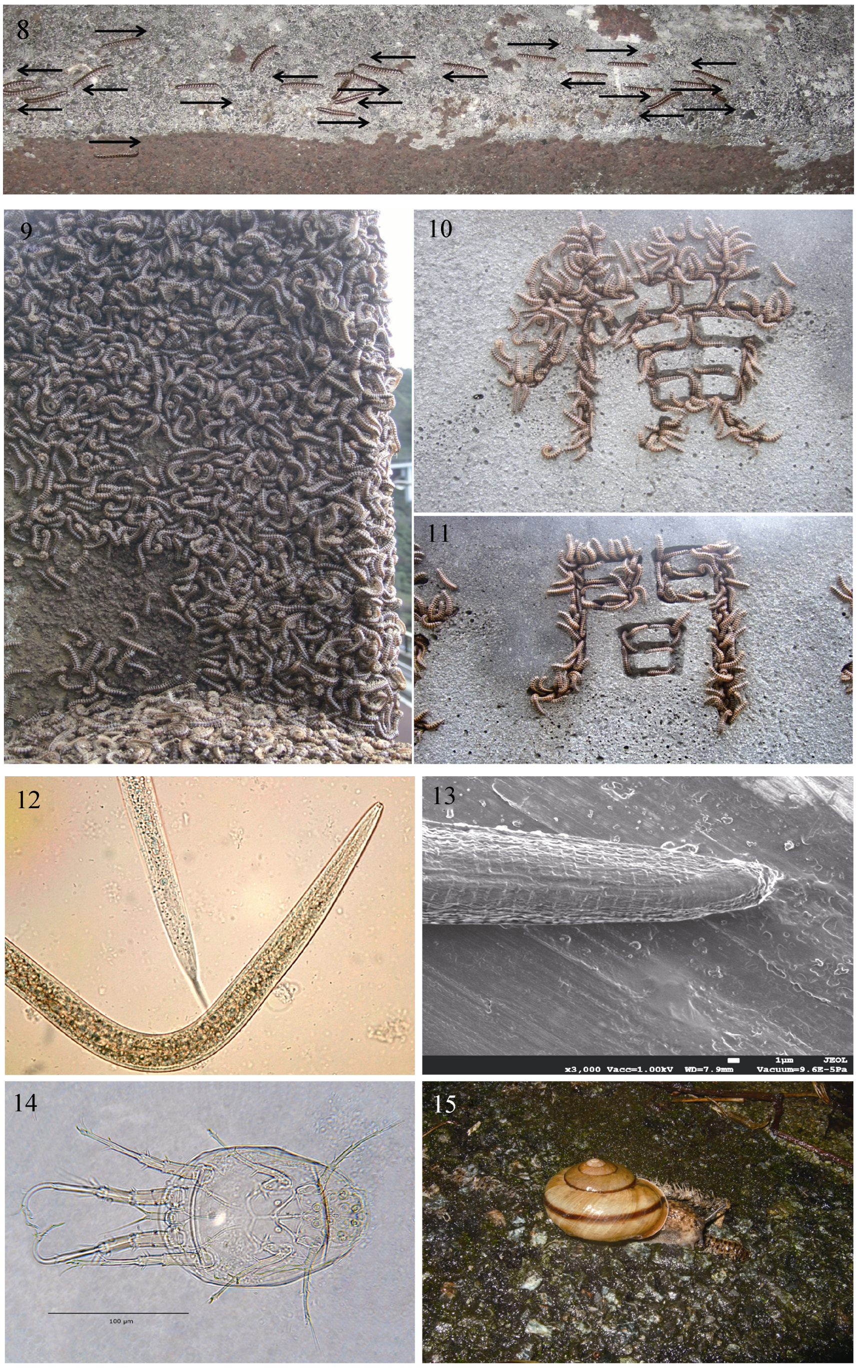

Figure 8 Two-way traffic with individuals from the right (arriving) and left (departing) passing each other

Figure 9 With winds predominantly from the west, dense aggregations began to form on the northern side and on top of the wall

Figure 10 Cracks and depressions gave the millipedes some protection against the wind and rain (here the word 'yoko' in the wall facing east)

Figure 11 Any hole or depression in the concrete serves the millipedes to hang on (here the word 'ma')

Figure 12 Light micrograph of rhabditid nematode from *C. hualienensis* (taken by Y. Takaku)

Figure 13 Scanning electron micrograph of rhabditid nematode from *C. hualienensis* (taken by Y.Takaku)

Figure 14 Light micrograph of deutonymph of *Histiostoma* sp. from the body of migratory *C. hualienensis* (prepared by H. Schikora)

Figure 15 During mild rain unidentified terrestrial snails were feeding on corpses of *C. hualienensis*.

On the outer surfaces of *C. hualienensis* numerous individuals of loosely attached tiny mites, no bigger than 0.3.mm, were present (Figure 14). They were identified by Dr. M. Farfan of the University of Illinois at Chicago as deutonymphs most likely belonging to the genus *Histiostoma* and almost certainly phoretic rather than parasitic. As with the nematodes when and how the mites 'boarded' the millipedes and what effect, if any, they had on their host is still unknown.

Macroscopically no animals other than some inactive, presumably hibernating snails were observed amongst the mass aggregations. Once a bright green approximately 5 mm long caterpillar was seen crawling on a cluster of *C. hualienensis*, but an attempt to capture it failed as it dropped and disappeared amongst multiple layers of dead millipedes on the ground. Nearby on the wall, but obviously not at all interested in the millipedes were occasionally some geckos (*Gekko hokouensis* Pope) and praying mantises. Under stones in close proximity with the millipedes were cockroaches (*Opisthoplatia orientalis* Burmeister) of both genders and at various stages in their life cycle. It was obvious, however, that cockroaches and sheltering millipedes avoided each other.
No animal was ever seen to feed on this readily available prey, but millipedes drowned in the rain were approached by large terrestrial snails and partially consumed by them (Figure 15).

DISCUSSION

The polydesmid *Chamberlinius hualienensis* is not the only species of millipede in Japan involved in swarming and forming mass aggregations. Various subspecies of the polydesmid *Parafontaria laminata* in the mountainous regions of Honshu at altitudes of around 1 000 m have had numerous outbreaks, listed by year, place and dominant local flora by Niijima & Shinohara (1988). Apart from the nuisance that so many animals create by invading dwellings and because of their unpleasant odour, they can also disrupt road and rail traffic as was first reported for Japan by Esaki (1934) after Verhoeff (1900) had already described a similar occurrence for France, albeit not of a migrating polydesmid but a iulid species of millipede. Members of the Julidae, so prominent in European outbreaks, do not feature in Japanese millipede mass aggregations, but apart from the polydesmid taxa mentioned above one other polydesmid family, namely the Strongylosomatidae may contain species in Japan that sometimes swarm (Esaki, 1934).

Possible reasons for swarming and mass aggregations

Comparison between *Parafontaria laminata* and *Chamberlinius hualienensis*

Clues as to why and when the two main migratory species groups in Japan swarm could possibly be gleaned from a comparison of the biologies of *P. laminata* and *C. hualienensis*, in the local vernacular known as 'kishayasude and 'yangbarutosakayasude', respectively. According to Fujiyama et al (2012) the temperate and sub-Arctic *P. laminata* has an 8-year cycle with single age groups per year and moults occurring once every 12 months. The tropical *C. hualienensis*, however, develops much faster and its immature individuals moult monthly. While *P. laminata* with an optimal temperature range of 10-20 ºC and able to survive subzero temperatures has a narrow food spectrum and occurs predominantly in the forests of hilly or mountainous areas, *C. hualienensis* dies below 0 °C, is most active between 20-30 °C, has a wide food spectrum and inhabits a range of habitats including forests and cultivated fields of both hilly and lowland areas.

What the two taxa have in common in addition to their rather similar size and appearance are their dietary requirements of decaying plant matter and the number of eggs per cluster. However, while in their lifetime *P. laminata* females lay their 300-600 eggs within one month, which then enter a period of dormancy, *C. hualienensis* females mate numerous times over a period of four months and lay their eggs not all at once. Moreover, neither their eggs nor any of their larval stages enter a dormancy period. Higa et al (1992) have counted 70 clusters of 300-600 eggs laid by 100 *C. hualienensis* pairs over a period of 4 months, but how many eggs one female lays over its lifetime is not known. In *P. laminata* adults and a small number of sub-adults make up the migratory swarms, which occur mostly in September and October and occasionally even earlier (Niijima & Shinohara 1988), but in *C. hualienensis* the swarming period lasts mostly from early October to early December and overwhelmingly consists of adult individuals (Fujiyama et al, 2012).

Population pressure and lack of food

The question as to what triggers the migrations, not only of polydesmids in Japan, but millipedes in general, has led to a number of suggestions that will be examined one by one. Lack of food and a population increase beyond sustainable levels have frequently been mentioned and given the often staggeringly large numbers of millipedes involved in the aggregations seems a reasonable suggestion and could perhaps be a contributing factor in some species and situations, e.g., the enormous initial population increases affecting non-native, i.e., invasive species during the first few years after their arrival at a new location as witnessed by the Portuguese *O. moreleti* in Australia. The species *C. hualienensis* on Hachijojima island may still be in that initial unchecked population growth phase given that (a) natural predators like toads and some millipede-consuming birds are absent from the island and (b) millipedes generally excrete defensive cyanide derivatives, one of which in *C. hualienensis* has been identified as the toxic substance mandelonitrite (Noguchi et al, 1997).

However, visual inspection of the areas in which the outbreak of *C. hualienensis* occurred showed an abundance of rotting and decaying plant matter providing ample food to millipede populations far greater than those seemingly occurring in the area. Although correlations between millipede mass outbreaks have been sought with dominant plant species of the areas in which outbreaks occurred (Niijima & Shinohara 1988; Kania & Tracz, 2005; Voigtländer, 2005), or soil types and habitat characteristics (Barlow, 1957; Helb, 1975; Tajovský, 1993; Voigtländer, 2011; Zimmermann, 2013) or co-inhabiting soil invertebrates (Niijima, 1998), such correlations did not turn out

very convincing and certainly do not apply to the euryoecious *C. hualienensis* and its mass outbreaks on Hachijojima island. Incidentally, a correlation between outbreaks and soil pH changes was rejected by Haacker (1968).

It was suggested by Shintaro Yamashita (pers. comm..) that millipedes choose concrete roads and walls to crawl on, because they could obtain calcium from there. Although the cuticle of millipedes is indeed calcium-rich (Enghoff et al, 2014), it is unlikely that they gather together for the purpose of calcium uptake, for aggregations have also been reported from tree trunks and other surfaces that contain no or little calcium. Moreover, millipedes frequently move along the rails of railway tracks (Verhoeff, 1900; Esaki, 1934), which contain no calcium at all, but allow millipedes to move along unimpededly.

A study of thermal preferences by Boccardo & Penteado (1995a) has led to the speculation that concrete and asphalt roads are preferred as migratory paths, because they retain heat. However, it is unlikely that this could be the main reason for the millipedes' choice of their migratory route. However, once a route has become established, an olfactory trail may well guide additional individuals along.

Reproduction and search for oviposition sites

Reproduction and a search for suitable oviposition sites by females has frequently been suggested to explain swarming in millipedes, but it does not explain why non-reproductive sub-adults, although in considerably smaller numbers, frequently participate in the mass migrations. Although a high proportion of *C. hualienensis* individuals were paired at the aggregation sites, pairing and copulations could also be observed at other times of the year and locations far away from the aggregation sites, which suggests that pairing may not be a cause of the mass migration, but the latter can provide individuals with an opportunity to mate, because of the proximity of so many individuals at one place at the same time. As with *C. hualienensis*, a skewed sex ratio favouring females has also been reported from many other migratory species of millipedes (Kania & Tracz, 2005), but according to Stojałowska (1968, cited in Kania & Tracz, 2005) the ratio between male and females can vary over a period of several months, adding support to the notion of male periodomorphosis (Fairhurst, 1969; Sahli, 1985).

Given the fact that males as well as females of all migratory millipedes appear to have a tendency of climbing upward and ascending walls as well as trees, it does not make much sense if they were in search of suitable oviposition sites, for eggs are usually laid into the soil and other humid habitats (Perttunen, 1953). Therefore, we may have to reject the idea that millipedes primarily swarm in order to mate and that the females then search for places to lay their eggs in.

Weather conditions and climatic factors

The suggestion that the migrations are related to a search for overwintering niches stems from the fact that some species like, for instance, *Parafontaria laminata* and *C. hualienensis* migrate in autumn, but in Europe with its more severe winters most of the mass migrations have been reported from late spring and early summer, i.e., many months before the advent of winter. In addition, as with the hypothesized search for oviposition sites, climbing upwards and exposing themselves to the elements can hardly be interpreted as an optimal strategy to find hibernation shelters or, for that matter, to avoid desiccation and enter a state of aestivation during the summer months.

Given that mass migratory outbreaks are not involving all populations of a given species, but are restricted to some, it seems that local weather conditions disrupting the habitat and environment in a particular area may play a role. Temperature extremes and heavy rains, for example, have frequently been noticed to precede an outbreak in both European spring migrations and Japanese autumn migrations. In the case of the Hachijojima outbreak of the *C. hualienensis* a very heavy downpour with 104 mm of rain in one day occurred on November 6th and could possibly have washed down from the hills huge numbers of millipedes that after cessation of the rains needed to climb to where they had been dislodged from. However, even that cannot be the full explanation, because swarms wandering towards Site II (the concrete support pylon of the viaduct) followed the path of a road that was leading down and not upward. Fleeing excessively wet areas so as not to be drowned and trying to reach drier ground has been suggested and could well be one reason, but seeing at least some *C. hualienensis* individuals wandering into shallow puddles and getting drowned does not tally with that idea. Neither does the fact that at least some species search for humid areas to lay their eggs in (Perttunen, 1953).

It has also sometimes been suggested that the weather during the previous year and in particular a mild winter and a warm spring before an outbreak year could have been influential in leading to the outbreak. However, for the outbreak of *C. hualienensis* reported in this paper it is an unlikely explanation, since the weather records of the previous winter and spring did not exhibit any unusual features. Moreover, locals assert that *C. hualienensis* outbreaks appear to follow roughly a 4-year cycle. Other than the locals' opinion, however, no hard evidence in support of a 4-year cycle of millipede outbreak on Hachijojima exist and in view of the monthly moults of immature individuals (Fujiyama et al, 2012) actually seems unlikely.

Their extremely well developed clawed tarsi and obviously strong thigmotaxis allows many millipedes generally and *C. hualienensis* in particular to crawl upside down along rough surfaces even during strong wind. Strong wind, however, is likely to affect the place on the aggregation site where millipedes come to rest, but as the observations on *C. hualienensis* have shown, while the initially preferred walls were facing west and east at Site 1, the preferred side individuals chose at Site II at the same time was north. The only clear evidence of a preferred side emerged towards late November and early December when winds blew mostly from the west and the remaining aggregation clusters had moved to vertical surfaces of concrete walls all facing north, away from the light, but surprisingly also away from the midday warmth.

Behavioural reactions in particular in relation to light and darkness

All species of millipedes, with few exceptions, avoid bright light

and usually occur in dark areas under the bark of trees, in the soil, under stones, amongst leaf litter and rotting vegetation, but there is some evidence that mass aggregations occur preferentially on lighter surfaces. Since aggregations of millipedes were indeed frequently reported to occur on white or at least not very dark surfaces (Voigtländer, 2005) and the fact that some migrations involving *O. sabulosus* occurred in bright sunlight (Dziadosz, 1966; Fairhurst, 1970; Verhoeff, 1900), has led some researchers to conclude that during their migrations millipedes became positively phototactic. However, contradictory observations, namely that migrating millipedes, including *O. sabulosus*, sought shelter during the day from the light and became active only at night also exist (Demange, 1960). One question we therefore have to examine is whether millipedes can see at all.

Iulid and spirobolid species, as has been known for over a hundred years, (Graber, 1880; Grenacher, 1880) as well as spirostreptids (Blanke & Wesener, 2014), glomerids (Bedini, 1970) and penicillate millipedes (Müller et al, 2007) possess eyes and undoubtedly can perceive differences in light intensity and perhaps even crude shapes (Nilsson & Kelber, 2007). An endogenous activity rhythm was reported in *Gymnostreptus olivaceus* (Schubart), but light as an exogenous synchronizer of the millipede's nocturnal activity seemed insufficient to block the start of the biological clock (Boccardo & Penteado, 1995b). Observations on *C. hualienesis* gave a different result in that light clearly inhibited the animals (this paper); yet, polydesmids are all eyeless, in fact they are often called "blind" (e.g., Mesibov, 2014). Although that is clearly wrong, as already v. Rath (1890) has shown in *Polydesmus complanatus* (Latzel) and observations on *C. hualienensis* (this paper) have confirmed, the question arises how an eyeless polydesmid can detect light and use it as an exogenous synchronizer of its activities.

The fact that individuals active at night almost immediately became immobile and sought shelters when light was shone on them and the fact that individuals continued to crawl around during the day when placed into a totally dark room demonstrates that eyeless polydesmids are not blind. Most likely intracerebral photoreceptors are responsible for the observed dark/light reactions, but candidates for receptors of this kind amongst Myriapoda have to date only been reported from the chilopod *Lithobius forficatus* L. by Jamault-Navarro (1992), various species of glomerids by Juberthie-Jupeau (1967) and the iulid millipede *Cylindroiulus truncorum* by Heithier & Melzer (2005). Polydesmid species have apparently not yet been studied with regard to intracerebral photoreceptors, but are expected to have them too, since these internal photoreceptive structures are also present in crustaceans (Bobkova et al, 2003), insects (Hariyama, 2000) and chelicerates (Spreitzer & Melzer, 2003) and, thus, seem an arthropod-wide trait.

Female *C. hualienensis* outnumbered males by on average 1.24: 1.0 when data were pooled. Under very wet conditions at night, however, females reached an even higher proportion. Since females individuals appear to be stronger than males and are also slightly larger, they are likely to be able to cope with adverse weather conditions better than males. Given the long march that presumably both males and females have behind them when they arrive at the aggregation sites, some weaker males may have perished on the way and this could explain the preponderance of females.

Commensals and parasites

The large numbers of internal nematodes that were collected from males and females of *C. hualienensis* presumably resided in the posterior intestine as is the case in other diplopodes (e.g., Travassos & Kloss, 1961) or in the haemolymph as with spiders (Lewbart, 2006). The worms most likely belonged to the Diplogastridae (*Fictor* sp.) and Rhabditidae (*Oscheius* cf. *necromena*) line of the Rhabditida. Nematodes are frequent associates as commensals or parasites of arthropods (Kaya & Gaugler, 1993) and have been reported from numerous species of temperate (e.g., Bowie, 1985), tropical (Malysheva & Van Luc, 2012; Malysheva & Spiridonov, 2013) and even desert millipedes (Upton et al, 1983). Some rhabditids like, for example, panagrolaimid nematodes in spiders are considered to be fatal to the infected individuals (Lewbart, 2006). In bark beetles of the family Ipidae it was shown by Yatsenkowsky (1924), cited in Grucmanova & Holusa (2013) that the worms can cause sterility, but an effect, if any, that these worms may have on the health and/or behaviour of *C. hualienensis* millipedes has yet to be demonstrated. It has, however, been reported by Schulte (1989) that the nematode *Rhabditis necromena* (=*Oscheius necromena*) negatively affects the invasive millipede *Ommatoiulus moreleti* in Australia and Kania & Tracz (2005) have reported 90% and 100% lethality of the millipede *O. sabulosus* when infected with nematodes of the species *Heterorhabditis bacteriophora* and *Steinernema carpocapsae*, respectively.

Equally unknown is the effect another species associated with *C. hualienensis* might have, namely the deutonymphs of a mite representing a species of the genus *Histiostoma*. Phoretic mites, collectively known as myriapodophile Acari (Rosenberg, 2009, p357) have been reported from various species of millipedes before (Farfan & Klompen, 2012), including polydesmids, but not from *C. hualienensis*. The question arises as to whether the nematodes and mites were introduced together with *C. hualienensis* from Taiwan to Japan or were acquired locally. If the latter is the case, one has to ask if all the millipedes at a time when their swarming phase commenced were already infected by nematodes and mites or whether the close proximity and bodily contacts between individuals in the aggregation clusters caused nematode and mite infestations to spread. A necromenic lifestyle in which an organism ascends a carrier and completes its development on the carrier's cadavers is a possible scenario and known from some Histiostomatidae (Wirth, 2009).

Parasites or commensals other than those mentioned above were not encountered, although millipedes generally possess a propensity towards internal microorganisms (Hopkin & Read, 1992) and certain microorganisms like bacteria and yeasts actually assist the millipedes in the task of digesting cellulose and also themselves serve as food (Byzov, 2006). However, in

another invasive species (the Portuguese *Ommatoiulus moreleti*), the native Australian nematode *Rhabditis necromena* Sudhaus and Schulte has been shown to be lethal to the invader because it introduces bacteria to which the millipede is not immune (Schulte, 1989). In Portugal itself, nematomorph worms of the genus *Gordius* are known to alter the behaviour of their hosts and were shown by Baker (1985) and Sahli (1986) to castrate males and to inhibit maturation of eggs in female *O. moreleti* individuals.

Since parasites can cause behavioural changes in their hosts we can not totally rule out the possibility that parasite infestations are a factor in millipede outbreaks. According to Dobson (1988) it is in the interest of the parasite to have a high density of host individuals and therefore manipulations by parasites are greatest under conditions of low host population densities and smallest at high host population densities. Moreover, it is known that some parasites that cause infections often alter a natural negative phototaxis "such that infected individuals become indifferent or attracted to light, whereas uninfected ones are strongly repulsed by it" (Cézally et al, 2014).

Reasons and means to control millipede outbreaks

Often described as beneficial on account of their habits to recycle dead and decaying plant matter (Schmidt, 1952; Anonymous, 2010), millipedes can also damage healthy plants and crops (Hopkin & Read, 1992). More importantly they can contain various vectors of plant and animal diseases. For example, in the migratory European species *O. sabulosus* Kania & Klapeć (2012) found *Citrobacter* species, known to cause a wide spectrum of infections in humans and being associated with neonatal meningitis and brain abscesses. Other pathogenic bacteria from millipedes were *Pantoea agglomerans* that "can cause infections in children that involve the bloodstream", *Enterobacter* that are "associated with wound, intra-abdominal, respiratory, urinary and blood stream infections representing an increasingly important nosocomial pathogen" and *Raoultella planticola* as well as *Salmonella arizonae*, two further species impacting on human health negatively (Kania & Klapeć, 2012). It is therefore important to understand the causes of the outbreaks of millipede mass migrations and to learn how such outbreaks can be controlled. However, what do we know so far?

Millipedes, because of their defensive secretions of benzaldehyde and hydrogen cyanide derivatives, are preyed upon by only very few insect species (e.g., assassin bugs of the subfamily Ectrichodiinae and some firefly larvae: Ohba, 1997) and hardly any mammals, birds, reptiles, and amphibians; control by vertebrate animals is thus not an option. Therefore, a variety of methods (reviewed by, to name but a few, Hopkin & Read, 1992; Kania & Tracz, 2005; Zimmermann, 2013) and categorizable as chemical (e.g., pesticides and poisons), physical (e.g., mechanical barriers, traps, glue-strips and other obstacles) and biological (e.g., parasitoids, parasites and pathogens) have been tried with variable rates of success. Pyrethroid insecticides have been effective, but since these chemicals are toxic not only for millipedes, but also for most other animals, including beneficial species like honeybees, biological control methods have been looked into as alternatives (Kania & Tracz, 2005). Baker (1985) and Sahli (1986) recommended the nematomorph worm *Gordius* sp. and Baker (1985), additionally, listed the parasitoid fly *Egina* sp. as agents in the control of the invasive species *O. moreleti* in Australia. Promising results were also obtained with the native Australian nematode *Rhabditis necromena* (Schulte, 1989), which carries bacteria to which *O. moreleti* is not resistant. Kania & Tracz (2005) reported 90% and 100% lethality of the millipede *O. sabulosus* when infected with the nematodes of the species *Heterorhabditis bacteriophora* and *Steinernema carpocapsae*, respectively.

CONCLUSION

While the search for biological control agents seems to result in promising advances, the search for common causes of mass migrations and aggregations in millipedes as well as an answer to the question how these animals orientate and locate their aggregation sites has so far been less successful. For some species in which outbreaks occur at regular intervals related to the species' life cycle, predictions of outbreak years and seasons are possible and alien, invasive species like *O. moreleti* in Australia and *C. hualienensis* on the island of Hachijojima, may exhibit population explosions in their new environment for some years following their arrival until a more balanced situation develops.

Amongst insects numerous species are known, which possess sedentary and migratory morphs that may or may not alternate on a regular basis; the dominance or the prediction of one or the other morph's occurrence is therefore often not at all possible (Roff & Fairbairn, 2007). What has come under scrutiny recently, however, is the genetic background for this form of polymorphism (Yang et al, 2014). It is thus at least thinkable that also in millipedes we could have two perhaps morphologically hard to distinguish but genetically non-identical morphs, one prone to migrate and the other to remain sedentary. It would certainly seem worthwhile to examine whether those specimens of *C. hualienensis* that migrate and those that stay behind differ in their gene expression profiles.

There is, however, as this review has shown, not a single suggestion amongst those that have been made to explain the cause or causes of an outbreak and mass migration in the past, which does not have its counter argument. Echoing Morse (1903) more than a hundred years ago, who concluded that each migration seemed to have its own cause, we are left with the possibility that mass migrations and aggregations in millipedes do not have a common cause at all, but represent phenomena that in some locations occur on a seasonal basis and in others not and that are identical in their outcomes of bringing together masses of conspecifics, but which have evolved for different purposes in different millipede taxa and therefore need to be examined not in their entirety (unless the emphasis is on a bio-mathematical treatment or has a modelling perspective, e.g., David, 2012), but on a case-to-case basis.

ACKNOWLEDGMENTS

The author is indebted to Prof. Dr. T. Hariyama, Dr. Y. Takaku and Tsutsui san of Hamamatsu Medical University for preparing light and scanning electron micrographs of the nematodes, Dr. Lynn Carta of the USDA-ARS Nematology Laboratory for identifying the nematodes found in *C. hualienensis* and Dr. S.V. Malysheva of the A.N. Severtsov's Institute of Ecology and Evolution in Moscow for information on myriapod nematode taxonomy as well as Drs. C.H.G. Müller and J. Rosenberg for supplying copies or pages of difficult to obtain publications. The author is further grateful to Dr. H.-B. Schikora for preparing the mite light-micrographs and Dr. Monica Farfan of the University of Illinois at Chicago for her information on Histiostomatidae. Thanks are also due to Mr. Isao Nagai of Nakanogo Elementary School and Mr. Kotaro Osawa (Hokkaido University student) for their help with some of the translations of weather tables and Japanese publications. Last but not least the author wishes to acknowledge the role that Mr. S. Yamashita (Hachijojima Councillor) has played in supporting the author in numerous and generous ways and the help that has come from the constructive comments that two anonymous referees had provided.

REFERENCES

Anonymous. 2006[2006-10-11]. Tausendfüssler überrennen Vorarlberg – News. http: //www.20min.ch/print/story/16609580 (in German).

Anonymous. 2010[2010-04-26]. Millipedes and centipedes in Atlanta. http: //www.callnorthwest.com/2010/04/millipedes-and-centipedes-in-atlanta/

Anonymous. 2011. Tausendfüssler-Plage. http: //www.beobachter.ch/wohnen/artikel/tausendfuessler-plage/_jede-nacht-krabbelten-tausendfuessler-die-waende-hoch/ (in German).

Anonymous. 2013. Millipedes suspected in Clarkson train crash. *Railway Digest (Australia),* November 2013: 24.

Baker GH. 1978. The distribution and dispersal of the introduced millipede *Ommatoiulus moreletii* (Diplopoda: Julidae) in Australia. *Journal of Zoology (London),* 185(1): 1-11.

Baker GH.1985. Parasites of the millipede *Ommatoiulus moreletii* (Lucas) (Diplopoda: Iulidae) in Portugal, and their potential as biological control agents in Australia. *Australian Journal of Zoology,* 33(1): 23-32.

Barlow CA. 1957. A factorial analysis of distribution in three species of diplopods. *Tijdschrift voor Entomologie,* 100: 349-426.

Becker R. 1929. Beitrag zur Diplopodenfauna Lettlands. *Folia Zoologica (Riga),* 1: 10-50 (in German).

Bedini C. 1970. The fine structure of the eye in *Glomeris* (Diplopoda). *Monitore Zoologico Italiano (N.S.),* 4(4): 201-219.

Bellairs V, Bellairs R, Goel S. 1967. Studies on an Indian polydesmoid millipede *Streptogonopus phipsoni*, life cycle and swarming behaviour of the larvae. *Journal of Zoology,* 199(1): 31-50.

Blanke A, Wesener T. 2014. Revival of forgotten characters and modern imaging techniques help to produce a robust phylogeny of the Diplopoda (Arthropoda, Myriapoda). – *Arthropod Structure and Development,* 43(1): 63-75.

Bobkova M, Greve P, Meyer-Rochow VB, Martin G. 2003. Description of intracerebral ocelli in two species of North American crayfish: *Orconectes limosus* and *Pacifastus leniusculus* (Crustacea, Decapoda, Astacidea). *Invertebrate Biology,* 122: 158-165.

Boccardo L, Penteado, CHS. 1995a. Preferencias termicas e respostas metabolicas em relacao a temperatura e ao tamanho em *Gymnostreptus olivaceus* Schubart, 1944 (Diplopoda, Spirostreptidae). *Revista brasileira de biologia,* 55 (3): 445-456 (in Portuguese with English summary).

Boccardo L,Penteado CHS. 1995b. Locomotor and metabolic actoivities of *Gymnostreptus olivaceus* (Diplopoda, Spirostreptida) at different photoperiod conditions. *Comparative Biochemistry and Physiology*, Pt A, 112(3-4): 611-617.

Boccardo L, Jucá-Chagas R, Penteado CHS. 2002. Migration and population outbreaks of millipedes in the coffee plantations, region Altoparanaíba, MG, Brazil. *Holos Environment,* 2(2): 220-223.

Boccardo L, Penteado CHS, Jucá-Chagas R. 1997. Swarming of millipedes, new case noticed in the district of Patrocinio, MG, Brazil. Journal of Advanced Zoology, 18(1): 62-63.

Bowie JY. 1985. New species of rhigonematid and thelostomatid nematodes from indigenous New Zealand millipedes. *New Zealand Journal of Zoology,* 12(4): 485-503.

Brade-Birks SG. 1922. Notes on myriapoda, 27. Wandering millipeds. *Annals and Magazine of Natural History (ser. 49),* 9(9): 208-212.

Brooks FE. 1919. A migratory army of millipeds. *Journal of Economic Entomology,* 12(6): 462-464.

Byzov BA. 2006. Intestinal microbiota of millipedes. *In*: König H, Varma A. Intestinal Microorganisms of Termites and other Invertebrates. Berlin: Springer, 373-384.

Ceuca T. 1984. Migrațiile la diplopode. *Nymphaea (Oradea),* 10: 237-242 (in Romanian with English summary).

Cézally F, Perrot-Minnot MJ, Rigaud T. 2014. Cooperation and conflict in host manipulation: interactions among macro-parasites and micro-organisms. *Frontiers in Microbiology,* 5: 248.

Chater A. 2004. A swarm of *Cylindroiulus londinensis* in Montgomeryshire. *Bulletin of the British Myriapod and Isopod Group,* 20: 51.

Cloudsley-Thompson JL. 1949. The significance of migration in myriapods. *Journal of Natural History Series 12,* 2(24): 947-962.

Cook OF. 1924. Swarming of desert millipeds. *Science N.S.,* 60(1552): 294.

Ćurić BPM, Makarov SE. 1995. The occurrence of swarming in *Megaphyllum unilineatum* (C.L. Koch, 1838) (Diplopoda: Julidae), with observations on a case of pedal anomaly. *Archives of Biological Sciences (Belgrade),* 47(1-2): 67-70.

David JF. 2012. First estimate of the intrinsic rate of increase of a millipede: *Polydesmus angustus* (Polydesmida: Polydesmidae) in a seasonal environment. *Annals of the Entomological Society of America,* 105(1): 90-96.

Demange JM. 1960. Sur un important rassemblement de *Schizophyllum sabulosum* L. (Myriapode-Diplopode). *Cahiers des Naturalistes du Bulletin National de Paris N.S.,* 16(4): 89-91 (in French).

Dobson AP. 1988. The population biology of parasite-induced changes in host behavior. *The Quarterly Reviews of Biology,* 63(2): 139-165.

Dziadosz C. 1966. Materiały do znajomości rozmieszczejnia krocinogów (Diplopoda) w Polsce. *Fragmenta Faunistica (Warszawa),* 13: 1-31 (in Polish).

Ehrnsberger R. 2002. Massenauftreten und Wanderung des Diplopoden *Ommatoiulus sabulosus* in Westniedersachsen. *Osnabrücker Naturwissenschaftliche Mitteilungen,* 28: 199-203 (in German).

Enghoff, H., Manno, N., Tchibozo, S., List, M., Schwarzinger, B., Schoefberger, W., Schwarzinger, & C., Paoletti, MG. (2014). Millipedes as food for humans: their nutritional and possible antimalarial value - A first

report. *Evidence-Based Complementary and Alternative Medicine*, ID 651768, doi:10.1155/2014/651768.

Esaki T. 1934. Diplopoda that disturb the movement of trains. *Shokubutsu oyobi Dobutsu,* 2: 821-833 (in Japanese).

Fairhurst CP. 1970. Activity and wandering in *Tachypodoiulus niger* (Leach) and *Schizophyllum sabulosum* (L.). *Bulletin du Muséum National d'Histoire Naturelle,* 41(S2): 61-66.

Farfan MA, Klompen H. 2012. Phoretic mite associations of millipedes (Diplopoda, Julidae) in the northern Atlantic region (North America, Europe). *International Journal of Myriapodology,* 7: 62-91.

Fontanetti CS, Calligaris IB, Souza TS. 2010. A millipede infestation of an urban area of the city of Campinas, Brazil and preliminary toxicity studies of insecticide bendiocarb to the *Urostreptus atrobrunneus* Pierozzi & Fontanetti, 2006. *Arquivos do Instituto Biológico* (São Paulo)*,* 77(1): 165-166.

Fujiyama S, Ishida T, Shah SK. 2012. Ecology of imigrated diplopoda, *Chamberlinius hualienensis* with special reference to that of *Parafontaria laminata armigera*. *The Annals of Environmental Science of Shinshu University,* 34: 110-116 (in Japanese).

Graber V. 1880. Ueber das unicorneale Tracheaten- und speciell das Arachnoiden- und Myriapoden-Auge. *Archiv für Mikroskopie und Anatomie,* 17: 58-94 (in German).

Grenacher H. 1880. Über die Augen einiger Myriapoden. Zugleich eine Entgegnung an V. Graber. *Archiv für mikroskopische Anatomie und Entwicklungsmechanik,* 18(1): 415-467 (in German).

Grucmanova S, Holusa J. 2013. Nematodes associated with bark beetles, with focus on the genus *Ips* (Coleoptera; Scolytinae) in Central Europe. *Acta Zoologica Bulgarica,* 65(4): 547-556.

Haacker U. 1968. Deskriptive, experimentelle und vergleichende Untersuchungen zur Autökologie rhein-mainischer Diplopoden. *Oecologia,* 1(1-2): 87-129 (in German with English summary).

Hagiwara Y, Kuwabara Y. 2008. Outbreak of the train millipede on the northern slope of Mt. Fuji. *Fujisan Kenkyu Report,* 2: 21-24 (in Japanese).

Hariyama T. 2000. The brain as a photoreceptor: intracerebral ocelli in then firefly. *Naturwissenschaften,* 87(7): 327-330.

Heithier N, Melzer RR. 2005. The accessory lateral eye of a diplopod, *Cylindroiulus truncorum* (Silvestri, 1896) (Diplopoda: Julidae). *Zoologischer Anzeiger,* 244(1): 73-78.

Helb HW. 1975. Zum Massenauftreten des Schnurfüssers *Schizophyllum sabulosum* (Myriapoda: Diplopoda). *Entomologia Germanica,* 1(3-4): 376-381 (in German).

Higa Y, Kishimoto T, Niijima K. 1992. Seasonal abundance of Yanbarutosa-kayasude in Okinawa. *Okinawa Ken Kogai Eisei Kenkyujo Houkoku* (Report of the Okinawa Prefectural Pollution Institute), 23: 72-76 (in Japanese).

Hopkin SP, Read HJ. 1992. The Biology of Millipedes. Oxford: Oxford University Press.

Jamault-Navarro C. 1992. Sur la présence d'une structure rhabdomérique localisée intracérébralement dans le protocérébron de *Lithobius forficatus* L. *Berichte des Naturwissenschaftlich-Medizinischen Vereins Innsbruck Supplement,* 10: 81-86 (in French).

Japanese Meteorological Agency. 2014. http: //www.data.jma.go.jp (in Japanese).

Juberthie-Jupeau L. 1967. Existence d'organes neuraux intracérébraux chez les Glomeridia (Diplopodes) épigés et cavernicoles. *Comptes Rendus hebdomadaires des Séances de l'Académie des Sciences (Paris),* 264: 89-92 (in French).

Kania G, Tracz H. 2005. Mass occurrence and migration of *Ommatoiulus sabulosus* (Linnaeus, 1758) (Diplopoda, Julida: Julidae) in Poland. *Peckiana,* 4: 57-66.

Kania G, Klapeć T. 2012. Seasonal activity of millipedes (Diplopoda) - their economic and medical significance. *Annals of Agricultural and Environmental Medicine,* 19(4): 649-650.

Kaya HK, Gaugler R. 1993. Entomopathogenic nematodes. *Annual Review of Entomology,* 38: 181-206.

Koch LE. 1985. Pincushion millipedes (Diplopoda: Polyxenida): their aggregations and identity in Western Australia. *Western Australian Naturalist,* 16(2-3): 30-32.

Korsós Z. 1998. Ikerszelvényes-invázió magyarországon. *Állattani Közlemények,* 83: 53-65 (in Hungarian).

Lawrence RF. 1952. Variation in the leg numbers of South African millipede *Gymnonstreptus pyrrhocephalus* C. Koch. *Annals and Magazine of Natural History Series,* 12: 1044-1051.

Lewbart GA. 2006. Invertebrate Medicine. Chichester (U.K.): Wiley-Blackwell, 211.

Lindgren LAH. 1942. Ett massuppträdande av en diplopod, *Cylindroiulus teutonicus* Pocock. *Fauna och Flora Uppsala,* 2: 79-81 (in Swedish).

Malysheva SV, Van Luc P. 2012. *Cattiena fansipanis* n. sp. (Nematoda: n Rhigonematida: Carnoyidae) from a millipede (Myriapoda: Diplopoda: Spirobolida) in North Vietnam. *Systematic Parasitology,* 81: 135-146.

Malysheva SV, Spiridonov SE. 2013. *Ichthyocephaloides sumbatus* n. sp. (Nematoda: Rhigonematoidea) from Indonesia and additional data on *Xystrognathus phrissus* Hunt, Pham Van Luc & Spiridonov, 2002. *Nematology,* 15(5): 575-588.

McKillup SC, Allen PG, Skewes MA. 1988. The natural decline of an introduced species following its initial increase in abundance: an explanation for *Ommatoiulus moreleti* in Australia. *Oecologia,* 77(3): 339-342.

Meidell B, Simonsen A. 1985. A mass occurrence of *Cylindroiulus londinensis* (Leach, 1815) in Norway. *Fauna Norvegica B,* 32(1): 47-48.

Mesibov R. 2014[2015-01-16]. External anatomy of polydesmida. http: //www.polydesmida.info/polydesmida.

Mitra TR. 1976. Millipedes entering houses. *The Entomologist's Monthly Magazine,* 112: 44.

Morse M. 1903. Unusual abundance of a myriapod, *Parajulus pennsylvanicus* (Brandt). *Science N.S.,* 18(445): 59-60.

Müller CHG, Sombke A, Rosenberg J. 2007. The fine structure of the eyes of some bristly millipedes (Penicillata, Diplopoda): Additional support for the homology of mandibulate ommatidia. *Arthropod Structure and Development,* 36(4): 463-476.

Niijima K. 1998. Effects of outbreak of the train millipede *Parafontaria laminata armigera* Verhoeff (Diplopoda: Xystodesmidae) on litter decomposition in a natural beech forest in Central Japan. 1. Density and biomass of soil invertebrates. *Ecological Research,* 13(1): 41-53.

Niijima K, Shinohara K. 1988. Outbreaks of the *Parafontaria laminate* group (Diplopoda: Xystodesmidae). *Japanese Journal of Ecology,* 38: 257-268 (in Japanese with English summary).

Nilsson DE, Kelber A. 2007. A functional analysis of compound eye evolution. *Arthropod Structure and Development,* 36(4): 373-385.

Noguchi S, Mori N, Higa H, Kuwahara Y. 1997. Identification of mandeloni-

trite as a major secretary compound of *Chamberlinius hualienensis* Wang (Polydesmidae, Paradoxosomatidae). *Japanese Journal of Environmental Entomology and Zoology,* 8: 208-214.

Ohba N. 1997. Breeding of the firefly, Rhagophthalmus ohbai (Coleoptera: Rhagophthalmidae). *Scientific Reports of Yokosuka City Museum*, 45: 51-55.

Ormerod EA. 1890. Manual of Injurious Insects with Methods of Prevention and Remedy for Their Attacks to Food Crops, Forest Tress, and Fruit, and with A Short Introduction to Entomology. London: WS Sonnenschein & Allen Publ., 150-151.

Paszlavszky J. 1879. Massenhaftes Erscheinen von Tausendfüsslern. *Verhandlungen der kaiserlich-königlichen zoologisch-botanischen Gesellschaft in Wien Jahrgang 1878,* 28: 545-552 (in German).

Perttunen V. 1953. Reactions of Diplopods to the Relative Humidity of the Air: Investigations on *Orthomorpha gracilis, Julus terrestris* and *Schizophyllum sabulosum*. *Annales Societatis Zoologicae-Botanicæ Fennicæ Vanamo,* 16(1): 1-69.

vom Rath O. 1890. Ueber die Fortpflanzung der Diplopoden (Chilognathen). *Berichte der Naturforschenden Gesellschaft Freiburg,* 5(1): 1-28 (in German).

Robinson WH. 2005. Urban Insects and Arachnids. Cambridge (U.K.): Cambridge University Press, 424-426.

Roff DA, Fairbairn DJ. 2007. The evolution and genetics of migration in insects. *Bioscience*, 57 (2): 155-164.

Rosenberg J. 2009. Die Hundertfüsser - Chilopoda: die neue Brehm Bücherei Band 285. Hohenwassersleben (Germnany): Westarp Wissenschafts-Verlagsgesellschaft (in German).

Sahli F. 1985. Périodomorphose et males intercalaires des diplopodes Julidae: une nouvelle terminologie. *Bulletin Scientifique de Bourgogne,* 38(1-2): 23-32 (in French).

Sahli F. 1986. Modifications des caractères sexuels secondaires males et stérilisé des femelles sous l'influence d'un *Gordius* parasite chez le diplopode julide *Ommatoiulus omeletti* (Lucas) au Portugal. *Bulletin Scientifique de Bourgogne,* 39(2): 587-598 (in French).

Sahli F. 1996. Déplacement en masse dans le sud-est de la France chez *Ommatoiulus sabulosus* (Myriapoda, Diplopoda, Julidae) avec invasions d'habitations. *In*: Geoffroy JJ, Mauries JP, Nguyen-Duy-Jacquemin M. Acta Myriapodologica. Paris: Mémoires du Museum National d'Histoire Naturelle, 169: 373-384 (in French).

Schmidt H. 1952. Nahrungswahl und Nahrungsverarbeitung bei Diplopoden (Tausendfüßlern). *Mitteilungen des Naturwissenschaftlichen Vereines für Steiermark,* 81/82: 42- 66 (in German).

Schulte F. 1989. The association between *Rhabditis necromena* Sudhaus and Schulte 1989 (Nematoda: Rhabditidae) and native and introduced millipedes in South Australia. *Nematologica,* 35(1): 82-89.

Scott H. 1958a. Migrant millipedes and entering houses 1953-1957. *The Entomologist's Monthly Magazine,* 94: 73-77.

Scott H. 1958b. Migrant millipedes entering houses 1958. *The Entomologist's Monthly Magazine,* 94: 252-256.

Spreitzer A, Melzer RR. 2003. The nymphal eyes of *Parabuthus transvaalicus* Purcell, 1899 (Buthidae): an accessory lateral eye in a scorpion. *Zoologischer Anzeiger,* 242(2): 137-143.

Stojałowska W. 1968. Materiały do poznania krocinogów (Diplopoda) Wyżyny Lubelskiej. *Folia Societatis Scientiarum Lublinensis B,* 7/8: 83-93 (in Polish).

Tajovský K. 1993. Diversity and structure of millipede communities (Diplopoda) in four different iotopes. *Ekologia (Bratislava),* 12(3): 277-283.

Takaku Y, Suzuki H, Ohta I, Ishii D, Muranaka Y, Shimomura M, Hariyama T. 2013. A thin polymer membrane, nano-suit, enhancing survival across the continuum between air and high vacuum. *Proceedings of the National Academy of Sciences of the United States of America,* 110(19): 7631-7635.

Thaler K. 1989. Kleintiere im Kulturland des Innsbrucker mittelgebirges. *In*: Köck L, Holaus K. 50 Jahre Landesanstalt für Pflanzenschutz und Samenprüfung. Rinn: Landesanstalt für Pflanzenschutz und Samenprüfung, 59-177 (in German).

Thuringer JM. 1924. A note on migration of Myriapoda. *Science N.S.,* 60(1543): 83.

Tömösváry Ö. 1878. A százlábúak vándorlásához. *Természettudományi Közlemények,* 10: 365-366 (in Hungarian).

Travassos PL, Kloss GR. 1961. Sur un curieux nématode de *Robertia leiperi* gen. et sp. nov., parasite de l'intestine postérieur de diplopode. *Journal of Helminthology,* 35(S1): 187-190 (in French).

Upton SJ, Crawford CS, Hoffman RL. 1983. A new species of thelastomatid (Nematoda: Thelastomatidae) from the desert millipede, *Orthoporus ornatus* (Diplopoda, Spirostreptidae). *Proceedings of the Helminthological Society (Washington),* 50(1): 69-82.

Verhoeff KW. 1900. Wandernde Doppelfüßler, Eisenbahnzüge hemmend. *Zoologischer Anzeiger,* 23: 465-473 (in German).

Verhulst PF. 1845. Recherches mathématiques sur la loi d'accroissement de la population. *Mémoires de l'Académie Royale des Sciences et Belles Lettres de Bruxelles,* 18: 1-42 (in French).

Viosca P Jr. 1925. Perambulating millipeds. *Science N.S.,* 61(1566): 19-20.

Voigtländer K. 2005. Mass occurrences and swarming behaviour of millipedes (Diplopoda: Julidae) in Eastern Germany. *Peckiana,* 4: 181-187.

Voigtländer K. 2011. Preferences of common Central European millipeds for different biotopes (Myriapoda, Diplopoda) in Saxony-Anhalt (Germany). *International Journal of Myriapodology,* 6: 61-83.

Wang YM. 1956. Records of myriapods on Formosa with description of new species (2). *Quarterly Journal of the Taiwan Museum,* 9(2): 155-159.

Wesener T, Schütte K. 2010. Swarming behaviour and mass occurrences in the world's largest giant pill-millipede species, *Zoosphaerium neptunus*, on Madagascar and its implication for conservation efforts (Diplopoda: Sphaerotheriida). *Madagascar Conservation and Development,* 5(2): 89-94.

Wirth S. 2009. Necromenic life style of *Histiostoma polypori* (Acari: Histiostomatidae). *Experimental and Applied Acariology,* 49(4): 317-327.

Yang X, Liu X, Xu X, Li Z, Li Y, Song D, Yu T, Zhu F. 2014. Gene expression profiling in winged and wingless cotton aphids, *Aphis gossypii* (Hemiptera: Aphididae). *International Journal of Biological Sciences*, 10(3): 257-267.

Yatsenkowsky AV. 1924. The castration of *Blastophagus* of pines by roundworms and their effect of the activity and life phenomena of Ipidae. *Publications of the Agriculture Institute of Western White Russia,* 3: 1-19.

Zimmermann K. 2013. Röns: St. Magnus und die Tausendfüssler. Dornbirn (Austria): Naturmonographie Jagdberggemeinden, 371-386 (in German).

Molecular characterization of an *IL-1β* gene from the large yellow croaker (*Larimichthys crocea*) and its effect on fish defense against *Vibrio alginolyticus* infection

Jun WU[1], Yu-Hong SHI[1], Xue-Heng ZHANG[1], Chang-Hong LI[1], Ming-Yun LI[1], Jiong CHEN[1,2,*]

[1] *Laboratory of Biochemistry and Molecular Biology*, *School of Marine Sciences*, *Ningbo University*, *Ningbo* 315211, *China*

[2] *Donghai Sea Collaborative Innovation Center for Industrial Upgrading Mariculture*, *Ningbo University*, *Ningbo* 315211, *China*

ABSTRACT

Interleukin 1β (IL-1β), the first interleukin to be characterized, plays a key role in regulating the immune response. In this study, we determined the cDNA and genomic DNA sequences of the *IL-1β* gene from the large yellow croaker, *Larimichthys crocea*. Phylogenetic analysis indicated that the *IL-1β* (*LcIL-1β*) gene was most closely related to that of European seabass (*Dicentrarchus labrax*), sharing 67.8% amino acid identity. In healthy large yellow croaker, LcIL-1β transcription was detected in all tested tissues, with the highest level found in the head kidney. Upon *Vibrio alginolyticus* infection, LcIL-1β transcription in all tested tissues was significantly upregulated. Intraperitoneal injection of recombinant LcIL-1β (rLcIL-1β) improved the survival rate and reduced the tissue bacterial load after *V. alginolyticus* infection. In addition, rLcIL-1β induced monocytes/macrophages (MO/MΦ) chemotaxis and increased phagocytosis and bactericidal activity *in vitro*. These results suggest that LcIL-1β plays an important role in the large yellow croaker immune response against *V. alginolyticus*.

Keywords: Interleukin 1β; Large yellow croaker; Survival rate; *Vibrio alginolyticus*; Monocytes/ macrophages

INTRODUCTION

Large yellow croaker (*Larimichthys crocea*) is one of the most abundant species in the Northwest Pacific basin, and is also an economically important aquaculture fish species in China. In recent years, farmed production of large yellow croaker has become intensive. However, the farming industry is now threatened with infectious disease outbreaks, with *Vibrio alginolyticus* regarded as the major bacterial pathogen (Chen et al, 2003; Li et al, 2009). Antibiotics have been used extensively for controlling large yellow croaker diseases, but drug residues in aquatic products and environments have become an increasing threat to human health (Mu et al, 2013). Thus, controlling diseases by understanding immune response modulation in fish species is critical.

The cytokine interleukin-1β (IL-1β) exerts a plethora of systemic and localized biological effects, and is central to the initiation and regulation of immune and inflammatory responses in animals (Hong et al, 2003). Many economically important teleost *IL-1β* sequences have been studied previously (Fujiki et al, 2000; Lu et al, 2013; Scapigliati et al, 2001; Zou et al, 1999). Some reports have shown that teleost IL-1β is tightly associated with the defense reaction of the host to pathogen infection. For example, *IL-1β* gene expression increased significantly in ayu (*Plecoglossus altivelis*) upon *Vibrio anguillarum* infection (Lu et al, 2013). Recombinant rainbow trout (*Oncorhynchus mykiss*) IL-1β enhanced their resistance to *Aeromonas salmonicida*, and increased the migration and phagocytic activity of its head kidney-derived leucocytes *in vitro* (Hong et al, 2003). An IL-1β derived peptide, P3, which corresponds to fragment 197-206 (YRRNTGVDIS) of the rainbow trout sequence, enhanced the phagocytic and bactericidal activity of rainbow trout head kidney leucocytes (Peddie et al, 2002). Recombinant European seabass (*Dicentrarchus labrax*) IL-1β stimulated the proliferation of thymocytes (Scapigliati et al, 2001). However,

Received: 23 March 2015; Accepted: 24 April 2015

Foundation items: This project was supported by the National 863 Project (2012AA10A403), the Natural Science Foundation of Ningbo City of China (2014A610187) and the Scientific Research Foundation of Graduate School of Ningbo University (G14041)

*Corresponding author, E-mail: jchen1975@163.com

the function of IL-1β in large yellow croaker remains unclear.

In the present study, we determined the cDNA and genomic DNA sequences of the *IL-1β* gene (*LcIL-1β*) from the large yellow croaker. LcIL-1β transcription was investigated in healthy fish and in *V. alginolyticus*-infected fish. The effect of intraperitoneal (i.p.) administration of recombinant LcIL-1β (rLcIL-1β) on the survival rate and tissue bacterial load in large yellow croaker following *V. alginolyticus* infection was investigated. We also studied the effect of rLcIL-1β on monocytes/macrophages (MO/MΦ) chemotaxis, phagocytosis and bactericidal activity *in vitro*.

MATERIALS AND METHODS

Fish

Healthy large yellow croaker (15.5±1.3 cm in length, weighing 76.2±5.8 g) were obtained from the Ningbo Hai-Wan Marine Breeding Center, Xiangshan county, Ningbo city, China. Fish without any pathological signs were kept in tanks maintained at 25-27 °C with regular feeding for at least one week prior to experimental use. All experiments were performed according to the Experimental Animal Management Law of China and approved by the Animal Ethics Committee of Ningbo University.

Bacterial challenge

The *V. alginolyticus* challenge was performed as reported previously (Li et al, 2014). Briefly, overnight cultured *V. alginolyticus* isolate ATCC 17749 was diluted 1:100 in fresh Tryptic Soy Broth Medium (TSB) and cultured at 28 °C. Cells were harvested in the logarithmic phase of growth, and diluted to the appropriate concentration in PBS. Four groups of fish were infected by i.p. injection of *V. alginolyticus* (6.5×10^4 CFU/g in 200 μL PBS), with PBS used in the control group. Each group contained at least three fish. The liver, spleen, heart, head kidney, trunk kidney, brain, intestine and gill were collected at 4, 8, 12, and 24 hours post injection (hpi), frozen in liquid nitrogen and stored at -80 °C until RNA extraction.

Determination of cDNA and genomic DNA sequences of *LcIL-1β*

The cDNA sequence of *LcIL-1β* was obtained from transcriptome analysis of large yellow croaker, and the correct sequence was confirmed using PCR amplification combined with sequencing on an ABI 3730 automated sequencer (Invitrogen, Shanghai, China). Genomic DNA of large yellow croaker was isolated from liver tissue using a DNA Extraction Kit (TaKaRa, Dalian, China). Primers gLcIL-1βF: 5'- ATGGAATCTGAGATGAAATGC -3' and gLcIL-1βR: 5'- TCAGGCCTGACCCTCAGT -3' were designed to amplify the genomic sequence. The PCR product was cloned and sequenced. The BLAST program (http://blast.ncbi.nlm.nih.gov/Blast.cgi) was used for sequence similarity searching. Protein analysis was performed using online software on the ExPASy Server (http://www.expasy.org/tools/). The ClustalW program (http://clustalw.ddbj.nig.ac.jp/) was used for multiple sequence alignment. MEGA version 5 was used for phylogenetic tree analysis (Tamura et al, 2011). Accession numbers of sequences used are provided in Table 1.

Real-time quantitative PCR (qPCR) analysis of LcIL-1β mRNA expression

QPCR was carried out as described previously (Chen et al, 2014; Lu et al, 2013). Briefly, total RNA was extracted from the

Table 1 ***IL-1β*** **sequences used for multiple sequence alignment and phylogenetic tree analysis**

GenBank accession no.	Species		Gene
	Latin name	English name	
NM_001280090	*Takifugu rubripes*	Tiger pufferfish	*IL-1β*
AB720983	*Paralichthys olivaceus*	Japanese flounder	*IL-1β*
AY257219	*Pagrus major*	Red sea bream	*IL-1β*
HF543937	*Plecoglossus altivelis*	Ayu	*IL-1β*
AJ535730	*Gadus morhua*	Atlantic cod	*IL-1β*
AJ245925	*Oncorhynchus mykiss*	Rainbow trout	*IL-1β*
AY617117	*Salmo salar*	Atlantic salmon	*IL-1β*
AJ550166	*Melanogrammus aeglefinus*	Haddock	*IL-1β*
AJ277166	*Sparus aurata*	Gilthead sea bream	*IL-1β*
AJ311925	*Dicentrarchus labrax*	European seabass	*IL-1β*
EF513753	*Lateolabrax japonicus*	Japanese seabass	*IL-1β*
AJ295836	*Scophthalmus maximus*	Turbot	*IL-1β*
EF582837	*Epinephelus coioides*	Orange-spotted grouper	*IL-1β*
FJ816103	*Cynoglossus semilaevis*	Half smooth tongue sole	*IL-1β*
AJ574910	*Tetraodon nigroviridis*	Spotted green pufferfish	*IL-1β*
FM210810	*Danio rerio*	Zebrafish	*IL-1β*
BT007213	*Homo sapiens*	Human	*IL-1β*

large yellow croaker liver, spleen, heart, head kidney, trunk kidney, brain, intestine and gill using the RNeasy® Mini Kit (Qiagen, Maryland, USA). First-strand cDNA was synthesized using AMV Reverse Transcriptase (TaKaRa). Primers LcIL-1βF: 5'- TGGGAATGTGCCTGGAGAAC -3' and LcIL-1βR: 5'-CTTCCGTCTTAAGAGGATCA -3' were designed to amplify a 100-base pair (bp) fragment of the *LcIL-1β* cDNA. As an internal control, primers Lcβ-actinF: 5'-GATGTGGATCAGCA AGCAGG-3' and Lcβ-actinR: 5'-GAGCTGAAGTTGTTGGGT GT-3' were designed to amplify a 120-bp fragment of β-actin cDNA (EU443733). QPCR was performed using SYBR premix Ex Taq (Perfect Real Time) (TaKaRa). The reaction mixture was incubated for 5 min at 95 °C, followed by 35 amplification cycles of 30 s at 95 °C, 30 s at 60 °C and 30 s at 72 °C in an RT-Cycler™ Realtime Fluorescence Quantitative PCR thermocycler (CapitalBio, Beijing, China). The LcIL-1β transcript was normalized relative to β-actin. Amplifications were performed in triplicate for each sample. The relative mRNA expression of LcIL-1β was calculated by the comparative Ct method ($2^{-\Delta\Delta Ct}$ method).

Prokaryotic expression, purification and refolding of rLcIL-1β

The ORF sequence of the *LcIL-1β* gene was amplified from a liver cDNA template with the following primers: LcIL-1βpF: 5'-C<u>CATATG</u>GAATCTGAGATGAAATGC-3' and LcIL-1βpR: 5'-G<u>GGATCC</u>TCAGGCCTGACCCTCAGT-3' (underlined bases are *Nde* I and *BamH* I sites, respectively). After restriction enzyme digestion, the amplicon was orientedly inserted into the pET28a vector. The recombinant pET28a-LcIL-1β plasmid was then transformed into *Escherichia coli* BL21(DE3) pLysS, and its expression was induced with IPTG. The purification and refolding of rLcIL-1β were carried out as described previously (Zhang et al, 2011), with some modifications. Briefly, a His Trap™ FF Crude chelating column (GE Healthcare, Shanghai, China) and 120-mL XK 16/100 column packed with Superdex 75 gel media (GE Healthcare) were used to purify and refold the recombinant protein. The eluted fraction containing refolded rLcIL-1β was then desalted on a Bio-Gel P-6 column (Bio-Rad, Shanghai, China). The size and purity of the peak fractions were monitored by 12% SDS-PAGE followed by Coomassie brilliant blue staining. The purified protein was lyophilized for further study.

Survival rate and bacterial load assays

Four groups of 20 fish were used in the survival rate assay. Thirty minutes after the large yellow croakers were intraperitoneally infected with 6.5×10^4 CFU/g *V. alginolyticus*, refolded *rLcIL-1β* in 200 µL PBS (0, 0.001, 0.01 or 0.1 µg/g body weight) were i.p. injected into the fish. The dose was in line with previous research on rainbow trout (Hong et al, 2003). Morbidity was monitored for nine days, and dead fish were collected daily. The same concentrations of refolded rLcIL-1β were i.p. injected into healthy fish and no impairment was found. Death was considered to be caused by the injected isolate only if the same isolate could be re-isolated as single colonies in pure culture from the head and liver of the moribund or dead fish. The Log-rank test was used to analyze survival rate.

Bacterial load was measured as colony-forming units per mg tissue as per prior study (Li et al, 2014). At 72 h post administration of rLcIL-1β, four groups of six fish were sacrificed, and the tissue samples (liver, spleen, kidney and blood) were collected. The samples from each fish were weighed and homogenized in 1 mL of sterile PBS (pH 7.2). Homogenates and blood were serially diluted in sterile PBS and then plated onto Thiosulfate Citrate Bile Salt (TCBS) agar plates for 12 h at 28 °C. Results were normalized as colonies/weight tissue (0.1 g) or colonies/blood volume (0.1 mL).

Primary culture of large yellow croaker head kidney-derived MO/MΦ

Large yellow croaker MO/MΦ were isolated as perviously described (Lu et al, 2013). Briefly, head kidney leucocyte-enriched fractions were obtained using a Ficoll density gradient (Invitrogen, Shanghai, China). Non-adherent cells were washed off and the attached cells were incubated with RPMI 1640 medium containing 10% FCS and 1% P/S throughout the experiment after overnight incubation at 24 °C. Over 95% of adherent cells were MO/MΦ according to morphological characteristics observed after Giemsa staining.

MO/MΦ chemotaxis, phagocytosis and bactericidal activity assays

The chemotaxis assay was carried out in a Chemotaxicell (Corning, Shanghai, China) following a modified Boyden chamber method (Zhang et al, 2011). Briefly, wells in the lower compartment were loaded with five concentrations (0.001, 0.01, 0.1, 1 and 10 µg/mL) of refolded rLcIL-1β, denatured rLcIL-1β and BSA dissolved in RPMI 1640. A polyvinylpyrrolidone (PVP)-free polycarbonate membrane with a pore size of 5 µm was placed in the lower compartment. Large yellow croaker MO/MΦ were added to the upper compartment. The chamber was sealed and incubated at 24 °C for 4 h. Cells that completely migrated to the lower compartment were counted in five random fields using a light microscope at 400× magnification. Each test was run in triplicate. The chemotactic index was calculated from the number of cells that migrated to the test samples divided by the number of cells that migrated to the medium only.

The phagocytosis assay was carried out following a modified method (Chen et al, 2014). Briefly, *E. coli* strain DH5α cells were labeled with FITC (FITC-DH5α). Large yellow croaker MO/MΦ were incubated with PBS, 0.001, 0.01 and 0.1 µg/mL rLcIL-1β for 4 h and subsequently incubated with FITC-DH5α at 24 °C for 0.5 h. The uptake of bacteria into cells was captured by a microscope and quantified by measuring fluorescence intensity using ImageJ software (http://rsb.info.nih.gov/ij/).

The bactericidal assay was carried out following a modified method (Chen et al, 2014). Briefly, large yellow croaker MO/MΦ were incubated with PBS, 0.001, 0.01 and 0.1 µg/mL rLcIL-1β at 24 °C for 24 h, and the cells were then washed twice to remove all traces of P/S. The cells were incubated with *V. alginolyticus* at an MOI of 20 for 0.5 h and subsequently washed in PBS to remove extracellular bacteria. The uptake

group cells were lysed with 0.05% Triton X-100 and the killing group wells were incubated for 2 h and then lysed with 0.05% Triton X-100. The cell lysates were plated on TCBS plates, and bacterial counts were enumerated after 12 h. Bacterial survival was determined by dividing the number of colonies in the killing group by those in the uptake group.

Statistical analysis

All data are described as means±*SEM*. Statistical analysis of the results was conducted by one-way ANOVA with SPSS version 13.0 (SPSS Inc, Chicago, USA), and P<0.05 was considered statistically significant.

RESULTS

Sequence comparison and phylogenetic analysis of the *LcIL-1β* gene

The *LcIL-1β* cDNA was deposited in GenBank under accession number KJ459927. The sequence consisted of 1274 nucleotides (nt), with a 768-nt ORF that encoded a 255-amino acid (aa) protein with an estimated molecular weight (MW) of 2.86×10^4 and a theoretical isoelectric point (pI) of 5.6. *LcIL-1β* contained two conserved cysteine residues (Cys^{162} and Cys^{232}), which were identified by Husain et al (2012). The IL-1 family signature motif [FCL]-X-S-[ASLV]-X_2-[PSR]-X_2-[FYLIV]-[LIV]-[SCAT]-T-X_7-[LIVMK] was reasonably well conserved in the fish IL-1β, and was identified as L_{209}VSVPYNNWYISTAKENNK PL_{229} in LcIL-1β (Figure 1). The cleavage site of IL-1β converting enzyme (ICE) (also known as Caspase-1), which is highly conserved in mammalian IL-1β, has not been found in fish IL-1β (Buonocore et al, 2005). Sequence comparisons showed that LcIL-1β shared the highest amino acid identity (67.8%) with that of European seabass. Large yellow croaker IL-1β was most closely related to that of European seabass, gilthead sea bream and red sea bream (Figure 2).

The genomic DNA sequence of *LcIL-1β* was amplified, sequenced and deposited in GenBank under accession number KP057877. The exons and introns of the *LcIL-1β* gene were identified by comparison with the cDNA sequence. The genomic DNA sequence of *LcIL-1β* was comprised of three introns and four exons that spanned approximately 1.8 kb, which is the same gene structure as European seabass, Atlantic halibut and spotted green pufferfish.

Alteration of LcIL-1β mRNA expression upon *V. alginolyticus* infection

The LcIL-1β transcript exhibited constitutive expression in all tested tissues of healthy large yellow croaker, including the liver, spleen, heart, head kidney, trunk kidney, brain, intestine and gill. The highest LcIL-1β transcription level was in the head kidney, followed by the gill (Figure 3A). When fish were infected with *V. alginolyticus*, LcIL-1β transcription significantly increased in almost all tested tissues at 4 or 8 hpi compared with that of the control group (Figures 3B-I). The most significant LcIL-1β transcription upregulation was observed in the head kidney (14.1-fold) at 12 hpi, followed by the gill (12.3-fold) at 24 hpi (Figure 3).

Prokaryotic expression, purification and refolding of rLcIL-1β

After IPTG induction, a protein band of expected MW (approximately 3.10×10^4: including intact LcIL-1β and an N-terminal histidine-tag) was observed by SDS-PAGE (Figure 4A). The purifying (Figure 4B) and refolding (Figure 4C) peaks were analyzed by SDS-PAGE (Figure 4D).

Effect of rLcIL-1β on survival rate of *V. alginolyticus*-infected fish

Under pathogen challenge, the 0.01 μg/g rLcIL-1β-treated group showed the highest survival rate out of all treatment groups. The survival rate of rLcIL-1β-treated fish was 30% in the group given 0.01 μg/g rLcIL-1β. However, at 0.1 μg/g rLcIL-1β, the survival rate appeared to be marginally inhibited. This mirrors the pattern previously described in rainbow trout *in vitro*, where IL-1 receptor saturation and/or receptor sensitization were suggested as possible mechanisms for post-optimal inhibition (Hong et al, 2003; Peddie et al, 2001). The 0.001 μg/g rLcIL-1β-treated group showed no significant increase in survival rate compared with the PBS-treated group, in which all fish were dead by day 6 (Figure 5).

Effect of rLcIL-1β on bacterial load in *V. alginolyticus*-infected fish

The plate count method was employed to assay bacterial load (Li et al, 2014). *Vibrio alginolyticus* was undetectable in the liver, spleen, kidney and blood of healthy fish. The number of CFU per 0.1 g of tissue or per 0.1 mL of blood in *V. alginolyticus*-infected fish is shown in Figure 6. Compared with the PBS-treated group, the 0.01 and 0.1 μg/g rLcIL-1β-treated groups both showed significant reductions in bacterial load in the liver, spleen, kidney and blood, while the 0.001 μg/g rLcIL-1β-treated group showed only a small amount of variation *(*Figure *6)*. The 0.01 μg/g rLcIL-1β-treated group achieved the best capacity for bacterial clearance in tissues. The bacterial loads in the liver, spleen, kidney and blood from the 0.01μg/g rLcIL-1β-treated group were 47±7, 17±2 and 126±23 CFU/0.1 g and 214±49 CFU/0.1 mL, respectively. For the control, the bacterial loads in the liver, spleen, kidney and blood from the PBS-treated group were 457±104, 1 202±198 and 1 862±289 CFU/0.1 g and 4 898 ±691 CFU/0.1 mL, respectively.

Effect of rLcIL-1β on MO/MΦ chemotaxis, phagocytosis and bactericidal activity

The refolded rLcIL-1β showed a dose-dependent chemotaxis activity to attract large yellow croaker MO/MΦ. The chemotactic index increased with increasing concentrations of refolded rLcIL-1β, showing a chemotactic index peak and reaching a maximum of 2.1 at 0.01 μg/mL (Figure 7A). In contrast, the denatured rLcIL-1β and BSA did not show evident chemotaxis activity. The phagocytosis ability of large yellow croaker MO/MΦ was significantly enhanced to approximately 1.6-fold after treatment with 0.01 μg/mL rLcIL-1β relative to that of treatment with PBS (Figure 7B). Moreover, a 0.001 or 0.1 μg/mL dose of rLcIL-1β also increased phagocytosis ability. Bacterial survival was determined by the CFU counting method to

assess the bacterial killing of large yellow croaker MO/MΦ (Figure 7C). Incubation with rLcIL-1β at 0.01 μg/mL significantly decreased bacterial survival to approximately 61% of treatment with PBS.

DISCUSSION

IL-1β, which is the first characterized interleukin, plays a key role in regulating the fish immune response. In the present study, we determined the cDNA and genomic DNA sequences of an *IL-1β* gene from large yellow croaker. *LcIL-1β* had typical sequence characteristics of the animal IL-1 family (Angosto et al, 2013). Sequence comparisons and phylogenetic tree analysis both confirmed LcIL-1β to be a distinct member of the fish IL-1β family (Husain et al, 2012). In mammals, ICE specifically cleaves IL-1β after residue Asp (Asp[116] in humans and Asp[117] in mice, respectively), yielding a C-terminal secreted active form (Reis et al, 2012). However, this ICE cleavage site

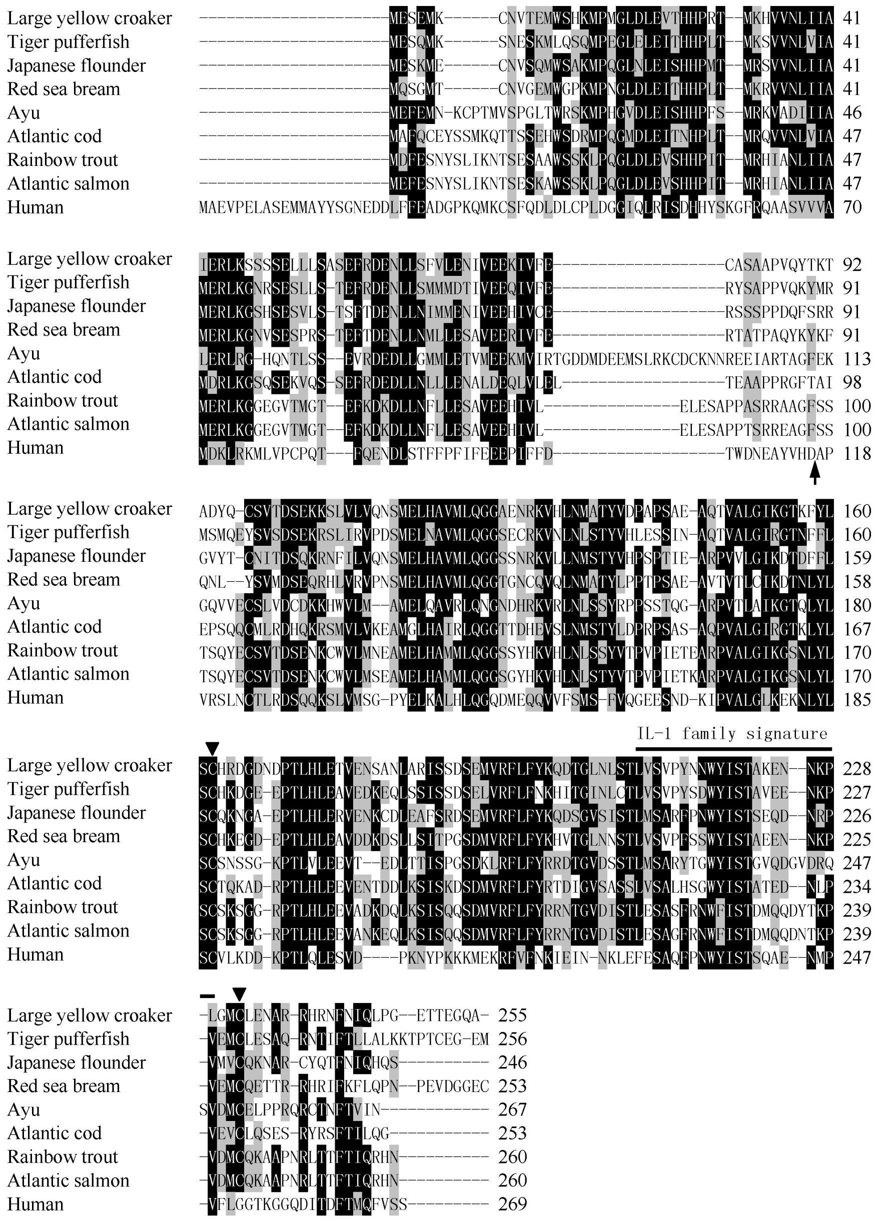

Figure 1 Multiple alignment of the LcIL-1β amino acid sequence with that of other related animal IL-1β sequences

Similar residues are marked with gray shading and identical residues with black shading. The ICE site in humans is indicated with an arrow. Two conserved cysteine residues are marked by "▼", and the IL-1 family signature is lined above the alignment. Accession numbers of sequences are provided in Table 1.

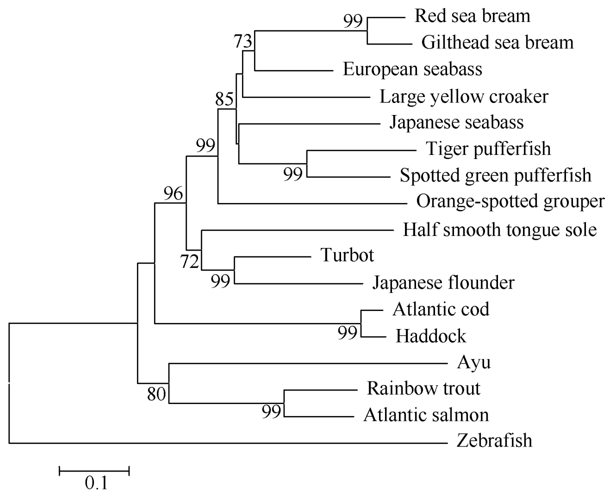

Figure 2 Phylogenetic tree analysis of IL-1β amino acid sequences of large yellow croaker and some related fish using the neighbor-joining method

The values at the forks indicate the percentage of trees in which this grouping occurred after bootstrapping the data (1 000 replicates; shown only when >60%). Scale bar shows number of substitutions per base. Accession numbers of sequences are provided in Table 1.

is not found in any known fish IL-1β, suggesting that fish Il-1β is possibly activated by another mechanism.

In teleosts, the tissue expression profile of IL-1β in healthy fish varies greatly in different species. For example, in half smooth tongue sole (*Cynoglossus semilaevis*) and ayu, high expression of IL-1β was observed in the head kidney, spleen and gill (Yu et al, 2012; Lu et al, 2013), but was not detected at all in haddock (*Melanogrammus aeglefinus*) (Corripio-Miyar et al, 2007). In this study, strong expression of LcIL-1β was observed in the head kidney and gill, similar to that reported in half smooth tongue sole and ayu. Previous studies have also revealed that IL-1β mRNA expression can be dramatically induced in fish upon bacterial infection (Cai et al, 2004; Lu et al, 2013). For example, *Yersinia ruckeri* infection significantly increased (thousand-fold) IL-1β transcription in the spleen of rainbow trout (Wang et al, 2009). The present study showed that *V. alginolyticus* infection induced the mRNA expression of LcIL-1β in all tested tissues of large yellow croaker, consistent with previous reports. This suggests that LcIL-1β was involved in the acute inflammatory response of these fish.

Recently, recombinant IL-1β (rIL-1β) was proven effective in promoting disease resistance in some fish (Hong et al, 2003; Buonocore et al, 2005). In rIL-1β-injected common carp, an increase in resistance to *Aeromonas hydrophila* infection was found compared with that of the control group (Kono et al, 2002).

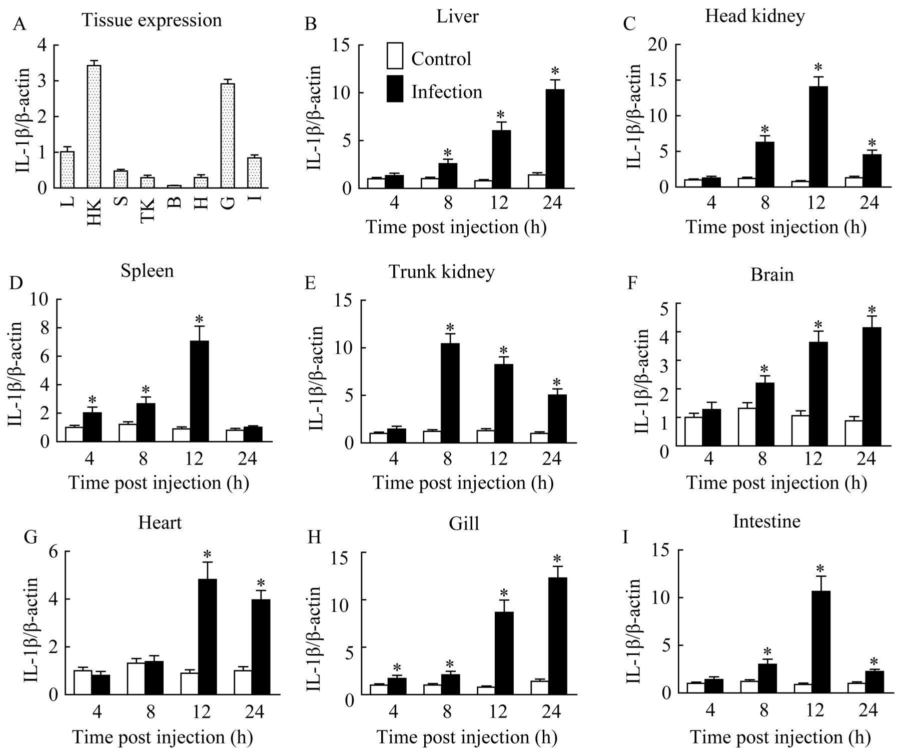

Figure 3 QPCR analysis of the relative mRNA expression of LcIL-1β in different tissues of healthy (A) and *V. alginolyticus*-challenged large yellow croaker (B-I)

A: tissue expression profile of LcIL-1β in healthy fish. L: liver; HK: head kidney; S: spleen; TK: trunk kidney; B: brain; H: heart; G: gill; I: intestine. Results from three fish are expressed as means±*SEM*. *: *P*<0.05 versus PBS group.

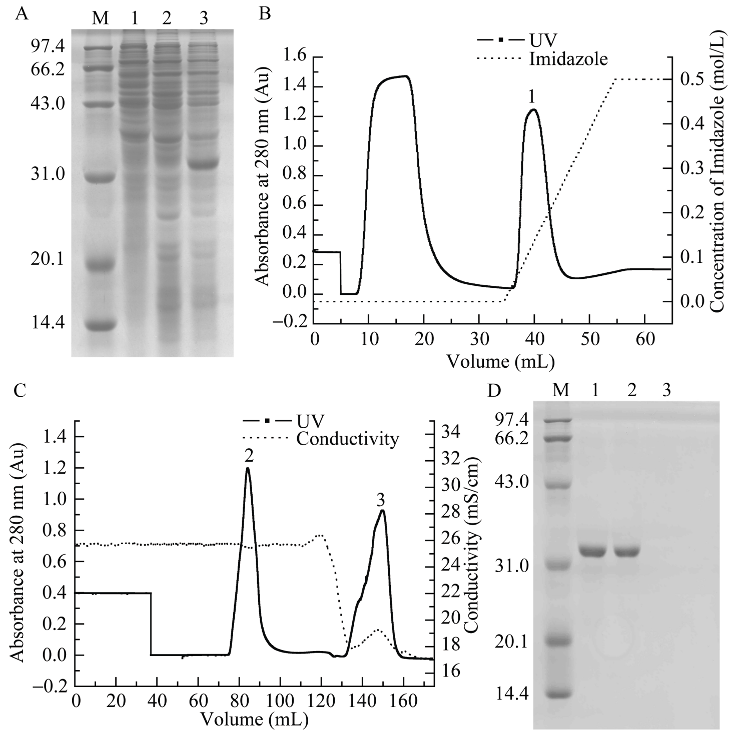

Figure 4 Prokaryotic expression, purification and refolding of rLcIL-1β

A: Bacterial lysates were electrophoresed on 12% SDS-PAGE gels. Lane M: protein marker; 1: *E. coli* BL21 (DE3) transformed with pET28a after IPTG induction; 2: *E. coli* BL21 (DE3) transformed with pET28a-LcIL-1β before IPTG induction; 3: *E. coli* BL21 (DE3) transformed with pET28a-LcIL-1β after IPTG induction. B: His affinity chromatography purification of rLcIL-1β using His Trap™ FF Crude column. C: Refolding of rLcIL-1β using urea gradient gel filtration on a Superdex 75 column. D: SDS-PAGE analysis of peaks in B and C. Lane M: protein marker; Lane 1: peak 1; 2: peak 2; 3: peak 3.

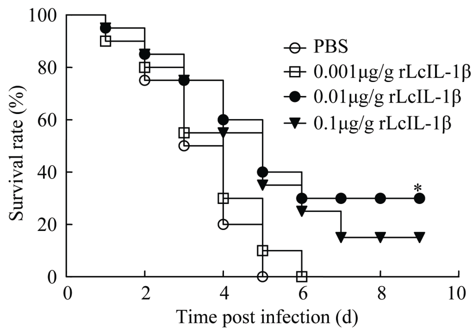

Figure 5 Effect of different doses of rLcIL-1β on the survival rate of *V. alginolyticus*-infected large yellow croaker

Fish (20 in each group) were i.p.injected with *V. alginolyticus* (6.5×10^4 CFU/g). At 0.5 hpi, 0.001, 0.01 or 0.1 μg/g rLcIL-1β was i.p.injected into fish, respectively. The control group received an equal volume of PBS. Fish were monitored for signs of sickness and mortality every 24 h for 9 days. Group survival rates for each treatment were analyzed by the Log-rank test. *: P<0.05 versus PBS-treated group.

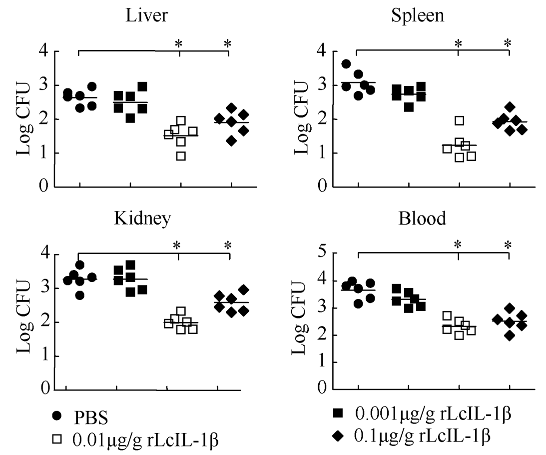

Figure 6 Effect of different doses of rLcIL-1β on bacterial loads in immune tissues and blood of large yellow croaker

Fish (6 in each group) were i.p.-injected with *V. alginolyticus* (6.5×10^4 CFU/g) and received 0.001, 0.01 or 0.1 μg/g of rLcIL-1β at 0.5 hpi, respectively. The control group received an equal volume of PBS. Fish were euthanized at 72 h post treatment of rLcIL-1β. Liver, spleen, kidney, and blood samples were collected. Homogenates and blood were cultured on TCBS agar plates. Colony numbers were normalized to volume (0.1 mL for blood) and tissue weight (0.1 g for liver, spleen and kidney). *: P<0.05 versus PBS-treated group.

In rainbow trout, i.p. injection of rIL-1β (starting at Ala[95]) prior to infection with *A. salmonicida* significantly reduced fish mortality (Hong et al, 2003). In this study, *V. alginolyticus*-infected large yellow croaker i.p. injected with a dose of 0.01 μg/g

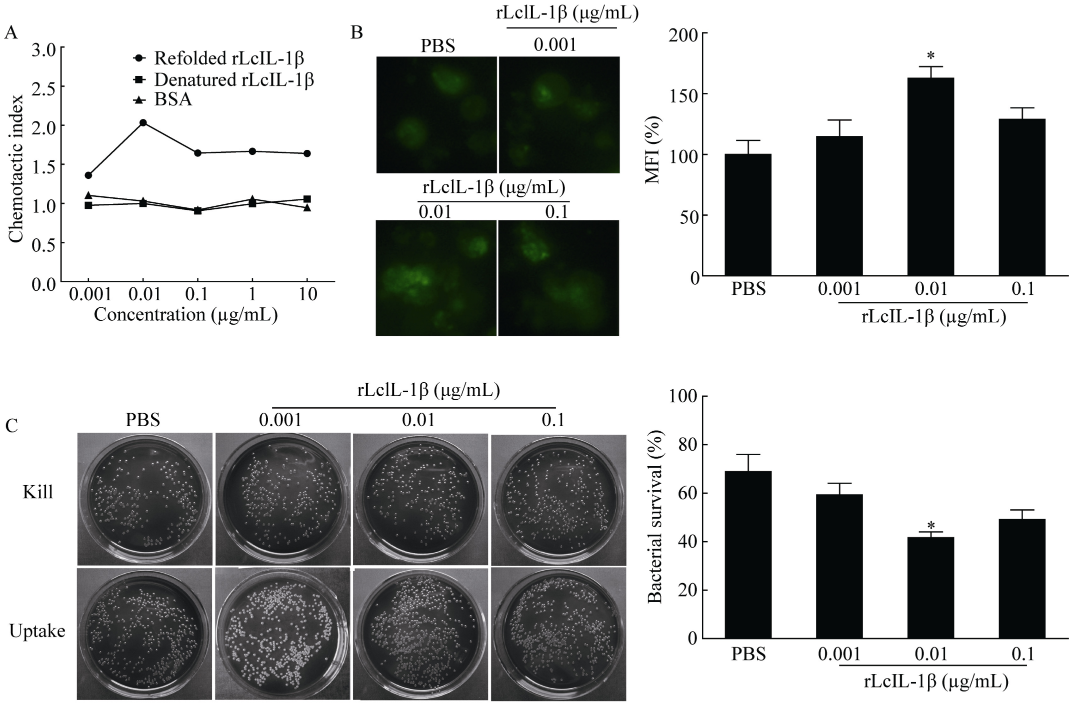

Figure 7 Effect of rLcIL-1β on MO/MΦ chemotaxis, phagocytosis and bactericidal activity

A: Dose-response relationship of refolded rLcIL-1β to attract large yellow croaker MO/MΦ. Denatured rLcIL-1β and BSA were used as controls. B: Fluorescence images of phagocytosis of FITC-DH5α in MO/MΦ treated with rLcIL-1β. Histogram represents mean fluorescence intensity (MFI) percentage of bacteria engulfed by cells. Magnification ratio: 400X. C: Plates display survival *V. alginolyticus* from MO/MΦ treated with rLcIL-1β. Histogram demonstrates effects of rLcIL-1β on bacterial killing. Data are representative of at least three independent experiments. *: $P<0.05$ versus PBS-treated group.

intact rLcIL-1β at 0.5 h following bacterial infection exhibited a survival rate of 30%, while all control fish died. The tissue bacterial load of rLcIL-1β-treated fish decreased significantly.

Research has shown that rIL-1β can induce cell migration (Ebisawa et al, 1992; Carrero et al, 2012) as well as increase phagocytosis and the bactericidal activity of leucocytes (Hong et al, 2003; Peddie et al, 2002). In humans, rIL-1β treatment induced significant migration of eosinophils (4 h, 5 ng/mL) (Ebisawa et al, 1992) and macrophages (4 h, 25 ng/mL) (Carrero et al, 2012). A rainbow trout IL-1β derived peptide, P3 (0.25 mM), enhanced phagocytosis and bactericidal activity of head kidney leucocytes *in vitro* (Peddie et al, 2001; Peddie et al, 2002). In the present study, the refolded rLcIL-1β showed chemotaxis activity to attract large yellow croaker MO/MΦ. The higher doses used (0.1, 1 and 10 μg/mL) were significantly less stimulatory, potentially attributable to rLcIL-1β toxicity for cells at this concentration or to receptor saturation (Buonocore et al, 2005). Incubation with 0.01 μg/mL rLcIL-1β demonstrated significant phagocytosis and bactericidal activity. This dose-response is consistent with that noted in humans (Ebisawa et al, 1992), rainbow trout (Hong et al, 2001) and European seabass (Buonocore et al, 2005).

IL-1β can induce the expression of macrophage-derived chemokine (MDC), which is involved in regulating leucocyte migration (Rodenburg et al, 1998) and enhancing phagocytosis and bactericidal activity of peritoneal macrophages (Matsukawa et al, 2000). IL-1β can also reduce pH and lead to acidification in alveolar macrophage endosomes, which is critical for the activation of cysteine proteases involved in bacterial degradation (Bird et al, 2009; Descamps et al, 2012). These results indicate that LcIL-1β[0] could play an important role in phagocytosis and bactericidal activity of large yellow croaker MO/MΦ.

In conclusion, we characterized an *IL-1β* gene in large yellow croaker, which was tightly involved in the fish innate immune response. Animal experiments showed that even full length rLcIL-1β treatment could increase the survival rate and decrease bacterial load in fish following bacterial infection. It could also induce cell migration and increase phagocytosis and bactericidal activity of MO/MΦ *in vitro*.

REFERENCES

Angosto D, Montero J, López-Muñoz A, Alcaraz-Pérez F, Bird S, Sarropoulou E, Abellán E, Meseguer J, Sepulcre MP, Mulero V. 2013. Identification and functional characterization of a new IL-1 family member, IL-1Fm2, in most evolutionarily advanced fish. *Innate Immunity,* **20**(5): 487-500.

Bird PI, Trapani JA, Villadangos JA. 2009. Endolysosomal proteases and their inhibitors in immunity. *Nature Reviews Immunology,* **9**(12): 871-882.

Buonocore F, Forlenza M, Randelli E, Benedetti S, Bossù P, Meloni S, Secombes CJ, Mazzini M, Scapigliati G. 2005. Biological activity of sea

bass (*Dicentrarchus labrax* L.) recombinant interleukin-1β. *Marine Biotechnology,* **7**(6): 609-617.

Cai ZH, Song LS, Gao CP, Wu LT, Qiu LH. 2004. Molecular cloning and expression of interleukin 1 beta (IL-1β) from red sea bream (*Pagrus major*). *Progress in Natural Science,* **14**(5): 396-402.

Carrero R, Cerrada I, Lledó E, Dopazo J, García-García F, Rubio MP, Trigueros C, Dorronsoro A, Ruiz-Sauri A, Montero JA, Sepúlveda P. 2012. IL1β induces mesenchymal stem cells migration and leucocyte chemotaxis through NF-κB. *Stem Cell Reviews and Reports,* **8**(3): 905-916.

Chen J, Chen Q, Lu XJ, Li CH. 2014. LECT2 improves the outcomes in ayu with *Vibrio anguillarum* infection via monocytes/macrophages. *Fish and Shellfish Immunology,* **41**(2): 586-592.

Chen XH, Lin KB, Wang XW. 2003. Outbreaks of an iridovirus disease in maricultured large yellow croaker, *Larimichthys crocea* (Richardson), in China. *Journal of Fish Diseases*, **26**(10): 615-619.

Corripio-Miyar Y, Bird S, Tsamopoulos K, Secombes CJ. 2007. Cloning and expression analysis of two pro-inflammatory cytokines, IL-1β and IL-8, in haddock (*Melanogrammus aeglefinus*). *Molecular Immunology,* **44**(6): 1361-1373.

Descamps D, Le Gars M, Balloy V, Barbier D, Maschalidi S, Tohme M, Chignard M, Ramphal R, Manoury B, Sallenave JM. 2012. Toll-like receptor 5 (TLR5), IL-1β secretion, and asparagine endopeptidase are critical factors for alveolar macrophage phagocytosis and bacterial killing. *Proceedings of the National Academy of Sciences of the United States of America,* **109**(5): 1619-1624.

Ebisawa M, Bochner BS, Georas SN, Schleimer RP. 1992. Eosinophil transendothelial migration induced by cytokines. I. Role of endothelial and eosinophil adhesion molecules in IL-1 beta-induced transendothelial migration. *The Journal of Immunology,* **149**(12): 4021-4028.

Fujiki K, Shin DH, Nakao M, Yano T. 2000. Molecular cloning and expression analysis of carp (*Cyprinus carpio*) interleukin-1β, high affinity immunoglobulin E Fc receptor γ subunit and serum amyloid A. *Fish and Shellfish Immunology,* **10**(3): 229-242.

Hong S, Peddie S, Campos-Pérez JJ, Zou J, Secombes CJ. 2003. The effect of intraperitoneally administered recombinant IL-1β on immune parameters and resistance to *Aeromonas salmonicida* in the rainbow trout (*Oncorhynchus mykiss*). *Developmental and Comparative Immunology,* **27**(9): 801-812.

Hong S, Zou J, Crampe M, Peddie S, Scapigliati G, Bols N, Cunningham C, Secombes CJ. 2001. The production and bioactivity of rainbow trout (*Oncorhynchus mykiss*) recombinant IL-1β. *Veterinary Immunology and Immunopathology,* **81**(1-2): 1-14.

Husain M, Bird S, Van Zwieten R, Secombes CJ, Wang T. 2012. Cloning of the IL-1β3 gene and IL-1β4 pseudogene in salmonids uncovers a second type of IL-1β gene in teleost fish. *Developmental and Comparative Immunology,* **38**(3): 431-446.

Kono T, Fujiki K, Nakao M, Yano T, Endo M, Sakai M. 2002. The immune responses of common carp, *Cyprinus carpio* L., injected with carp interleukin-1β gene. *Journal of Interferon & Cytokine Research,* **22**(4): 413-419.

Li HX, Lu XJ, Li CH, Chen J. 2014. Molecular characterization and functional analysis of two distinct liver-expressed antimicrobial peptide 2 (LEAP-2) genes in large yellow croaker (*Larimichthys crocea*). *Fish and Shellfish Immunology,* **38**(2): 330-339.

Li SY, Ao JQ, Chen XH. 2009. Molecular and functional characterization of a cystatin analogue in large yellow croaker (*Pseudosciaena crocea*). *Molecular Immunology,* **46**(8-9): 1638-1646.

Lu XJ, Chen J, He YQ, Shi YH. 2013. Molecular characterization of an IL-1β gene from ayu, *Plecoglossus altivelis*. *Fish and Shellfish Immunology,* **34**(5): 1253-1259.

Matsukawa A, Hogaboam CM, Lukacs NW, Lincoln PM, Evanoff HL, Kunkel SL. 2000. Pivotal role of the CC chemokine, macrophage-derived chemokine, in the innate immune response. *The Journal of Immunology,* **164**(10): 5362-5368.

Mu YN, Wan X, Lin KB, Ao JQ, Chen XH. 2013. Liver proteomic analysis of the large yellow croaker (*Pseudosciaena crocea*) following polyriboinosinic: polyribocytidylic acid induction. *Fish Physiology and Biochemistry,* **39**(5): 1267-1276.

Peddie S, Zou J, Cunningham C, Secombes CJ. 2001. Rainbow trout (*Oncorhynchus mykiss*) recombinant IL-1β and derived peptides induce migration of head-kidney leucocytes *in vitro*. *Fish and Shellfish Immunology,* **11**(8): 697-709.

Peddie S, Zou J, Secombes CJ. 2002. A biologically active IL-1β derived peptide stimulates phagocytosis and bactericidal activity in rainbow trout, *Oncorhynchus mykiss* (Walbaum), head kidney leucocytes *in vitro*. *Journal of Fish Diseases,* **25**(6): 351-360.

Reis MIR, Do Vale A, Pereira PJ, Azevedo JE, Dos Santos NM. 2012. Caspase-1 and IL-1β processing in a teleost fish. *PLoS One,* **7**(11): e50450.

Rodenburg RJ, Brinkhuis RF, Peek R, Westphal J, Van Den Hoogen FH, Van Venrooij WJ, Van De Putte LB. 1998. Expression of macrophage-derived chemokine (MDC) mRNA in macrophages is enhanced by interleukin-1β, tumor necrosis factor alpha, and lipopolysaccharide. *Journal of Leukocyte Biology,* **63**(5): 606-611.

Scapigliati G, Buonocore F, Bird S, Zou J, Pelegrin P, Falasca C, Prugnoli D, Secombes CJ. 2001. Phylogeny of cytokines: molecular cloning and expression analysis of sea bass *Dicentrarchus labrax* interleukin-1β. *Fish and Shellfish Immunology,* **11**(8): 711-726.

Tamura K, Peterson D, Peterson N, Stecher G, Nei M, Kumar S. 2011. MEGA5: Molecular evolutionary genetics analysis using maximum likelihood, evolutionary distance, and maximum parsimony methods. *Molecular Biology and Evolution,* **28**(10): 2731-2739.

Wang TH, Bird S, Koussounadis A, Holland JW, Carrington A, Zou J, Secombes CJ. 2009. Identification of a novel IL-1 cytokine family member in teleost fish. *The Journal of Immunology,* **183**(2): 962-974.

Yu Y, Zhong QW, Li CM, Jiang LM, Sun YY, Wang XB, Wang ZG, Zhang QQ. 2012. Molecular cloning and characterization of interleukin-1β in half-smooth tongue sole *Cynoglossus semilaevis*. *Veterinary Immunology and Immunopathology,* **146**(3-4): 270-276.

Zhang RC, Chen J, Li CH, Lu XJ, Shi YH. 2011. Prokaryotic expression, purification, and refolding of leukocyte cell-derived chemotaxin 2 and its effect on gene expression of head kidney-derived macrophages of a teleost fish, ayu (*Plecoglossus altivelis*). *Fish and shellfish Immunology,* **31**(6): 911-918.

Zou J, Grabowski PS, Cunningham C, Secombes CJ. 1999. Molecular cloning of interleukin 1β from rainbow trout *Oncorhynchus mykiss* reveals no evidence of an ICE cut site. *Cytokine,* **11**(8): 552-560.

ZOOLOGICAL RESEARCH

Selective recruitment of host factors by HSV-1 replication centers

Feng-Chao LANG[1,2], Xin LI[1,2], Olga VLADMIROVA[3], Zhuo-Ran LI[1,2], Gui-Jun CHEN[1], Yu XIAO[1], Li-Hong LI[1], Dan-Feng LU[1,2], Hong-Bo HAN[4], Ju-Min ZHOU[1,*]

[1] *Key Laboratory of Animal Models and Human Disease Mechanisms of Chinese Academy of Sciences & Yunnan Province, Kunming Institute of Zoology, Chinese Academy of Sciences, Kunming Yunnan* 650223, *China*

[2] *University of Chinese Academy of Sciences, Beijing* 100049, *China*

[3] *The Wistar Institute, Gene Expression and Regulation Program, Philadelphia PA* 19104, *USA*

[4] *Biology & Chemistry Engineering College, Panzhihua University, Panzhihua Sichuan* 617000, *China*

ABSTRACT

Herpes simplex virus type 1 (HSV-1) enters productive infection after infecting epithelial cells, where it controls the host nucleus to make viral proteins, starts viral DNA synthesis and assembles infectious virions. In this process, replicating viral genomes are organized into replication centers to facilitate viral growth. HSV-1 is known to use host factors, including host chromatin and host transcription regulators, to transcribe its genes; however, the invading virus also encounters host defense and stress responses to inhibit viral growth. Recently, we found that HSV-1 replication centers recruit host factor CTCF but exclude γH2A.X. Thus, HSV-1 replication centers may selectively recruit cellular factors needed for viral growth, while excluding host factors that are deleterious for viral transcription or replication. Here we report that the viral replication centers selectively excluded modified histone H3, including heterochromatin mark H3K9me3, H3S10P and active chromatin mark H3K4me3, but not unmodified H3. We found a dynamic association between the viral replication centers and host RNA polymerase II. The centers also recruited components of the DNA damage response pathway, including 53BP1, BRCA1 and host antiviral protein SP100. Importantly, we found that ATM kinase was needed for the recruitment of CTCF to the viral centers. These results suggest that the HSV-1 replication centers took advantage of host signaling pathways to actively recruit or exclude host factors to benefit viral growth.

Keywords: HSV-1; CTCF; γH2AX; Viral replication cente; RNA Pol II

INTRODUCTION

Herpes simplex virus type I (HSV-1) belongs to the herpes family of DNA viruses, and infects numerous cell types during the productive phase of infection, but enters latency in neuronal cells. HSV-1 infects more than 80% of the population (Roizman & Whitley, 2013), and when activated from latency, it is responsible for oral and genital herpes, keratitis and in rare but often fatal cases, herpes encephalitis (Knipe & Howley, 2007). HSV-2 is similar to HSV-1 in genome and there is common co-infection in HIV-1 infected people (Lai et al, 2003; Zhou et al, 2014).

The outcome of HSV-1 infection is determined by complex interactions between the virus and the host cell and immune system. At a cellular level, the incoming virus first releases its linear DNA into the nucleus, which quickly circularizes and becomes chromatinized (Conn & Schang, 2013). With the help of tegument proteins ICP0 and VP16 (Wysocka & Herr, 2003) and host transcription machinery, HSV-1 starts transcribing the viral genome, first the immediate early genes (IE) and then the early genes (E), to prepare viral DNA synthesis and modify host responses. With the onset of viral DNA replication, the virus also makes late genes and finally assembles viral particles (Everett, 2014; Knipe & Howley, 2007). Viral replication usually occurs about 6 hours post infection (hpi). Replicating viral genomes first appear at pre-replication centers marked by viral protein ICP8 (Knipe et al, 1982), a single strand DNA binding

Received: 09 March 2015; Accepted: 09 April 2015

Foundation items: This work was supported by grants from the Yunnan Provincial Government (2013FA051; 2011HA005), the National Science Foundation of China (NSFC 81471966 to JZ and NSFC 31200964 to YX), and the common project of the Panzhihua Science and Technology Bureau from China (2012CY-S-22(9) to HH)

[*]Corresponding author, E-mail: zhoujm@mail.kiz.ac.cn

protein, and then gradually form distinct replication centers or compartments. These centers grow quickly in size and finally merge into larger regions occupying much of the cellular nucleus. Unlike the viral genome during the pre-replication stage, the rapidly replicating HSV-1 genome is only partially chromatinized (Lacasse & Schang, 2010, 2012).

The incoming virus triggers a number of host responses, including activation of the interferon pathway (Griffiths et al, 2013; Lafaille et al, 2012; Shen et al, 2014), DNA damage response (Lilley et al, 2011; Smith et al, 2014; Volcy & Fraser, 2013), apoptosis (Prasad et al, 2013; Wang et al, 2011) and other host defense mechanisms that limit viral growth. Many viral genes are designed to deal with these host responses to ensure viral transcription, genome synthesis and assembly. For example, the viral protein ICP34.5 is a key viral factor that interferes with the interferon γ pathway (Pasieka et al, 2006; Rasmussen et al, 2011; Wang et al, 2014). Likewise, the viral IE protein ICP0 can quickly counter host transcription silencing of PML, SP100, RNF8 and RNF168 activity by degrading these proteins, and prevent host silencing complex CoREST from inhibiting viral genes (Ferenczy et al, 2011; Roizman, 2011; Wang et al, 2012). HSV-1 can also produce viral-host shutoff (VHS) factor to degrade host mRNAs (Barzilai et al, 2006; Esclatine et al, 2004; Taddeo et al, 2006, 2013), while viral protein ICP27 can inhibit host mRNA splicing (Nojima et al, 2009; Sedlackova et al, 2008), thus reducing cellular protein synthesis.

During lytic infection, the interactions between the incoming virus and the host are dynamic and complex, with well-organized viral replication centers. Indeed several proteins have been implicated in the organization of the replication centers. Nuclear lamin A, a structure protein playing an essential role in the organization of the host nucleus, is important for HSV-1 replication center organization (Silva et al, 2008) and host transcription regulator HCF-1 is needed for proper replication center formation (Peng et al, 2010). The host DNA damage response (DDR), in particular, has an intriguing interaction with replicating HSV-1. The incoming virus firstly activates the host DDR, probably due to the linear ends of its genome, and then reactivates the host DDR during viral genome replication, which exhausts host DNA replication factors (Burke et al, 2005). The DDR recruits a number of factors to the viral replication centers, some of which are beneficiary to viral growth, including RAD51 (Wilkinson & Weller, 2004), Fanconi Anemia factor FANCD2 (Karttunen et al, 2014) and ATM (Weitzman & Weitzman, 2014), and some of which inhibit viral transcription and are harmful to viral growth (Everett & Murray, 2005; Lilley et al, 2011; Parkinson et al, 1999; Song et al, 2000; Weitzman et al, 2004), including RNF8, RNF168 and host silenced chromatin. Recent research has shown that the host chromatin mark of DNA damage sites, γH2A.X, is recruited towards the replication centers but is prevented from entering, instead forming a cage-like structure surrounding the ICP4 or ICP8 marked viral genomes (Wilkinson & Weller, 2006). This finding strongly suggests that replicating viral genomes selectively recruit or exclude host factors. Thus, examination of the selective recruitment or exclusion of host factors by the HSV-1 replication center can help illuminate new regulatory mechanisms of viral-host interactions.

Although many important details of viral-host interaction are known, how the quickly replicating virus interacts with host chromatin and host DDR is still not well understood. Thus, we analyzed the interaction of HSV-1 replication centers with host chromatin and host DDR factors. We found that host modified histones H3K9me3 and H3K4me3 were excluded from the replication centers and host RNA polymerase II (RNA Pol II) was recruited, though dynamic changes in phosphorylated RNA Pol II recruitment were observed as small replication centers began to merge. Host DDR factors 53BP1 and BRCA1 were recruited but host RNF8 was excluded. Importantly, the recruitment of host organizer CTCF was enhanced by the ATM kinase pathway. Taken together, these findings provide further evidence that viral replication centers are highly organized and actively recruit or exclude host factors to facilitate viral growth.

MATERIAL AND METHODS

Cells and virus

The BJ, HeLa, 293T and Vero cells were obtained from American Type Culture Collection. ATM+/+ and ATM-/- cells were kindly provided by Matthew Weitzman from University of Pennsylvania Perelman School of Medicine, Philadelphia. Cells were grown in Dulbecco's modified Eagle's medium (DMEM; Gibco, USA) supplemented with 10% fetal bovine serum (FBS), penicillin (100 U/mL), and streptomycin (100 μg/mL) in a humidified 5% CO_2 atmosphere at 37 °C. The HSV-1 was gifted by Professor Qi-Han LI from the Institute of Medical Biology, Chinese Academy of Medicine Science. The virus was grown and titrated on Vero cells. Viral infections were done according to standard protocols. Briefly, cultured cells were replaced with serum free DMEM, followed by adding the virus and incubating for 1 hour with occasional rotation to get an even spread. The culture medium was then replaced by regular DMEM with 10% FBS and 1% antibiotics. Cell treatment was with ATM inhibitor KU55933, with cells treated with 20 uM KU55933 for 1 hour before HSV-1 infection. During the HSV-1 infection process, KU55933 was not removed from the medium.

Antibodies

CTCF polyclonal antibodies, H3K4me3 and SP100 were made by GLS Biochem (Shanghai, China), CTCF monocle antibodies were from Millipore, Germany. Antibodies against γH2A.X, RNA Pol II Ser2P, RNA Pol II Ser5P, H3, H3K9me3, 53BP1, BRCA1, RNF8 and RNF168 were obtained from Abcam Cambridge, UK. Monoclonal antibody against ICP4 was a gift from Gerd Maul's laboratory at the Wistar Institute (Everett et al, 2004; Showalter et al, 1981). The H3S10p antibody was presented from Ping ZHENG's laboratory at the Kunming Institute of Zoology, Chinese Academy of Sciences. Alexa Fluor® 594 Goat Anti-Mouse IgG (H+L) Antibody and Alexa Fluor® 488 Goat Anti-Rabbit IgG (H+L) Antibody were from Life Technologies, USA.

Immunofluorescence

The BJ, HeLa, ATM+/+ and ATM-/- cells were seeded on glass

coverslips in 24-well plates one day before infection and used for infections at a multiplicity of infection (MOI) of 5 PFU/cell. At 5 or 6 hpi, cells were fixed with 4% paraformaldehyde at 4 °C for 60 min and extracted with 0.2% Triton X-100 in PBS for 10 min. Nuclei were visualized by staining with Hoechst 33342. Images were acquired using a Nikon 80i, Japan.

RESULTS

HSV-1 replication centers excluded modified histones

To determine how the replicating HSV-1 genomes interacted with the host chromatin, we conducted double immunostaining using an antibody against the viral protein ICP4 to label the viral replication centers and antibodies against histones in infected cells. In human primary fibroblast BJ cells, we infected with the 17+ strain of HSV-1 at an MOI of 5 and let the infection go for 6 hours, a time point when HSV-1 replication centers are well organized and recruitment or exclusion of host proteins is obvious. Due to the heterogeneity of cells and variation in the number of incoming viruses in each cell, we saw viral replication at various stages in different cells, from early small but distinct replication centers to large fused replication centers occupying most of the cellular nucleus.

We tested the localization of unmodified histone H3, modified histones H3 lysine 4 trimethylation (H3K4me3), H3 lysine 9 trimethylation (H3K9me3) and H3 serine 10 phosphorylation (H3S10p). Representative staining results are shown in Figures 1A-1D. Histone H3 did not show particular recruitment or exclusion in HSV-1 replication centers (Figure 1A). We highlighted a large replication center by dashed lines based on ICP4 staining, and the corresponding area on the H3 staining showed no difference in intensity from the surrounding areas outside the replication center (arrows). However, active chromatin mark H3K4me3 was clearly excluded from these centers (Figure 1B). We highlighted two centers with dashed circles (arrows), which indicated that the circled H3K4me3 (red) signal areas were obviously weaker than the surrounding area. In the merged image, ICP4 positive areas had little H3K4me3, confirming its exclusion. Likewise, H3K9me3, a mark of heterochromatin, was also excluded by replicating HSV-1 genomes. In Figure 1C, the dashed circle of the fused replication center (arrow) shows a reduction in the H3K9me3 signal, and the merged image shows mostly ICP4. Finally, we tested the serine10 phosphorylated form of histone H3, and found that in infected cells, H3S10p appeared to form clusters of staining signals and did not usually overlap with the ICP4 signals, although they appeared in close proximity in many cases, as shown in Figure 1D (arrows).

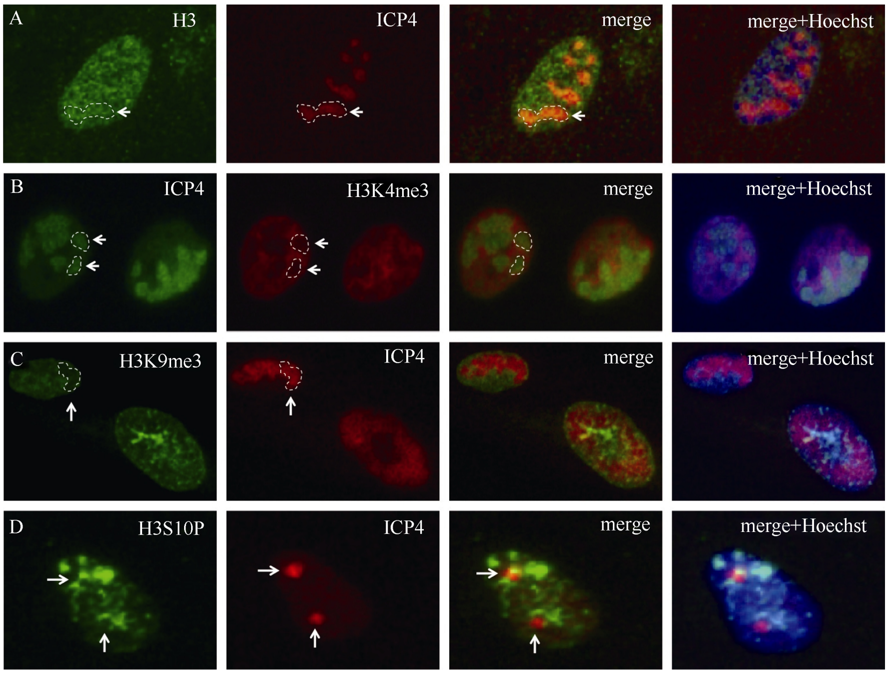

Figure 1 Recruitment or exclusion of histone and modified histone with HSV-1 replication centers

All cells were infected with HSV-1 at MOI=5 or 6 hours before fixing for immunofluorescent staining. In each row, cells were stained with two different antibodies, and images were merged to examine how the staining signals related to viral replication centers. A**:** Double staining with histone H3 (green) and ICP4 (red) antibodies. B**:** Double staining using ICP4 (red) and modified histone H3K4me3 (green). White arrows point to two of the viral replication centers, where H3K4me3 is very weak compared with the surrounding area. Merged images show green viral foci areas, suggesting a lack of red signal in the same area. C**:** Double staining with modified histone H3K9me3 (green) and ICP4 (red). Dashed circle shows part of a large fused replication center, where H3K9me3 is excluded. D**:** Cells double stained by modified histone H3S10P (green) and ICP4 (red). Arrows point to two distinct replication centers. H3S10P shows large clustered staining, which does not overlap with ICP4. Magnification ratio: 400X.

RNA polymerase II showed dynamic interaction with replicating viral genome

RNA Pol II is known to interact with replicating viruses and is highly phosphorylated in virally infected cells (Egloff & Murphy, 2008; Jenkins & Spencer, 2001). However, how dynamic RNA Pol II interacts with the HSV-1 genome as the virus transits from transcription to replication at 6 hpi is not known. To understand this dynamic interaction, we conducted double staining of ICP4 and RNA Pol II (Figure 2A). The ICP4 labeled early replication centers were colocalized with the RNA Pol II signal (orange arrows), with merged staining showing colocalization. We then stained antibodies specifically recognizing the serine 2 phosphorylated (Ser2P) form of RNA Pol II, which marks the elongating form of RNA polymerase (Kwak & Lis, 2013; Zhou et al, 2012). Figure 2B shows two infected cells, the left cell contains several distinct replication centers and the right cell contains large well-developed centers. Ser2P was recruited by smaller to intermediate sized replication centers (orange arrows), but not by large, well-developed centers (white arrows). This demonstrated that the elongating form of RNA Pol II associated more with early replicating viral genomes, but less with genomes in fully developed replication centers. We next examined the recruitment of serine 5 phosphorylated RNA Pol II. Similar to RNA Pol II Ser2P, the RNA Pol II Ser5P signal was also recruited to viral centers, but much more strongly (comparing orange arrows in Figures 2B and 2C), an observation consistent with reports that viral factor ICP22 degrades RNA Pol II Ser2P (Fraser & Rice, 2007; Zaborowska et al, 2014). In the present study, RNA Pol II Ser5P was recruited into viral centers in both early individual foci and late fused foci, although there was a drop in intensity in the RNA Pol II Ser5P signal in later fused replication centers. This could be seen by comparing orange arrows (marking individual viral center) with white arrows (well-developed, fused center), and the merged images in Figure 2C. The merged image shows that the smaller individual replication centers were mostly green and the large fused foci were orange, suggesting that the former had more RNA Pol II Ser5P than the latter. This result showed a reduction in RNA Pol II recruitment in fully developed replicating centers. Taken together, these findings suggest that active transcription occurred in smaller replication centers, but not in large fused ones.

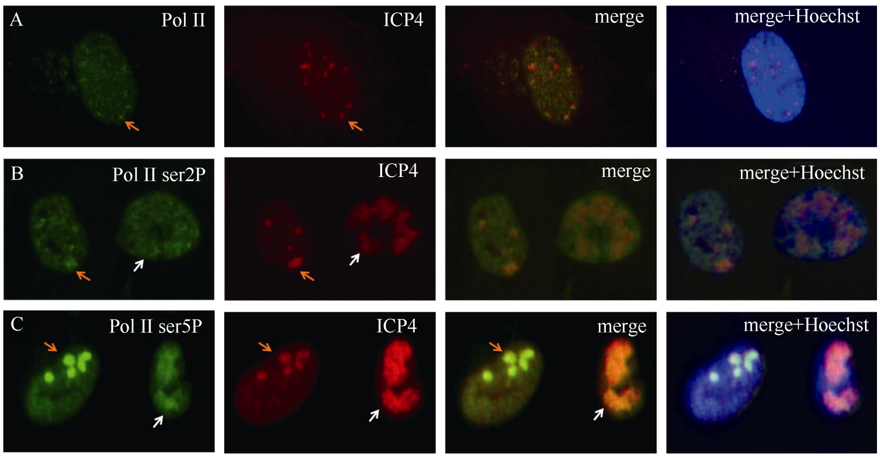

Figure 2 Recruitment of RNA Pol II by replicating HSV-1

BJ cells were infected with HSV-1 for 6 hours at MOI=5 and fixed for immunostaining. A. Double staining using ICP4 (red) and RNA Pol II (green) antibodies showing recruitment of total RNA Pol II to ICP4 labeled HSV-1 replication centers. B: Double staining using ICP4 (red) and Ser2 phosphorylated RNA Pol II (green) antibodies. Orange arrows show a well-defined replication center. White arrows show large fused replication centers. C: Immunostaining with ICP4 antibody (red) highlighting viral replication centers and Ser5 phosphorylated RNA Pol II antibody (green) showing paused RNA polymerase. Orange arrows indicate a cluster of well-defined replication centers, white arrows indicate late stage fused replication centers. Magnification ratio: 400X.

Interaction between HSV-1 replication centers and DDR factors

To determine the potential interaction of DDR factors with the replicating viral genome, we surveyed four DDR factors, 53BP1, BRCA1, RNF8 and RNF168, using immunofluorescent staining. 53BP1 is a key DNA damage repair factor involved in nonhomologous end joining (NHEJ) double strand break (DSB) repair (Taylor & Knipe, 2004; Weitzman & Weitzman, 2014). Only a few studies have explored whether 53BP1 plays a role in DNA virus infection (Bailey et al, 2009; Salsman et al, 2012). BRCA1 is another key regulator of host DDR and mediates a homologous recombination type of DSB repair (Yun & Hiom, 2009), though its role in HSV-1 infection has not yet been established. RNF8 and RNF168 are two essential ubiquitin ligases needed to modify histones and other DDR factors during DNA damage repair (Lilley et al, 2010; Mattiroli et al, 2012). They are reported to restrict HSV-1 infection (Mattiroli et al, 2012), however, how RNF8 and RNF168 relate to HSV-1 replication centers is not known. To characterize the relationship between viral replication centers and these DDR factors, we double stained using CTCF or ICP4 to label the viral replication centers.

CTCF can be recruited to the HSV-1 replication compartment and colocalized with ICP4 (Figures 4C and 4E). However,

because some commercial antibodies are not compatible with ICP4 (for example, mouse derived 53BP1 antibody and ICP4), we used rabbit derived CTCF antibody to label HSV-1 replication centers in certain experiments. As shown in Figure 3A, the 53BP1 and CTCF signals colocalized quite well, suggesting that 53BP1 was recruited by the viral centers. Similarly, BRCA1 was also recruited by these centers (Figure 3B, arrows), although the staining signals were weaker. Conversely, RNF8 was excluded by the HSV-1 replication centers. We circled two well-defined replication centers with dashed lines (Figure 3C, white arrows), which shows much weaker RNF8 signals compared with ICP4. RNF168 staining was too weak to determine recruitment or exclusion. The weak RNF168 signal was probably due to degradation by the viral ICP0 protein (Chaurushiya et al, 2012; Lilley et al, 2010). In contrast to the results of Lilley et al (2010), RNF8 showed less degradation than RNF168, as seen in Figures 3C and 3D. This may be due to differences between the cell line, antibody and infection period. Taken together, our results demonstrated that HSV-1 replication centers selectively recruited two DDR factors, 53BP1 and BRCA1, and excluded RNF8, which suggests that 53BP1 and BRCA1 may be beneficial to viral growth.

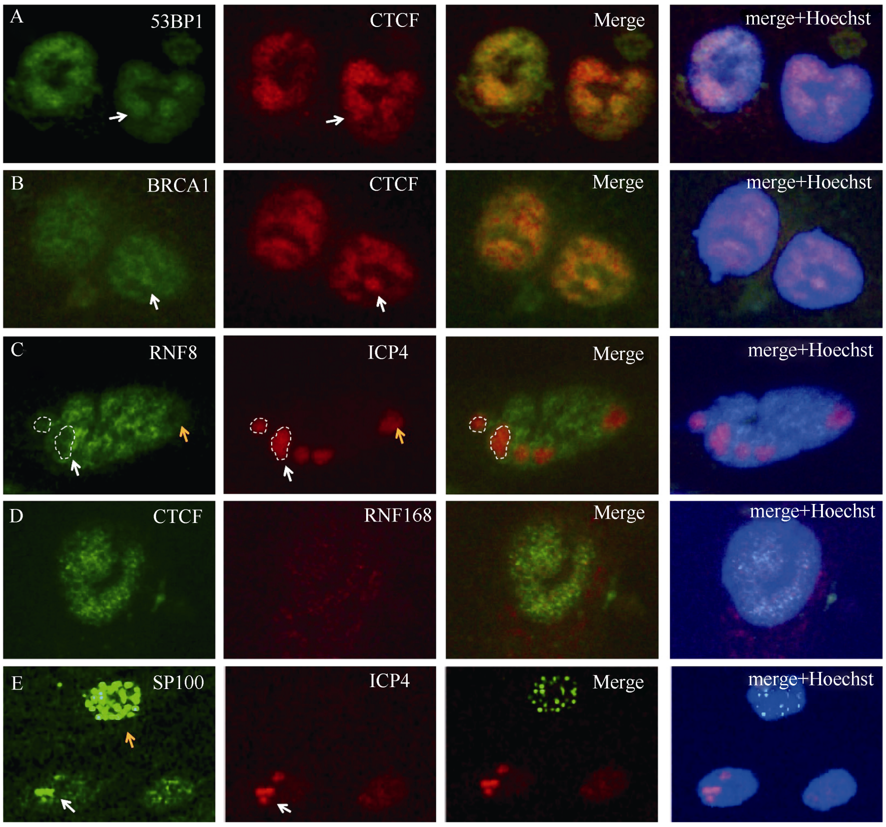

Figure 3 Recruitment or exclusion between HSV-1 replication centers and cellular DDR factors

Each row of panels was double stained using two antibodies. Red and green signals were merged to show how the two signals relate to each other (overlap or mutual exclusion). Nucleus was stained with Hoechst33342 to show nucleus outline. A: Double staining using 53BP1 (green) and CTCF antibodies (red). White arrows show a viral replication center, highlighting overlap between two proteins. B: Double staining using CTCF (red) and BRCA1 (green) antibodies. Arrows show a viral replication center. Merged signals show overlap of these two proteins in the replication center. C: Double staining using ICP4 (red) and RNF8 (green). Dashed circles show two HSV-1 replication centers highlighting apparent exclusion of RNF8 by replication centers. Orange arrows show a large replication center and the absence of RNF8 staining. D: Double staining of CTCF (green) and RNF168 proteins (red). E: Double staining of SP100 (green) and ICP4 (red). White arrows show a cluster of three replication centers and co-localization of SP100 with these centers. Orange arrow show an uninfected cell where SP100 shows punctate staining. Magnification ratio: 400X.

Cellular antiviral defense factor SP100 interacted with HSV-1 replication centers

SP100 is a key cellular antiviral defense protein normally stored in the promyelocytic leukemia protein (PML) bodies. HSV-1 protein ICP0 specifically targets the PML bodies and degrades their components (Everett & Murray, 2005; Gu et al, 2013; Negorev et al, 2009). This can be seen in the uninfected cell in Figure 3E (orange arrow), where SP100 staining exhibited a strong, punctate pattern. In infected cells, however, this pattern disappeared in Figure 3E (white arrow). To determine if SP100 was recruited by the viral replication centers, we increased the amount of exposure to offset the effect of degradation of SP100

by ICP0. The staining results clearly showed that SP100 was recruited by the viral replication centers (Figure 3E, white arrows), which suggests a possible direct interaction of SP100 with the HSV-1 genome to inhibit viral gene transcription.

CTCF recruitment was facilitated by the ATM kinase pathway

HSV-1 lytic infection activates the host DDR, as marked by the activation of ATM kinase, a key signaling kinase (Lilley et al, 2005). In the present study, several members of the host DDR were recruited to or towards the HSV-1 replication foci, including ATM, γH2A.X, 53BP1 (Figure 3A) and BRCA1 (Figure 3B). ATM kinase has been shown to affect HSV-1 replication (Lilley et al, 2011). To investigate whether CTCF recruitment was affected by the host DDR, we tested the effect of ATM inhibitor (ATMi) KU55933 on CTCF recruitment by the replicating viral foci (Hickson et al, 2004). As a control experiment, we monitored the behavior of γH2A.X. As shown in Figures 4A-4B, ATMi slightly inhibited the recruitment of γH2A.X to the HSV-1 replication center. Before adding ATMi, more γH2A.X was recruited to the ICP4 foci and it was distributed in a broad area around the foci, while in ATMi-treated cells, less γH2A.X was recruited and it was located in a much tighter area, which overlapped almost exactly with the ICP4 foci. The reduction in γH2A.X recruitment indicated that ATMi indeed inhibited the host DDR. Similarly, recruitment of

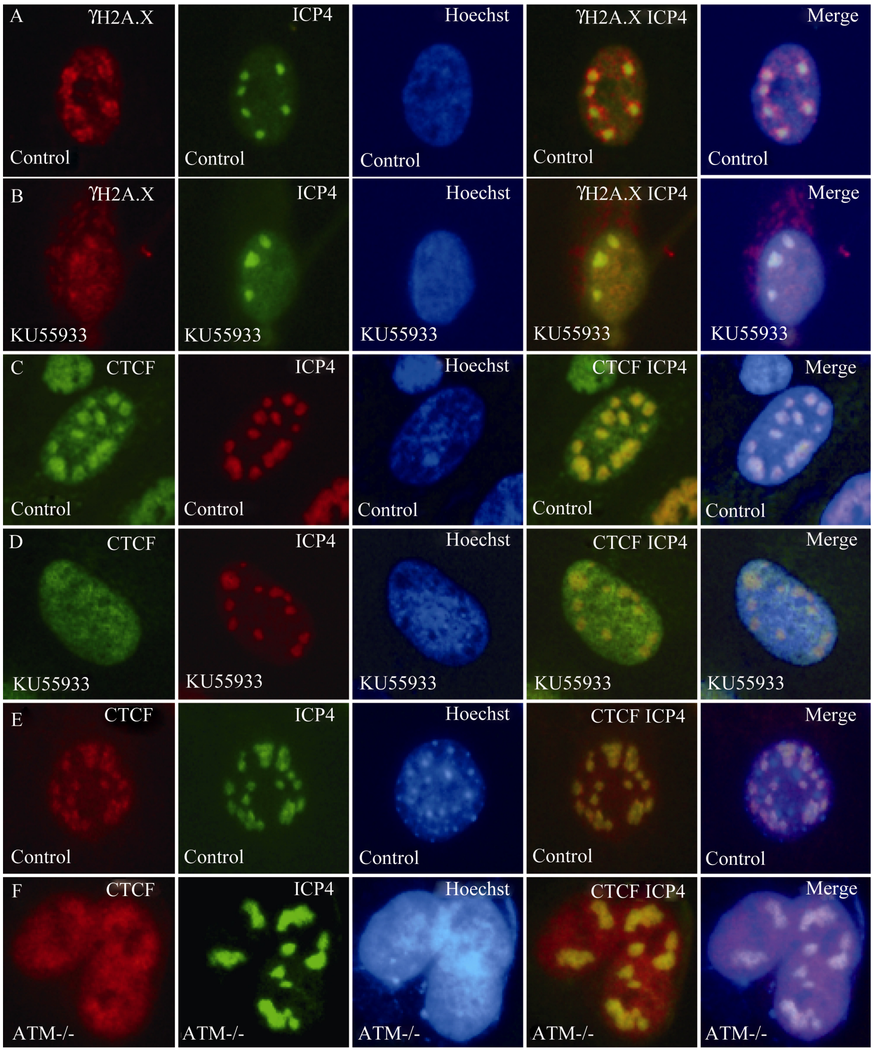

Figure 4 CTCF recruitment into HSV-1 replication centers facilitated by ATM pathway

To investigate whether CTCF recruitment was affected by the ATM pathway, we tested the effect of ATM inhibitor (ATMi) KU55933. A: BJ cells infected with HSV-1 17+ and fixed for immunostaining with either polyclonal antibodies against γH2A.X (red) or monoclonal antibody against viral protein ICP4 (green). Merged image shows γH2A.X recruitment to the viral replication centers and occupation of large areas around the viral foci. B: Reduced recruitment of γH2A.X, and colocalization with ICP4 when ATM inhibitor was added 1 hour prior to infection. C: CTCF (red) and ICP4 (green) showing clear colocalization at 6 hpi. D: Significant inhibition of CTCF recruitment after addition of ATMi. E: CTCF (red) and ICP4 (green) colocalization in mouse MEF cells. F: Less prominent CTCF recruitment and less defined staining in MEF cells deficient of ATM. Magnification ratio: 400X.

CTCF by the viral foci was also noticeably reduced by ATMi, as the inhibitor led to only slight thickening of the CTCF signal around viral replication centers, while the control showed a well-defined CTCF staining pattern (Figures 4C and 4D).

We quantified the effect of ATMi on overall HSV-1 foci appearance as well as the degree of CTCF recruitment by counting the HSV-1 infected cells that exhibited different types ICP4 staining: that is, forming foci, no foci but with high levels of diffused staining, and low levels of diffused ICP4 staining (Figure 5A). Ku55933 treatment of cells reduced the number of ICP4 positive cells by a third, or increased uninfected cells by a half, indicating inhibition of HSV-1 infection by the ATMi (Figure 5B). Consistent with this, the percentage of ICP4 cells with ICP4 foci was also reduced by about a third, while the proportion of diffused ICP4 staining increased. In ICP4 foci positive cells, about 90% of cells also recruited CTCF; however, in Ku55933-treated cells, only about 40% of cells recruited CTCF (Figure 5B).

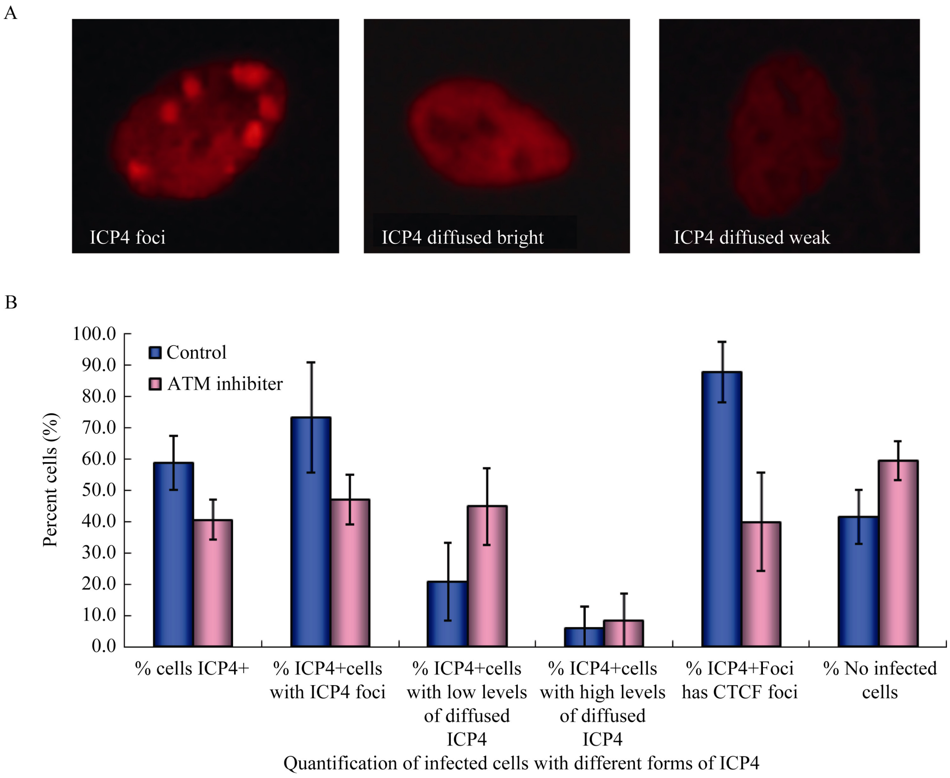

Figure 5 Inhibition of HSV-1 foci formation and CTCF recruitment into viral replication centers by ATMi

BJ cells were infected with HSV-1 17+ at 1 MOI and were fixed and stained with ICP4 antibody at 6 hpi. A**:** ICP4 staining is classified as "*ICP4 foci"* to represent clearly formed, defined viral foci; "*ICP4 diffused, bright"* to designate high levels of ICP4 staining but no foci formation; "*ICP4 diffused, weak"* to denote detectable ICP4 staining without foci formation. B**:** In control DMSO treated cells, a majority of infected cells display ICP4 foci while a smaller portion contain diffused staining. In cells treated with ATM inhibitor KU55933, the portion of foci forming cells is much smaller, about 20% of infected cells, while about half the infected cells show weak diffused staining and a third show strong diffused staining. At 1 MOI, ATMi also inhibited the number of cells infected by HSV-1, about a third drop percentage wise. At the same time, γH2A.X and CTCF recruitment into ICP4 foci were reduced by the inhibitor. Magnification ratio: 400X.

We also tested the effect of mouse MEF cells deficient of ATM (Lilley et al, 2011). The control MEF cells (Figure 4E) displayed a similar pattern of HSV-1 foci and CTCF recruitment to that of human BJ cells (Figures 4C and 4E). In the mutant cells, recruitment was significantly reduced (Figure 4F) compared with that observed in Figure 4E. These results strongly suggest that the ATM pathway facilitated CTCF recruitment into the HSV-1 replication centers.

DISCUSSION

We surveyed the interactions between HSV-1 replication centers and host chromatin, host RNA Pol II and host DDR factors. We found that viral replication centers selectively excluded modified histone H3, but not unmodified H3 (Figure 1). RNA Pol II was highly recruited to the centers, but there was a dynamic shift in the amount of recruitment as viral replication centers transited from small distinct foci to large fused centers (Figure 2). The host DDR factors also exhibited selective recruitment or exclusion from viral centers. BRCA1 and 53BP1 were recruited, but RNF8 was excluded (Figure 3). We found that the recruitment of host epigenetic regulator CTCF was regulated by ATM kinase (Figure 4 and 5), suggesting that recruiting host factors was an active process.

Interaction of host chromatin with HSV-1 replication centers

Immunostaining of histone H3 and modified histone H3 (H3K9me3, H3K4me3 and H3S10p) showed differential staining results. H3 interacted with the viral replication centers, but was not enriched in these centers (Figure 1A), while H3K9me3, H3K4me3 and H3S10p were all excluded by the replication centers (Figures 1B-D). H3K9me3 is a heterochromatin mark, and its exclusion was expected as the replicating virus was poorly chromatinized and unlikely to form heterochromatin. In contrast, the exclusion of H3K4me3, an active chromatin mark interacting with highly transcribed gene promoters, was rather unexpected. The functional implication of this exclusion is interesting and merits further investigation.

We also observed strong recruitment of RNA Pol II (Figure 2A), consistent with a previous study (Dai et al, 2006). However, we found that as the viral replication centers grew in size, RNA Pol II Ser2P quickly disappeared from these centers (Figure 2B). Similarly, RNA Pol II Ser5P also became weaker as small viral foci merged into large ones (Figure 2C). This suggests that as the virus began genome replication, the transcription of the viral genes was gradually reduced. Since transcription and DNA replication are incompatible, it is possible that as more viral genomes started rapid DNA synthesis, transcription and thus RNA Pol II recruitment was inhibited. How this process is regulated is an interesting and important question.

Replicating HSV-1 genome and host DDR

HSV-1 has a complex interaction with host responses. HSV-1 lytic infection activates the host DDR, either due to replicative stress resulting from depletion of host DNA replication factors, or from exposed double strand DNA ends from the linear genome (Smith et al, 2014). Host DDR will trigger apoptosis and transcription silencing, which are both deleterious to HSV-1 growth. However, some DDR components are needed for viral replication (Karttunen et al, 2014). Clearly, HSV-1 has successfully dealt with host DDR, i.e., taking advantage of host DDR factors that are beneficial, such as ATM, and inhibiting or degrading host DDR factors that are harmful for viral growth. For example, RINF8 and RNF168 are destroyed by ICP0 (Chaurushiya et al, 2012; Lilley et al, 2010). Although it is not clear how many DDR factors affect HSV-1 lytic infection, the recruitment or exclusion of certain DDR factors clearly indicates an active choice by the HSV-1 replication center. Previous research showed that γH2A.X was recruited by HSV-1 replication centers, but it did not co-localize with the replication centers exactly (Wilkinson & Weller, 2006). In this study, we found that cellular 53BP1 and BRCA1 were recruited by the viral replication center, while RNF8 was excluded. This suggests that 53BP1 and BRCA1 may play positive roles in viral growth, while RNF8 (and RNF168) may play a restrictive one. Consistent with this analysis, the positive role of 53BP1 and the inhibitory roles of RNF8 and RNF168 have been reported earlier (Bailey et al, 2009; Salsman et al, 2012).

Recruitment of CTCF and its implications

CTCF interacts with a consensus sequence through its zinc finger DNA binding domain (Burke et al, 2005; Klenova et al, 1993; Moon et al, 2005). Other than DNA methylation, which interrupts CTCF binding to its target, no other reported mechanism can regulate CTCF binding to DNA (Filippova et al, 2001; Teif et al, 2014). However, various studies, especially whole genome ChIP-seq studies, have revealed that CTCF binding to genomic sites is dynamic and regulated in a tissue specific manner, not all of which can be explained by DNA methylation of its binding sites (Shukla et al, 2011). In an earlier study (submitted, results in “CTCF interacts with the lytic HSV-1 genome to promote viral transcription and replication center organization”), we provided evidence that CTCF was recruited by HSV-1 replication centers and played a role in keeping γH2A.X from entering viral replication centers. In the present study, we showed that CTCF recruitment was facilitated by the ATM kinase pathway. The inhibition of ATM by Ku55933 also reduced γH2A.X aggregation around the HSV-1 foci, and inhibition may have caused infiltration of γH2A.X, a possibility consistent with the reduced recruitment of CTCF (Figure 4D). This ATM-assisted CTCF recruitment is reminiscent of the recruitment of host DDR factors to double strand DNA breaks (Matsuoka et al, 2007). Can CTCF participate in the host DDR? In a separate study, we found evidence that CTCF was recruited through the ATM pathway to double strand DNA breaks and participated in host DDR (unpublished). This new property of CTCF, if established, further suggests that HSV-1 could take advantage of host DDR to quickly recruit CTCF to organize the viral genome and replication centers, and facilitate viral transcription. Indeed, our CTCF ChIP-seq data (unpublished) suggested that 6 hour after HSV-1 infection, even though the total HSV-1 DNA per cell was less than that of the host, the recruitment of CTCF by HSV-1 had led to the loss of approximately 90% of CTCF binding peaks in the host genome, underscoring dramatic host genome reorganization.

REFERENCES

Bailey SG, Verrall E, Schelcher C, Rhie A, Doherty AJ, Sinclair AJ. 2009. Functional interaction between Epstein-Barr virus replication protein Zta and host DNA damage response protein 53BP1. *Journal of Virology,* **83**(21): 11116-11122.

Barzilai A, Zivony-Elbom I, Sarid R, Noah E, Frenkel N. 2006. The herpes simplex virus type 1 vhs-UL41 gene secures viral replication by temporarily evading apoptotic cellular response to infection: Vhs-UL41 activity might require interactions with elements of cellular mRNA degradation machinery. *Journal of Virology,* **80**(1): 505-513.

Burke LJ, Zhang R, Bartkuhn M, Tiwari VK, Tavoosidana G, Kurukuti S, Weth C, Leers J, Galjart N, Ohlsson R, Renkawitz R. 2005. CTCF binding and higher order chromatin structure of the H19 locus are maintained in mitotic chromatin. *The EMBO Journal,* **24**(18): 3291-3300.

Chaurushiya MS, Lilley CE, Aslanian A, Meisenhelder J, Scott DC, Landry S, Ticau S, Boutell C, Yates JR, 3rd, Schulman BA, Hunter T, Weitzman MD. 2012. Viral E3 ubiquitin ligase-mediated degradation of a cellular E3: viral mimicry of a cellular phosphorylation mark targets the RNF8 FHA domain. *Molecular Cell,* **46**(1): 79-90.

Conn KL, Schang LM. 2013. Chromatin dynamics during lytic infection with herpes simplex virus 1. *Viruses,* **5**(7): 1758-1786.

Dai-Ju JQ, Li L, Johnson LA, Sandri-Goldin RM. 2006. ICP27 interacts with the C-terminal domain of RNA polymerase II and facilitates its recruitment to herpes simplex virus 1 transcription sites, where it undergoes proteasomal degradation during infection. *Journal of Virology,* **80**(7): 3567-3581.

Egloff S, Murphy S. 2008. Cracking the RNA polymerase II CTD code. *Trends in Genetics,* **24**(6): 280-288.

Esclatine A, Taddeo B, Evans L, Roizman B. 2004. The herpes simplex virus 1 U_L41 gene-dependent destabilization of cellular RNAs is selective and may be sequence-specific. *Proceedings of the National Academy of Sciences of the United States of America,* **101**(10): 3603-3608.

Everett RD. 2014. HSV-1 biology and life cycle. *Methods in Molecular Biology,* **1144**: 1-17.

Everett RD, Murray J. 2005. ND10 components relocate to sites associated with herpes simplex virus type 1 nucleoprotein complexes during virus infection. *Journal of Virology,* **79**(8): 5078-5089.

Everett RD, Sourvinos G, Leiper C, Clements JB, Orr A. 2004. Formation of nuclear foci of the herpes simplex virus type 1 regulatory protein ICP4 at early times of infection: localization, dynamics, recruitment of ICP27, and evidence for the de novo induction of ND10-like complexes. *Journal of Virology,* **78**(4): 1903-1917.

Ferenczy MW, Ranayhossaini DJ, Deluca NA. 2011. Activities of ICP0 involved in the reversal of silencing of quiescent herpes simplex virus 1. *Journal of Virology,* **85**(10): 4993-5002.

Filippova GN, Thienes CP, Penn BH, Cho DH, Hu YJ, Moore JM, Klesert TR, Lobanenkov VV, Tapscott SJ. 2001. CTCF-binding sites flank CTG/CAG repeats and form a methylation-sensitive insulator at the *DM1* locus. *Nature Genetics,* **28**(4): 335-343.

Fraser KA, Rice SA. 2007. Herpes simplex virus immediate-early protein ICP22 triggers loss of serine 2-phosphorylated RNA polymerase II. *Journal of Virology,* **81**(10): 5091-5101.

Griffiths SJ, Koegl M, Boutell C, Zenner HL, Crump CM, Pica F, Gonzalez O, Friedel CC, Barry G, Martin K, Craigon MH, Chen R, Kaza LN, Fossum E, Fazakerley JK, Efstathiou S, Volpi A, Zimmer R, Ghazal P, Haas J. 2013. A systematic analysis of host factors reveals a Med23-interferon-λ regulatory axis against herpes simplex virus type 1 replication. *PLoS Pathogens,* **9**(8): e1003514.

Gu HD, Zheng Y, Roizman B. 2013. Interaction of herpes simplex virus ICP0 with ND10 bodies: a sequential process of adhesion, fusion, and retention. *Journal of Virology,* **87**(18): 10244-10254.

Hickson I, Zhao Y, Richardson CJ, Green SJ, Martin NM, Orr AI, Reaper PM, Jackson SP, Curtin NJ, Smith GCM. 2004. Identification and characterization of a novel and specific inhibitor of the ataxia-telangiectasia mutated kinase ATM. *Cancer Research,* **64**(24): 9152-9159.

Jenkins HL, Spencer CA. 2001. RNA polymerase II holoenzyme modifications accompany transcription reprogramming in herpes simplex virus type 1-infected cells. *Journal of Virology,* **75**(20): 9872-9884.

Karttunen H, Savas JN, Mckinney C, Chen YH, Yates JR, 3rd, Hukkanen V, Huang TT, Mohr I. 2014. Co-opting the fanconi Anemia genomic stability pathway enables herpesvirus DNA synthesis and productive growth. *Molecular Cell,* **55**(1): 111-122.

Klenova EM, Nicolas RH, Paterson HF, Carne AF, Heath CM, Goodwin GH, Neiman PE, Lobanenkov VV. 1993. CTCF, a conserved nuclear factor required for optimal transcriptional activity of the chicken c-myc gene, is an 11-Zn-finger protein differentially expressed in multiple forms. *Molecular and Cellular Biology,* **13**(12): 7612-7624.

Knipe DM, Quinlan MP, Spang AE. 1982. Characterization of two conformational forms of the major DNA-binding protein encoded by herpes simplex virus 1. *Journal of Virology,* **44**(2): 736-741.

Kwak H, Lis JT. 2013. Control of transcriptional elongation. *Annual Review of Genetics,* **47**: 483-508.

Lacasse JJ, Schang LM. 2010. During lytic infections, herpes simplex virus type 1 DNA is in complexes with the properties of unstable nucleosomes. *Journal of Virology,* **84**(4): 1920-1933.

Lacasse JJ, Schang LM. 2012. Herpes simplex virus 1 DNA is in unstable nucleosomes throughout the lytic infection cycle, and the instability of the nucleosomes is independent of DNA replication. *Journal of Virology,* **86**(20): 11287-11300.

Lafaille FG, Pessach IM, Zhang SY, Ciancanelli MJ, Herman M, Abhyankar A, Ying SW, Keros S, Goldstein PA, Mostoslavsky G, Ordovas-Montanes J, Jouanguy E, Plancoulaine S, Tu E, Elkabetz Y, Al-Muhsen S, Tardieu M, Schlaeger TM, Daley GQ, Abel L, Casanova JL, Studer L, Notarangelo LD. 2012. Impaired intrinsic immunity to HSV-1 in human iPSC-derived TLR3-deficient CNS cells. *Nature,* **491**(7426): 769-773.

Lai W, Chen CY, Morse SA, Htun Y, Fehler HG, Liu H, Ballard RC. 2003. Increasing relative prevalence of HSV-2 infection among men with genital ulcers from a mining community in South Africa. *Sexually Transmitted Infections,* **79**(3): 202-207.

Lilley CE, Carson CT, Muotri AR, Gage FH, Weitzman MD. 2005. DNA repair proteins affect the lifecycle of herpes simplex virus 1. *Proceedings of the National Academy of Sciences of the United States of America,* **102**(16): 5844-5849.

Lilley CE, Chaurushiya MS, Boutell C, Everett RD, Weitzman MD. 2011. The intrinsic antiviral defense to incoming HSV-1 genomes includes specific DNA repair proteins and is counteracted by the viral protein ICP0. *PLoS Pathogens,* **7**(6): e1002084.

Lilley CE, Chaurushiya MS, Boutell C, Landry S, Suh J, Panier S, Everett RD, Stewart GS, Durocher D, Weitzman MD. 2010. A viral E3 ligase targets RNF8 and RNF168 to control histone ubiquitination and DNA damage responses. *The EMBO Journal,* **29**(5): 943-955.

Matsuoka S, Ballif BA, Smogorzewska A, Mcdonald ER, 3rd, Hurov KE, Luo J, Bakalarski CE, Zhao ZM, Solimini N, Lerenthal Y, Shiloh Y, Gygi SP, Elledge SJ. 2007. ATM and ATR substrate analysis reveals extensive protein networks responsive to DNA damage. *Science,* **316**(5828): 1160-1166.

Mattiroli F, Vissers JHA, Van Dijk WJ, Ikpa P, Citterio E, Vermeulen W, Marteijn JA, Sixma TK. 2012. RNF168 ubiquitinates K13-15 on H2A/H2AX to drive DNA damage signaling. *Cell,* **150**(6): 1182-1195.

Moon H, Filippova G, Loukinov D, Pugacheva E, Chen Q, Smith ST, Munhall A, Grewe B, Bartkuhn M, Arnold R, Burke LJ, Renkawitz-Pohl R, Ohlsson R, Zhou JM, Renkawitz R, Lobanenkov V. 2005. CTCF is conserved from *Drosophila* to humans and confers enhancer blocking of the *Fab-8* insulator. *EMBO Reports,* **6**(2): 165-170.

Negorev DG, Vladimirova OV, Maul GG. 2009. Differential functions of interferon-upregulated Sp100 isoforms: herpes simplex virus type 1 promoter-based immediate-early gene suppression and PML protection from ICP0-mediated degradation. *Journal of Virology,* **83**(10): 5168-5180.

Nojima T, Oshiro-Ideue T, Nakanoya H, Kawamura H, Morimoto T, Kawaguchi Y, Kataoka N, Hagiwara M. 2009. Herpesvirus protein ICP27 switches PML isoform by altering mRNA splicing. *Nucleic Acids Research,* **37**(19): 6515-6527.

(Roizman BK DM, Whitley RJ) Knipe DM, Howley PM. 2007. Fields Virology. 5[nd] ed. Philadelphia, PA: Lippincott Williams & Wilkins.

Parkinson J, Lees-Miller SP, Everett RD. 1999. Herpes simplex virus type 1 immediate-early protein vmw110 induces the proteasome-dependent degradation of the catalytic subunit of DNA-dependent protein kinase. *Journal of Virology,* **73**(1): 650-657.

Pasieka TJ, Baas T, Carter VS, Proll SC, Katze MG, Leib DA. 2006. Functional genomic analysis of herpes simplex virus type 1 counteraction of the host innate response. *Journal of Virology,* **80**(15): 7600-7612.

Peng H, Nogueira ML, Vogel JL, Kristie TM. 2010. Transcriptional coactivator HCF-1 couples the histone chaperone Asf1b to HSV-1 DNA replication components. *Proceedings of the National Academy of Sciences of the United States of America,* **107**(6): 2461-2466.

Prasad A, Remick J, Zeichner SL. 2013. Activation of human herpesvirus replication by apoptosis. *Journal of Virology,* **87**(19): 10641-10650.

Rasmussen SB, Horan KA, Holm CK, Stranks AJ, Mettenleiter TC, Simon AK, Jensen SB, Rixon FJ, He B, Paludan SR. 2011. Activation of autophagy by α-herpesviruses in myeloid cells is mediated by cytoplasmic viral DNA through a mechanism dependent on stimulator of IFN genes. *The Journal of Immunology,* **187**(10): 5268-5276.

Roizman B. 2011. The checkpoints of viral gene expression in productive and latent infection: the role of the HDAC/CoREST/LSD1/REST repressor complex. *Journal of Virology,* **85**(15): 7474-7482.

Roizman B, Whitley RJ. 2013. An inquiry into the molecular basis of HSV latency and reactivation. *Annual Review of Microbiology,* **67**: 355-374.

Salsman J, Jagannathan M, Paladino P, Chan PK, Dellaire G, Raught B, Frappier L. 2012. Proteomic profiling of the human cytomegalovirus ul35 gene products reveals a role for UL35 in the DNA repair response. *Journal of Virology,* **86**(2): 806-820.

Sedlackova L, Perkins KD, Lengyel J, Strain AK, Van Santen VL, Rice SA. 2008. Herpes simplex virus type 1 ICP27 regulates expression of a variant, secreted form of glycoprotein C by an intron retention mechanism. *Journal of Virology,* **82**(15): 7443-7455.

Shen GH, Wang KZ, Wang S, Cai MS, Li ML, Zheng CF. 2014. Herpes simplex virus 1 counteracts viperin via its virion host shutoff protein UL41. *Journal of Virology,* **88**(20): 12163-12166.

Showalter SD, Zweig M, Hampar B. 1981. Monoclonal antibodies to herpes simplex virus type 1 proteins, including the immediate-early protein ICP 4. *Infection and Immunity,* **34**(3): 684-692.

Shukla S, Kavak E, Gregory M, Imashimizu M, Shutinoski B, Kashlev M, Oberdoerffer P, Sandberg R, Oberdoerffer S. 2011. CTCF-promoted RNA polymerase II pausing links DNA methylation to splicing. *Nature,* **479**(7371): 74-79.

Silva L, Cliffe A, Chang L, Knipe DM. 2008. Role for A-type lamins in herpesviral DNA targeting and heterochromatin modulation. *PLoS Pathogens,* **4**(5): e1000071.

Smith S, Reuven N, Mohni KN, Schumacher AJ, Weller SK. 2014. Structure of the herpes simplex virus 1 genome: manipulation of nicks and gaps can abrogate infectivity and alter the cellular DNA damage response. *Journal of Virology,* **88**(17): 10146-10156.

Song B, Liu JJ, Yeh KC, Knipe DM. 2000. Herpes simplex virus infection blocks events in the G1 phase of the cell cycle. *Virology,* **267**(2): 326-334.

Taddeo B, Zhang WR, Roizman B. 2006. The UL41 protein of herpes simplex virus 1 degrades RNA by endonucleolytic cleavage in absence of other cellular or viral proteins. *Proceedings of the National Academy of Sciences of the United States of America,* **103**(8): 2827-2832.

Taddeo B, Zhang WR, Roizman B. 2013. The herpes simplex virus host shutoff RNase degrades cellular and viral mRNAs made before infection but not viral mRNA made after infection. *Journal of Virology,* **87**(8): 4516-4522.

Taylor TJ, Knipe DM. 2004. Proteomics of herpes simplex virus replication compartments: association of cellular DNA replication, repair, recombination, and chromatin remodeling proteins with ICP8. *Journal of Virology,* **78**(11): 5856-5866.

Teif VB, Beshnova DA, Vainshtein Y, Marth C, Mallm JP, Höfer T, Rippe K. 2014. Nucleosome repositioning links DNA (de)methylation and differential CTCF binding during stem cell development. *Genome Research,* **24**(8): 1285-1295.

Volcy K, Fraser NW. 2013. DNA damage promotes herpes simplex virus-1 protein expression in a neuroblastoma cell line. *Journal of Neurovirology,* **19**(1): 57-64.

Wang S, Long J, Zheng CF. 2012. The potential link between PML NBs and ICP0 in regulating lytic and latent infection of HSV-1. *Protein & Cell,* **3**(5): 372-382.

Wang XJ, Patenode C, Roizman B. 2011. US3 protein kinase of HSV-1 cycles between the cytoplasm and nucleus and interacts with programmed cell death protein 4 (PDCD4) to block apoptosis. *Proceedings of the National Academy of Sciences of the United States of America,* **108**(35): 14632-14636.

Wang Y, Yang Y, Wu SF, Pan S, Zhou CD, Ma YJ, Ru YX, Dong SX, He B, Zhang CZ, Cao YJ. 2014. p32 is a novel target for viral protein ICP34.5 of herpes simplex virus type 1 and facilitates viral nuclear egress. *Journal of Biological Chemistry,* **289**(52): 35795-35805.

Weitzman MD, Carson CT, Schwartz RA, Lilley CE. 2004. Interactions of viruses with the cellular DNA repair machinery. *DNA Repair,* **3**(8-9): 1165-1173.

Weitzman MD, Weitzman JB. 2014. What's the damage? The impact of pathogens on pathways that maintain host genome integrity. *Cell Host & Microbe,* **15**(3): 283-294.

Wilkinson DE, Weller SK. 2004. Recruitment of cellular recombination and repair proteins to sites of herpes simplex virus type 1 DNA replication is dependent on the composition of viral proteins within prereplicative sites and correlates with the induction of the DNA damage response. *Journal of Virology,* **78**(9): 4783-4796.

Wilkinson DE, Weller SK. 2006. Herpes simplex virus type I disrupts the ATR-dependent DNA-damage response during lytic infection. *Journal of Cell Science,* **119**(Pt 13): 2695-2703.

Wysocka J, Herr W. 2003. The herpes simplex virus VP16-induced complex: the makings of a regulatory switch. *Trends in Biochemical Sciences,* **28**(6): 294-304.

Yun MH, Hiom K. 2009. CtIP-BRCA1 modulates the choice of DNA double-strand-break repair pathway throughout the cell cycle. *Nature,* **459**(7245): 460-463.

Zaborowska J, Baumli S, Laitem C, O'reilly D, Thomas PH, O'Hare P, Murphy S. 2014. Herpes Simplex Virus 1 (HSV-1) ICP22 protein directly interacts with cyclin-dependent kinase (CDK)9 to inhibit RNA polymerase II transcription elongation. *PloS One,* **9**(9): e107654.

Zhou Q, Li TD, Price DH. 2012. RNA polymerase II elongation control. *Annual Review of Biochemistry,* **81**: 119-143.

Zhou YH, Liang YB, Pang W, Qin WH, Yao ZH, Chen X, Zhang CY, Zheng YT. 2014. Diverse forms of HIV-1 among Burmese long-distance truck drivers imply their contribution to HIV-1 cross-border transmission. *BMC Infectious Diseases,* **14**: 463.

Social organization of Shortridge's capped langur (*Trachypithecus shortridgei*) at the Dulongjiang Valley in Yunnan, China

Ying-Chun LI[1, †], Feng LIU[1, †], Xiao-Yang HE[2], Chi MA[3], Jun SUN[2], Dong-Hui LI[2], Wen XIAO[3, *], Liang-Wei CUI[1,4, *]

[1] *Forestry Faculty*, *Southwest Forestry University*, *Kunming*, *Yunnan* 650224, *China*

[2] *Nujiang Administration Bureau*, *Gaoligongshan National Nature Reserve*, *Liuku*, *Yunnan* 673100, *China*

[3] *Institute of Eastern-Himalaya Biodiversity Research*, *Dali University*, *Dali*, *Yunnan* 671003, *China*

[4] *College of Life Sciences, Northwest University, Xi'an, 710069, China*

ABSTRACT

Non-human primates often live in socially stable groups characterized by bonded relationships among individuals. Social organization can be used to evaluate living conditions and expansion potential. Bisexual group size, ratio of males to females and group composition are essential elements determining the type of social organization. Although the first report on Shortridge's capped langurs (*Trachypithecus shortridgei*) was in the 1970s, until now, the species only inhabits forests of the Dulongjiang valley in northwest Yunnan, China, with c. 250-370 individuals in 19 populations. To understand its social organization, we collected data from five groups of Shortridge's langurs at Silaluo in the Dulongjiang valley during August 2012-October 2013. Family groups consist of one adult male, 2–3 adult females and up to five young. Group size averaged 8 (7-9) individuals. The ratio of adult males to females (M/F) was 1:2.9, infants to adult females was (I/F) 1:2.2; and ratio of adults to immatures was 1:1.2, indicating the potential of a population increasing. Birth season was during March-July and the inter-birth interval was two years.

Keywords: *Trachypithecus shortridgei*; Social organization; One-male, multi-female group; Multi-male, multi-female group; Group size

INTRODUCTION

Social organization, including group size, sexual composition and bonded relationships among individuals (Kappeler & van Schaik, 2002), is the most basic characterization of non-human primate societies (Clutton-Brock & Harvey, 1977; Crook & Gartlan, 1966; Eisenberg et al, 1972). Three fundamental types of social organization can be categorized into solitary, pair-living and group-living speceis (Kappeler & van Schaik 2002). Solitary individuals typically forage alone (Boinski & Garber, 2000) and their activities are desynchronized with each other both spatially and temporally (Charles-Dominique, 1978). Except for orangutan, most solitary primate species are nocturnal (Kappeler & van Schaik, 2002). Pair-living species refer to couples of one adult male and one adult female (Kappeler, 1999), such as gibbons. Most primates live in bisexual groups (van Schaik & Kappeler, 1997), which are much more stable compared with other mammals, and consist of more than two adults. Group living primates displayed a diversity with respect to the size, sex ratio and temporal stabitliy of compositioin. Accordingly, polyandrous, polygynous and multi-male, multi-female groups (MMGs) have been diistinguished (Kappeler, 2000). Variation in the number of adult males is the most prominent feature of primate group composition (Hamilton & Bulger, 1992; Preuschoft & Paul, 2000; van Hooff, 2000), and can thus be categorized as one-male, multi-female groups (OMGs) or MMGs. The number of adult males in each bisexual group related to the predatory pressure (van Schaik & Hőrstermann, 1994), is positively associated with the number of adult females (Mitani et al, 1996) and temporal overlap of female receptive periods (Nunn, 1999).

Received: 15 December 2014; Accepted: 05 March 2015

Foundation items: This study was supported by the Yunnan Green Environmental Development Fund, the Central Financial Assistance Fund, the National Natural Science Foundation of China (31160422, 30960084), the Program for New Century Excellent Talents in University (NCET-12-1079), the China Postdoctoral Science Foundation (2013M542379) and the Key Subject of Wildlife Conservation and Utilization in Yunnan Province

*Corresponding authors, E-mails: gcuilw@gmail.com; xiaowen.dali@gmail.com

†Authors contributed equally to this work

Group size is another vital feature of the social organization of group living primates, and may be influenced by birth rate, morality rate and the transfer of individuals (Kappeler & van Schaik, 2002). Significant variations can be found in colobine species, e.g., group size in Mentawai langurs (*Presbytis potenziani*) is less than four, whereas, golden snub-nosed monkeys (*Rhinopithecus roxellana*) can include approximately 400 individuals (Grueter, 2013; Newton & Dunbar, 1994). Social organization of langurs includes monogamy, such as found in Mentawai langurs (*P. potenziani*); matrilineal-harem, such as seen in Sumatran surilis (*P. melalophos*), maroon leaf monkeys (*P. rubicunda*), Nilgiri langurs (*Trachypithecus johnii*), Gee's golden langurs (*T. geei*), capped langurs (*T. pileatus*), dusky leaf monkeys (*T. obscurus*), proboscis monkeys (*Nasalis larvatus*), and Northern plains gray langurs (*Semnopithecus entellus*) at Abu and Jodhpur; matrilineal-multimale, such as observed in Northern plains gray langurs (*S. entellus*) at Orcha and Rajaji; and patrilineal-multimale, such as found in black-and-white colobus (*Colobus polykomos*), olive colobus (*Procolobus verus*) and western red colobus (*P. badius*) monkeys. However, the most typical social organizaiton is the one-male, multi-female unit (OMU). A large population can be composed of several OMUs, and one or several all-male units (AMUs) (Cui et al, 2008; Grueter, 2013; Kirkpatrick, 1996; Li et al, 2014; Newton & Dunbar, 1994; Qi et al, 2009, 2014).

Group size of *Trachypithecus* species can range from a dozen to approximately 100, and their social organization includes OMGs and MMGs (Koenig & Borries, 2012; Fan et al, 2014). Bisexual groups of white-headed langurs (*T. leucocephalus*) are composed dominantly of OMGs, occasionaly of MMGs (9.1%, *n*=11), with 3-30 individuals in each group. Non-breeding individuals can live solitarily or in groups (Jin et al, 2009; Li & Rogers, 2004). Non-breeding groups are either AMUs or include males (82.6%) and juvenile females (17.4%) (Jin et al, 2009). A bisexual group usually lives in an OMG with 6-12 individuals in François' langurs (*T. francoisi*) (Hu et al, 2011; Zhou et al, 2009). Bisexual groups of Delacour's langurs (*T. delacouri*) mostly live mostly in OMG,s, and occasionally in two-male, multi-female groups (TMGs), with 5-30 individuals in each group (Harding, 2011). Golden langur (*T. geei*) groups, which inhabit the rubber forests of Assam in India, usually consist of 7-26 (17.3 on average) individuals. Among three observed groups, two were TMGs with 19 and 26 individuals, respectively, and one was an OMGs with only seven individuals (Medhi et al, 2004). Silvered langur (*T. cristatus*) groups consist of 7-40 individuals (Timmins et al, 2013), one OMG includes seven individuals (Boonratana, 1998). Small OMGs and occasionally MMGs have been found in capped langurs (*T. pileatus*) (Green, 1981; Mukherjee, 1978; Mukherjee et al, 1995; Stanford, 1991). Most Phayre's leaf monkeys (*T. phayrei*) form bisexual groups (Bose, 2003; Koenig & Borries, 2012; Mukherjee, 1982) or AMUs (Mukherjee, 1982). Each group consists of 6-33 (Koenig & Borries, 2012) up to 45 individuals (Zheng, 1993), including 1-5 adult males and 3-12 adult females. Large groups of Indochinese gray langurs (*Trachypithecus crepusculus*) (60-100 individuals, *n*=6) were observed at Wuliangshan Mountain (Fan et al, 2014). Bisexual groups of Phayre's leaf monkeys include OMGs (48.4%), TMGs (24.9%) and three-male, multi-female groups (15.9%) (Koenig & Borries, 2012). The diverse social organization of *Trachypithecus* species are adaptations to diverse habitat environments (including natural and social environments) and are also the result of both environmental pressure and phylogeny.

Shortridge's capped langurs (*Trachypithecus shortridgei*) (Wroughton, 1915) are now considered as a separate species from capped langurs (*T. pileatus*) (Groves, 2001) and to only distribute in the Dulongjiang valley, northwest Yunnan, China (Cui et al, 2015) and northeastern Myanmar (Groves, 2001; Htun et al, 2008; Pocock, 1939). *T. shortridgei* is categorized as Endangered on the IUCN Red List (Htun et al, 2008) and is listed in CITES Appendix I (CITES, 2014). In China it is a Category I protected species under Chinese animal conservation laws, and in Myanmar it is protected under the national Wildlife Protection Law (Htun et al, 2008).. In India, capped langur (*Trachypithecus pileatus*) groups usually consist of 8-11 individuals (Solanki, 2007, 2008), usually forming OMGs and occasionally TMGs (Mukherjee, 1978) or MMGs (Green, 1981; Mukherjee, 1978; Mukherje et al, 1995; Solanki, 2007; Stanford, 1991, 1987, 1988). Non-breeding individuals live solitarily or in AMGs (Choudhury, 1988; Green, 1981; Stanford, 1991, 1988).

Although Shortridge's langurs were first found in China since 1972, little is known about this species. Community interview indicated that they live in bisexual groups of 10-30 individuals, and only 19 groups with 250-370 individuals have been found in the Dulongjiang region of Yunnan, China (Cui et al, 2015). To date, knowledge on their social organization remains very little. In this study, we aim to clarify some basic information of *T. shotridgei*: (1) whether its bisexual group size is 10-30 or approximately 10 indicdiuals similar to that of *T. pileatus*; (2) whether its social organization is OMG or MMG; (3) the number of adult females in bisexual group and (4) the age-sexal composition of bisexual group and its dynamic trends.

MATERIALS AND METHODS

Study area

The study area is located in the Dulongjiang region, Gongshan County, northwest Yunnan, China, and neighbors with Chayu in Tibet to the north and with Kachin in Myanmar to the south and west. East and west of Dulongjiang River are the west side of Gaoligongshan Mountain and the east side of the Dandanglika Mountains, respectively. The Gaoligongshan Mountain and Dandanglika Mountains are south-north oriented, descending from north to south and are featured with significant altitudinal differences (4 000 m maximum) and steepness. Under the influence of southwest monsoon and topographic features, the climate of the Drung River Basin is quite mild. Average yearly temperature was 14.5 °C during 2010-2012; the difference in average monthly temperature was 15.0 °C; the highest and lowest average temperature occurred in August (21.6 °C) and January (6.6 °C). The rain season is from February to October; average yearly precipitation was 2 745.1 mm, with two peak periods of precipitation from March to April and from June to September, respectively. The Drung region is characterized by

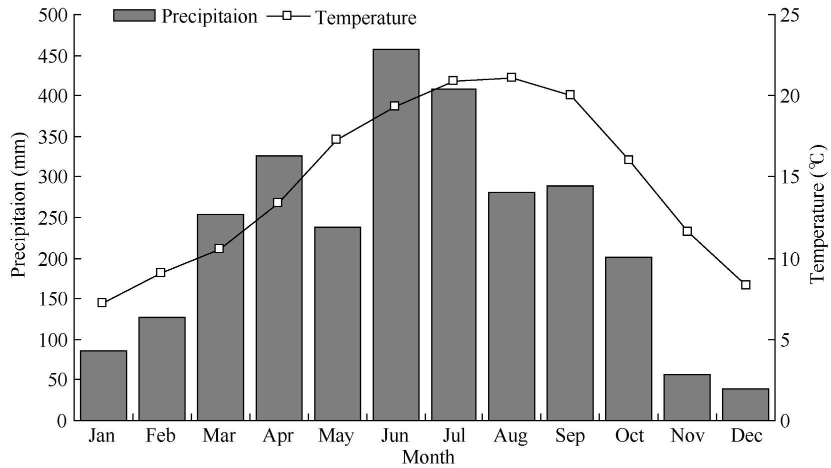

Figure 1 Average monthly temperature and precipitation in the Dulongjiang valley from January 2010 to December 2012

dense forests and obvious vertical zonality in vegetation. The vegetation type from low to high altitude is monsoonal evergreen broad-leaved forests (1 200–1 500 m), montane moist evergreen broad-leaved forests (1 500–2 400 m), mixed broadleaf-conifer forests (2 400–2 800 m), cold temperate coniferous forests (2 800–3 000 m), frigid-temperate coniferous forest (3 000–3 700 m) and alpine scrubs and meadows (>3 700 m) (He & Li, 1996).

Study subject

The study subjects included five groups (group A, B, C, D, E) of Shortridge's langurs inhabiting the Silaluo region (N27°47′, E98°19′) in the Dulongjiang valley. Age-sex composition of the species was distinguished according to body size, body color and other morphological features (Table 1). Except for one adult female with a chopped tail (its length is approximately 10 cm), others were not individually differentiated.

Method

Although an observing location (1 500 m a.s.l.) with open view was found on the mountain facing the activity areas of the langurs, the steep terrain and dense forests inhibited our observation. Therefore, all observations were conducted along the road opposite the activity areas of the monkey, so we only observed activities of the groups in areas between the riverside (approximately 1 420 m) and the elevation of 1 700 m.

From August 2012 to September 2013 (except December 2013), surveys were conducted daily during 0700–1830 in Silaluo-Pukawang region of the Dulongjiang valley. When monkeys were sighted, we observed them in the distance of 60-800 m by binoculars (Olympus 10×42 EXWP I) or monoculars (Leica Televid 77, 8×42). Age–sex compositions of the groups were recorded when they were crossing areas with open view (such as naked rocks or forest gaps). A topographic map (1: 50 000) of the study area was subdivided into small squares (250 m×250 m) and the locations of groups were recorded on the map every 30 min.

Due to the steep terrain and dense forests, it was not possible to continuously track groups or recognize individuals, so the birth season was only roughly estimated based on information acquired from group observations and the number and morphological chacteristics of infants.

Table 1 Features of different age-sex classes of *Trachypithecus shortridgei*

Age/Gender	Features
Adult males	Largest (15-20%) and stronger than adult females; black face, hand and foot, and tip of tail; tail is long and strong, and light black except for white ventro-base; small black spots on top of head; color from center to peripheral of the back transits from black to gray-black; gray-black in lateral thigh; color from waist to base of tail is silvery white; other body parts is silver; whiskers long and obvious along both sides of face; penis occasionally shown.
Adult females	Larger than juveniles; body color close to males; whiskers less obvious than males; tail long and slim; nipples flesh-color or pink, long and downward; usually found around infants.
Juveniles	Larger than infants; face and extremities black; back and lateral limbs gray-black; abdomen and internal limbs silver; whiskers appears along both sides of face; tail slim and black; tip of tail white in juveniles 1-2 years old.
Infants	Under a year old; an orange body except flesh-colored face, limbs and ears, but with a black line in the center and lateral back; face and extremities black and base of tail silver in two-month-olds; silver body, tail silver to black from base to tip in eight-month-olds; top of head white; long and white whiskers; usually accompanied by females or juveniles.

RESULTS

Bisexual groups of Shortridge's langur at the Dulongjiang valley were composed of one-male, multi-female and their immatures. Average group size was 8 (7-9) individuals, including one adult male, 2-3 adult females and up to five offspring. The ratio of adult males to females (M/F) was 1:2.9; infants (I/F) to females was 1:2.2 and adults to immature individuals (Ad/Im) was 1:1.2. Although a possible solitary male was observed at Qinlangdang south (30 km straight distance) of our study area and 12 single male individuals were previously surveyed at Pianma, Lushui; neither a all-male group nor solitary males were observed in our study area. The increasing size of group D was directly resulted from the birth of infants in the group. However, as we were unable to recognize individuals, it was not possible to determine the underlying mechanisms of variations in the number of individuals (Table 2).

One infant in group D was born sometime between 9 March and 6 April 2013. According to its morphological characteristics, we assumed the infant to be two weeks old on 6 April. Another infant in group D was born sometime during 7 April-23 May, 2013. One infant in group E was approximately 1-2 weeks old when it was first sighted and it was assumed born sometime during 22-31July 2013. Therefore, we concluded that the brith season of Shortridge's langurs in the Dulongjiang valley was from March to July.

In 2012, 11 females gave birth to six infants (birth rate=0.55), and three infants were produced by six females (birth rate=0.5) in 2013, which demonstrated an overall birth rate of 0.56 during the study period. From 2012 to 2013, three infants were produced by three females in group D. These results indicate that Shortridge's langurs produce one infant every two years.

This study ran for 299 days (2 343.9 h), of which 69 days was used for observation and 63 days for scanning record (273 h). Thirty-nine habitat squares, totaling 2.44 km^2, were utilized by the five groups. Although habitat overlap among the different groups was 33%, no direct competition was observed. We therefore assumed that the monkeys might avoid competition through using habitats at different time periods.

DISCUSSION

Group size in colobine varies from three to several hundred, living in small families or larger group (Newton & Dunbar, 1994). Shortridge's langurs at the Dulongjiang valley usually live in small groups of 7-9 (8 on average) individuals, which were much smaller than those estimated in community interviews (10-30 individuals, Cui et al, 2015), but were comparable with group sizes (approximately 10 individuals) of capped langur (*T. pileatus*) (Kumar & Solanki, 2008; Solanki et al, 2007), Delacour's langur (*T. delacouri*) (Workman, 2010), white-headed langur (*T. leucocephalus*) (Jin et al, 2009), purple-faced langur (*T. vetulus*) (Vandercone et al, 2012), François' langur (*T. francoisi*) (Huang et al, 2006, 2007; Li & Wei, 2012) and Gee's golden langur (*T. johnii*) (Roy et al, 2012); whereas, smaller than those of other species, such as cantor's dusky leaf monkey (*T. obscurus halonifer*) (Md-Zain & Ch'ng, 2011) and Javan lutung (*T. auratus sondaicus*) (Tsuji et al, 2013).

Group size is affected by the spatial and temporal distribution of food resources, predator pressures and foraging strategies of individuals. When predator pressure is low and food patches are small and/or abundant, group sizes are usually small; when food patches are large and food is high in variety but low in abundance, group sizes are usually large. When population densities are high, populations are limited by habitat quality (Newton & Dunbar, 1994). Fan et al (2014) found that large groups of Indochinese gray langurs (*Trachypithecus crepusculus*) were dependent on the high variety of food resources. The high overlap (33%) of habitats observed in the Shortridge's langurs at the Dulongjiang valley indicated that habitat limitations may have confined population expansion. During our study, no natural enemies of the Shortridge's langurs were found, suggesting low predator pressure, whereas, human activities (such as illegal hunting) may have disturbed the populations. The small Shortridge's langur populations may be the result of all these interactions. However, the specific factors underlying population size can only be determined by systematic research in gradient environments (various habitat qualities and human disturbance).

Bisexual groups of many *Trachypithecus* species are OMGs, though MMGs are occasionally observed (Kirkpatrick, 2007; Newton & Dunbar, 1994). Bisexual groups in Shortridge's langurs at the Dulongjiang valley usually included one male adult, 2-3 female adults and up to five immature offspring, which is quite similar with that of *T. vetulus* (Vandercone et al, 2012), *T. francoisi* (Huang et al, 2006, 2007; Li & Wei, 2012), *T. obscurus* (Md-Zain & Ch'ng, 2011), *T. phayrei* (Koenig et al, 2004), *T. johnii* (Roy et al, 2012) and *T. auratus* (Tsuji et al, 2013).

The number of male adults in a breeding group is irrelevant to population density, weather conditions and male mortality rate (Newton & Dunbar, 1994), but is correlated with predator pressure, number of females and reproduction synchronicity (Kappeler & van Schaik, 2002; Mitani et al, 1996; Nunn, 1999; van Schaik & Hőrstermann, 1994). For example, predator pressure (such as eagles) increased the numbers of adult males from one to two in breeding groups of howler monkeys and colobus monkeys, whereas, breeding groups of langurs that inhabit the same environment, but without predator pressure, are composed of OMG (van Schaik & Hőrstermann, 1994). The number of males is also affected by the number of females, which are restrained by food resources and population size (Andelman, 1986; Crockett & Eisenberg, 1987; Dunbar, 1988; Terborgh, 1986). The reproduction strategy of males depends on the number of estrous females that can be monopolized by males, which is correlated with both the number of adult females and their reproduction synchronicity (Emlen & Oring, 1977, Wrangham, 1980). Moreover, the percentage of OMGs is also influenced by the number of adult females and their reproduction synchronicity (Srivastava & Dunbar, 1996). Theoretically, one male HanumanLangur (*Semnopithecus entellus*) can monopolize up to 12 adult females, but once the number of females has exceeded this limitation, more than one male would be expected in a breeding group (Newton, 1988).

Table 2 Social organization of Shortridge's capped langur (*Trachypithecus shortridgei*) at the Dulongjiang Valley, Yunnan, China

Period	Code	Group composition	M	F	J	I	GS	M:F	I:F	Ad:Im	Birth rate	Home range (km²)
16 Aug-22 Nov 2012	A	M, F, F, J, J, J, I02	1	2	3	1	7	1:2	1:2	1:1.3	0.5	0.56
04 Sep 2012-22 Mar 2013	B	M, F, F, F, J, J, J, I_{02}, I_{02}	1	3	3	2	9	1:3	1:1.5	1:1.3	0.67	0.88
23-29 Mar 2013	C	M, F, F, F, J, J, J, I_{02}, I_{02}	1	3	3	2	9	1:3	1:1.5	1:1.3	0.67	0.38
12 Jan-08 Mar 2013		M, F, F, Fb, J, J, I_{02}	1	3	2	1	7	1:3	1:3	1:0.8	0.33	1.06
06 Apr 2013	D	M, F, F, Fb, J, J, J_{02}, I_{03}	1	3	3	1	8	1:3	1:3	1:1	0.33	
23 May-10 Sep 2013		M, F, F, Fb, J, J, J_{02}, I_{03}, I_{03}	1	3	3	2	9	1:3	1:1.5	1:1.3	0.67	0.38
06-10 Aug 2013	E	M, F, F, F, J, J, I_{03}	1	3	2	1	7	1:3	1:3	1:1.3	0.5	
Mean±*SD*			1±0	2.9±0.4	2.7±0.5	1.4±0.5	8±1 (7-9)	1:2.9	1:2.2	1:1.2		0.65±0.31

M: Adult male; F: Adult male; Fb: Adult female with chopped tail; J: Juvenile; GS: Group size; I_{02}: Infant born in 2012; I_{03}: Infant born in 2013; Ad: Adults; Im: Immature individuals; Color of tails of two infants in group B turned from orange to gray on 22 March 2012; Color of tip (tip of 1/6) of the tail of one infant in group C was orange on 23-29 March 2012; Group E in the activity area of group B at 06-10 August 2013; Group E was either an independent group or evolved from group B or C (i.e, through death or migrations).

Table 3 Summary of *Trachypithecus* social organization

Species	SO (%)	AM	AF	IEI	Infant	MGS (range, n)	M:F	I:F	Ad:Im	Habitat	Source
T. shortridgei	OMG (100)	1	2.9(2-3)	2.7(2-3)	1.4(1-2)	8 (7-9, 5)	1:2.9	1:2.2	1:1.2	Evergreen-deciduous forest	This study
T. pileatus	OMG (75)	1	4.7(4-5)	1.3(0-2)	0.7(0-2)	8.3 (7-9, 3)	1:4.7	1:7	1:0.5	Evergreen-deciduous forest	Solanki et al, 2007
	TMG (25)	2	4	1	0	7 (7, 1)	1:2	0:4	1:0.2		
	OMG (90)					7.5 (7-9, 24)	1:3.6			Evergreen-deciduous forest	Kumar & Solanki, 2008
	MMG(10)										
T. delacouri	OMG (71)	1(1-1)	5.4(2-8)	1.6(0-3)	3.6(0-6)	10.8 (4-16, 5)	1:5.4	1:1.5	1:0.7	Limestone karst	Workman, 2010
	TMG (29)	2(2-2)	1.5(1-2)	2(1-3)	0	5.0 (4-6, 2)	1:0.8	0:3	1:0.4		
T. geei	OMG (33)	1	2	3	1	7 (7, 1)	1:2	0:2	1:1.3	Nature forest	Medhi et al, 2004
	TMG (67)	2	4.5(2-7)	10(4-16)	6 (6-6)	22.5 (19-26, 2)	1:4.5	1:0.8	1:2.5		
T. leucocephalus	OMU(91)	1	4.9(3-9)	3.8(0-8)	1.6(0-5)	9.7(5-14, 10)	1:4.9	1:3.1	1:0.4	Disturbed and natural vegetation	Li & Rogers, 2004
	TMU(9)	2	3			5 (5-5, 1)	1:1.5				
	OMG (100)	1	5.1(1-14)	2.6(0-10)	2.9 (0-9)	11.7 (3-30)	1:5.1	1:1.8	1:0.8	Limestone karst	Jin et al, 2009
	OMG (100)	2.3(2-3)	3.0 (1-5)	3.3(0-9)	1.0(0-2)	9.7(3-19)	1:1. 3	1:3	1:0.8		
T. vetulus	OMG (100)	1	6		4	11	1:6	1:1.5	1:0.6	Dry zone forest	Vandercone et al, 2012
T. francoisi	OMG (100)	1	3		5	9	1:3	1:0.6	1:1.3	Limestone karst	Huang et al, 2006
	OMG (100)	1	5		3	9	1:5	1:1.7	1:0.5	Limestone karst	Huang et al, 2007
	OMG (100)	1	2.8(2-3)	1.5(0-3)	0	5 (4-6, 4)	1:2.8	0:2.8	1:0.4	Limestone karst	Li & Wei, 2012
T. obscurus	OMG (100)	1	5	11	1	18	1:5	1:5	1:2	-	Md-Zain & Ch'ng, 2011
T. phayrei	OMG (100)	1	4	4	3	9	1:4	1:1.3	1:0.8	Evergreen forests	Koenig et al, 2004
T. p. crepusculus	OMG/MMG	1-5	3-12	0-12	1-11	19(6-33)	1:3.5	1:1.3	1:1.1	Dry evergreen forest	Koenig & Borries, 2012
T. crepusculus	MMG	10-11	30-31	30	20	90-91	1:3	1:1.5	1:1.3	Evergreen broad	Fan et al, 2014
T. johnii	OMG (100)	1	2.0 (2-2)	4(2-6)	0.5(0-1)	7.5 (6-9, 2)	1:2	1:4	1:0.5	Evergreen-deciduous forest	Roy et al, 2012
T. auratus	OMG (100)	1	14	8	1	24	1:14	1:14	1:0.7	-	Tsuji et al, 2013

SO: Social organization; AM: Adult male; AF: Adult female; IEI: Immature except infants; MGS: Mean group size; OMG: One-male, multi-female group; TMG: Two-male, multi-female group; MMG: Multi-male, multi-female group; %: Percentage of different social organizations in the report.

Extreme reproductive synchronicity (either too high or too low) decreases the ability of males to monopolize females, and only moderate reproduction synchronicity can enhance the monopolization (Emlen & Oring, 1977). Monopolizaiton ability of the male can also be enhanced by the concentrated distribution of females and its more non-feeding time (van Schaik & van Van Hoof, 1983). On average, only five adult females were observed in OMGs of white-headed langur, which may result from low overall numbers of adult females (Jin et al, 2009). OMGs of Shortridge's langur at the Dulongjiang valley had only three adult females, whereas, the number of adult females in OMGs of other species of *Trachypithecus* are usually 4-5 (ranging from 2 to 14) (Table 3). Although the reproduction synchronicity of female Shortridge's langurs cannot be precisely determined, the scattered birth pattern suggests low synchrony. According to our study, females basically moved within the view field of males and the feeding time of adult males was 5.9%. Therefore, the number of adult males was correlated with both low predator pressure and the small number of adult females.

Although OMGs of Shortridge's langurs at the Dulongjiang valley contained only a few adult females, the ratio of adults to immature individuals (1:1.2) indicated their increasing potential. The ratio of OMGs in genus of Trachypithecus is 0.5-2, but that of most of other species is less than 1:1 (Solanki et al, 2007; Workman, 2010; Jin et al, 2009; Vandercone et al, 2012; Koenig et al, 2004; Koenig & Borries 2012; Roy et al, 2012; Tsuji et al, 2013), suggesting a significant trend of decreasing population. In the future, factors influencing population increase, such as human disturbance, habitat quality and inter-specific competition, should be explored.

Bisexual groups of genus of *Trachypithecus* are composed typically of OMGs and occasionally of MMGs. For example, MMGs in *T. leucocephalus* and *T. pileatus* account for 9-10% and 10-25%, respectively; and TMGs in *T. delacouri* and *T. geei* account for 29% and 67%, respectively (Table 3). The number of adult males in MMGs is mostly two and occasionally three (Koenig & Borries, 2012) and theri adult females are less than those in OMGs (*T. Pileatus*: Solanki et al, 2008; *T. delacouri*: Workman, 2010; *T. leucocephalus*: Li & Rogers, 2004; Jin et al, 2009), but the number of adult females in MMGs and OMGs of white-headed langurs (*T. Leucocephalus*) exhibit no differences. These phenomena indicate that MMG is not a strategy of males to monopolize more females (Jin et al, 2009). The occurrence of MMGs in white-headed langurs is the result of male replacement (Jin et al, 2009; Li & Rogers, 2004), which finally changes into OMGs or non-breeding groups (Jin et al, 2009). So the formation of MMGs in species of colobus may be age-graded or is only a temporary phenomenon during the process of male replacement (Jin et al, 2009; Sterck & Hooff, 2000).

Other than bisexual groups, there are also non-breeding groups and solitary males. Non-breeding groups mainly consist of males and occasionally females, suggesting that males play vital roles in sex dispersal (Jin et al, 2009; Kirkpatrick, 2007; Newton & Dunbar, 1994). In our study, no all-male group or a solitary male were observed, although 12 solitary males were previously reported in Fugong and Lushui counties near Myanmar. A similar phenomenon was also reported in species of colobus (Jin et al, 2009; Kirkpatrick et al, 1998; Newton & Dunbar, 1994). All-male groups were reported in white-headed langurs, but no in Shortridge's cpped langurs, which are important for promoting genetic communication among different populations and in avoiding inbreeding. However, the reason why all-male groups were not observed in our study is worth future exploration, for instance, wether they were poached or immigrated into other groups.

Under the influence of the warm and humid current brought by the southeast monsoon, the Dulongjiang valley experiences high precipitation, and has small yearly temperature variations (≤15 °C), with an average yearly temperature of 14.5 °C. The vegetation consists predominately of monsoon evergreen broad-leaved forests, warm temperate evergreen broad-leaved forest and broad-leaved deciduous forest, which provides many kinds of plant speices and abundant food resources for wild animals. Shortridge's langurs at the Dulongjiang valley have a long birth period (March to July) and scattered birth pattern. At the Pakhui Wildlife Sanctuary in India, the average highest and lowest yearly temperature is 28 °C and 19 °C, respectively, and the yearly average precipitation is 2 040 mm. Its optimal weather results in various vegetations, dominated by tropical ever-green and semi-evengreen broad-leaved forests and semitropical forest (Champion & Seth, 1968). Although local capped langur (*T. pileatus*) exhibits a birth peak, the birth pattern is very scattered (December to April next year) (Solanki et al, 2007). The scattered birth patterns in these two primates are likely adaptations to abundant food and mild seasonal changes in weather conditions and food resources. Conversely, blank-and-white snub-nosed monkeys inhabit temperate zones at high altitude with low temperatures, resulting in food shortage and severely seasonal changes in weather and food resources, and thus strict birth seasonality is found in their birth patterns. To ensure successful reproduction and increase fitness, these two primate species use different birth patterns to cope with specific environmental pressures.

In summary, Shortridge's langurs at the Dulongjiang valley are composed of one-male, multi-female groups without all-male groups, but with solitary males, which usually keeped distances from the breeding groups. There were, on average, eight individuals in each group and large habitat overlap between groups. The number of adult females in bisexual group was usually 2-3, smaller than the number in most species of *Trachypithecus*, which suggests a possible correlation between small number of adult females and limited suitable habitat and illegal hunting. Age structure of Shortridge's langurs indicated a trend of increasing potential. In the future, suitable habitat and threatening factors regarding Shortridge's langurs should be explored, and their population densities should be more precisely evaluated, from which feasible protection suggestions can be established.

ACKNOWLEDGEMENTS

Special thanks are given to the Nujiang Administrative Bureau of Gaoligongshan Nature Reserve for their support, Ding SQ and Meng XJ for their field assistance, and two anonymous reviewers for their useful suggestions.

REFERENCES

Andelman SJ. 1986. Ecological and social determinants of cercopithecine mating systems. *In*: Rubenstein DI, Wrangham RW. Ecological Aspects of Social Evolution: Birds and Mammals. Princeton: Princeton University Press, 201-216.

Boinski S, Garber PA. 2000. On the Move: How and Why Animals Travel in Groups. Chicago: University of Chicago Press.

Boonratana R. 1998. Wildlife survey training at Dong Hua Sao and Phou Xiang Thong National Biodiversity Conservation Areas, Lao RDR. IUCN/LSFP, Vientiane.

Bose J. 2003. 'Search for a Spectacle': *A conservation Survey of Phayre's Leaf Monkey (Trachypithecus phayrei)* in Assam and Mizoram. Wildlife Trust of India.

Charles-Dominique P. 1978. Solitary and gregarious prosimians: evolution of social structures in primates. *In*: Chivers DJ, Joysey KA. Recent Advances in Primatology, vol. 3. Evolution. London: Academic, 139-149.

Champion SHG, Seth SK. 1968. A Revised Survey of the Forest Types of India. Delhi: Manager of Publications.

Choudhury A. 1988. Phayre's leaf monkey (*Trachypithecus phayrei*) in Cachar. *Journal of Bombay Natural History Society*, **85**: 485-492.

Clutton-Brock TH, Harvey PH. 1977. Primate ecology and social organization. *Journal of Zoology,* **183**(1): 1-39.

CITES. 2014. Convention on International Trade in Endangered Species of Wild Fauna and Flora. Appendices I, II and III. Http://www.cites.org/eng/app/appendices.php [accessed 20 November 2014].

Crockett CM. Eisenberg JF. 1987. Howlers: variation in group size and demography. *In*: Smutes BB, Cheney DL, Seyfarth RM, Wrangham RW, Stuhsaker TT. Primate Societies. Chicago: University of Chicago Press, 54-68.

Crook JH, Gartlan JS. 1966. Evolution of primate societies. *Nature,* **210**(5042): 1200-1203.

Cui LW, Huo S, Zhong T, Xiang ZF, Xiao W, Quan RC. 2008. Social organization of black-and-white snub-nosed monkeys (*Rhinopithecus bieti*) at Deqin, China. *American Journal of Primatology,* **70**(2): 169-174.

Cui LW, Li YC, Li JF, He XY, Ma C, Scott MB, Li DH, Sun J, Sun WM, Xiao W. 2015. Distribution and conservation status of Shortridge's capped langurs (*Trachypithecus shortridge*i) in Yunnan, China. Oryx, (in press).

Dunbar RIM. 1988. Primate Social Systems. Beckenham: Croom Helm.

Eisenberg JF, Muckenhirn NA, Rudran R. 1972. The relation between ecology and social structure in primates. *Science,* **176**(4037): 863-874.

Emlen ST, Oring, LW. 1977. Ecology, sexual selection, and the evolution of mating systems. *Science,* **197**(4300): 215-223.

Fan PF, Garber P, Ma C, Ren GP, Liu CM, Chen XY, Yang JX. 2014. High dietary diversity supports large group size in Indo-Chinese gray langurs in Wuliangshan, Yunnan, China. *American Journal of Primatology,* doi: 10.1002/ajp.22361.

Green KM. 1981. Preliminary observations on the ecology and behavior of the capped langur, *Presbytis pileatus*, in the Madhupur Forest of Bangladesh. *International Journal of Primatology,* **2**(2): 131-151.

Groves CP. 2001. Primate Taxonomy. Washington and London: Smithsonian Institution Press.

Grueter CC. 2013. The Biology of the Snub-nosed Monkeys, Douc Langurs, Proboscis Monkeys, and Simakobus. New York: Nova Science Publishers, Inc.

Hamilton W, Bulger J. 1992. Facultative expression of behavioral differences between one-male and multimale savanna baboon groups. *American Journal of Primatology,* **28**(1): 61-71.

Harding LE. 2011. *Trachypithecus delacouvi* (Primates: Cercopithecidae). *Mammalian Species,* **43**(1): 118-128.

He DM, Li H. 1996. The Synthetical reserch of Dulong river and Dulong nationality. *In*: He DM, Li H. The Synthetical reserch of Dulong river and Dulong nationality. Kunming. Kunming: Yunnan Science and Technology Press, 1-24.

Htun S, Long YC, Richardson M. 2008. *Trachypithecus shortridgei*. *In*: IUCN 2014. The IUCN Red List of Threatened Species, Version 2014. 3 [online]. Available: Http: www.iucnredlist.org [Accessed 4 May 2015].

Hu G, Dong X, Luo HZ, Su XW, Li DY, Zhou CQ. 2011. The distribution and population dynamics of François' langur over the past two decades in Guizhou, China and threats to its survival. *Acta Theriologica Sinica,* **31**(3): 306-311. (in Chinese)

Huang CM, Zhou QH, Li YB, Cai XW, Wei FW. 2006. Activity rhythm and diurnal time budget of François langur (*Trachypithecus françoisi*) in Guangxi, China. *Acta Theriologica Sinica,* **26**(4): 380-386. (in Chinese)

Huang ZH, Zhou QH, Li YB, Wei SM, Wei H, Huang SM. 2007. Daily activity pattern and time budget of François langur *Trachypithecus françoisi* in Longgang Nature Reserve, China. *Acta Zoologica Sinica,* **53**(4): 589-599. (in Chinese)

Jin T, Wang DZ, Zhao Q, Yin LJ, Qin DG, Ren WZ, Pan WZ. 2009. Social organization of white-headed langurs (*Trachypithecus leucocephalus*) in the Nongguan Karst Hills, Guangxi, China. *American Journal of Primatology,* **71**(3): 206-213.

Kappeler PM. 1999. Convergence and nonconvergence in primate social systems. *In*: Fleagle JG, Janson CH, Reed KA. Primate Communities. Cambridge: Cambridge University Press, 158-170.

Kappeler PM. 2000. Primate males: History and theory. *In*: Kappeler PM. Primate Males. Cambridge: Cambridge University Press, 3-7.

Kappeler PM, van Schaik CP. 2002. Evolution of primate social systems. *International Journal of Primatology,* **23**(4): 707-740.

Kirkpatrick RC. 1996. Ecology and Behavior of the Yunnan Snub-Nosed Langur *Rhinopithecus bieti* (Colobinae). Ph. D. dissertation. University of California, Davis.

Kirkpatrick PC. 2007. The Asian colobines: diversity among leaf-eating monkeys. *In*: Campbell CJ, Fuentes A, MacKinnon KC, Panger M, Bearder SK. Primates in Perspective. New York: Oxford University Press, 186-200.

Kirkpatrick RC, Long YC, Zhong T, Xiao L. 1998. Social organization and range use in the Yunnan snub-nosed monkey *Rhinopithecus bieti*. *International Journal of Primatology,* **19**(1): 13-51.

Koenig A, Borries C. 2012. Social organization and male residence pattern in Phayre's leaf monkeys. *In*: Kappeler PM, Watts DP. Long-Term Field Studies of Primates. Berlin: Springer, 215-236.

Koenig A, Larney E, Lu A, Borries C. 2004. Agonistic behavior and dominance relationships in female Phayre's leaf monkeys: preliminary results. *American Journal of Primatology,* **64**(3): 351-357.

Kumar A, Solanki GS. 2008. Population status and conservation of capped langurs (*Trachypithecus pileatus*) in and around Pakke Wildlife Sanctuary, Arunachal Pradesh, India. *Primate Conservation,* **23**: 97-105.

Li GS, Chen YX, Sun WM, Wang XW, Huang ZP, Li YP, Xiang ZF, Ding W, Xiao W, Li M. 2014. Preliminary observation of population status and social organization of *Rhinopithecus strykeri* in Pianma Town, Nujiang County, China. *Acta Theriologica Sinica,* **34**(4): 323-328. (in Chinese)

Li YB, Wei ZY. 2012. Survey on distdbufion and populafion of *Trachypithecus francois*i in Nongdeng, Fusui of Guangxi. *Journal of Anhui Agricultural Sciences*, **40**(26): 12952-12953, 12956. (in Chinese)

Li ZY, Rogers E. 2004. Social organization of white-headed langurs *Trachypithecus leucocephalus* in Fusui, China. *Folia Primatologica,* **75**(2): 97-100.

Md-Zain BM, Ch'ng CE. 2011. The activity patterns of a group of cantor's dusky leaf monkeys (*Trachypithecus obscurus halonifer*). *International Journal of Zoological Research,* **7**(1): 59-61.

Medhi R, Chetry D, Bhattacharjee PC, Patiri BN. 2004. Status of *Trachypithecus geei* in a rubber plantation in Western Assam, India. *International Journal of Primatology,* **25**(6): 1331-1337.

Mitani JC, Gros-Louis J, Manson JH. 1996. Number of males in primate groups: Comparative tests of competing hypotheses. *American Journal of Primatology,* **38**(4): 315-332.

Mukherjee RP. 1978. Further observations on the golden langur (*Presbytis geei* KHAJURIA, 1956) with a note to capped langur (*Presbytis pileatus* BLYTH, 1843) of Assam. *Primates,* **19**(4): 737-747.

Mukherjee RP. 1982. Survey of non-human primates of Tripura. *Zoological Journal of the Linnean Society,* **34**: 70-81.

Mukherjee RP, Chaudhuri S, Murmu A. 1995. Population survey of South-Asian non-human primates in and around Darjeeling. *Primate Report,* **41**: 23-32.

Newton PN. 1988. The variable social organization of Hanuman langurs (*Presbytis entellus*), infanticide, and the monopolization of females. *International Journal of Primatology,* **9**(1): 59-77.

Newton PN, Dunbar RIM. 1994. Colobine monkey society. *In*: Davies AG, Oates JF. Colobine Monkeys: Their Ecology, Behaviour, and Evolution. Cambridge: Cambridge University Press, 311-346. Nunn CL. 1999. The number of males in primate social groups: A comparative test of the socioecological model. *Behavioral Ecology and Sociobiology,* **46**(1): 1-13.

Pocock RI. 1939. The Fauna of British India, Including Ceylon and Burma. Mammalia 1: Primates and Carnivora (in part), Families Felidae and Viverridae. London: Taylor & Francis.

Preuschoft S, Paul A. 2000. Dominance, egalitarianism, and stalemate: An experimental approach to male-male competition in Barbary macaques. *In*: Kappeler PM. Primate Males: Causes and Consequences of Variation in Group Composition. Cambridge: Cambridge University Press, 205-216.

Qi XG, Garber PA, Ji WH, Huang ZP, Huang H, Zhuang P, Guo ST, Wang XW, He G, Zhang P, Li BG. 2014. Satellite telemetry and social modeling offer new insights into the origin of primate multilevel societies. *Nature Communications*, **5**: Article number: 5296 doi: 10.1038/ncomms6296.

Qi XG, Li BG, Garber PA, Ji WH, Watanabe K. 2009. Social dynamics of the golden snub-nosed monkey (*Rhinopithecus roxellana*): female transfer and one-male unit succession. *American Journal of Primatology,* **71**(8): 670-679.

Roy D, Ashokkumar MA, Desai AA. 2012. Foraging ecology of Nilgiri Langur (*Trachypithecus johnii*) in Parimbikulam Tiger Reserve, Kerala, India. *Asian Journal of Conservation Biology,* **1**(2): 92-102.

Solanki GS, Kumar A, Sharma BK. 2007. Reproductive Strategies of *Trachypithecus pileatus* in Arunachal Pradesh, India. *International Journal of Primatology,* **28**(5): 1075-1083.

Solanki GS, Kumar A, Sharma BK. 2008. Winter food selection and diet composition of capped langur (*Trachypithecus pileatus*) in Arunachal Pradesh, India. *Tropical Ecology,* **49**(2): 157-166.

Srivastava A, Dunbar RIM. 1996. The mating system of Hanuman langurs: a problem in optimal foraging. *Behavioral Ecology and Sociobiology,* **39**(4): 219-226.

Stanford, CB. 1987. Ecology of the capped langur (*Presbytis pileata*) in Bangladesh. *American Journal of Primatology,* **12**(3): 373.

Stanford, CB. 1988. Ecology of the capped langur and Phayre's leaf monkey in Bangladesh. *Primate conservation*, (9): 125-128.

Stanford CB. 1991. Social dynamics of intergroup encounters in the capped langur (*Presbytis pileata*). *American Journal of Primatology,* **25**(1): 35-47.

Sterck EHM, Hooff JARAM. 2000. The number of males in langur groups: monopolizability of females or demographic processes. *In*: Kappeler PM. Primate Males: Causes and Consequences of Variation in Group Composition. Cambridge: Cambridge University Press, 120-129.

Terborgh J. 1986. The social systems of new world primates: adaptionist's view. *In*: Else JG, Lee PC. Primate Ecology and Conservation. Cambridge University Press, 199-211.

Timmins RJ, Steinmetz R, Poulsen MK, Evans TD, Duckworth JW, Boonratana R. 2013. The Indochinese silvered leaf monkey *Trachypithecus germaini* (*Sensu lato*) in Lao PDR. *Primate Conservation,* **26**: 75-87.

Tsuji A, Widayati KM, Hadi I, Suryobroto B, Watanabe K. 2013. Identification of individual adult female Javan lutungs (*Trachypithecus auratus sondaicus*) by using patterns of dark pigmentation in the pubic area. *Primates,* **54**(1): 27-31.

Vandercone RP, Dinadh C, Wijethunga G, Ranawana K, Rasmussen DT. 2012. Dietary Diversity and Food Selection in Hanuman Langurs (*Semnopithecus entellus*) and Purple-Faced Langurs (*Trachypithecus vetulus*) in the Kaludiyapokuna Forest Reserve in the Dry Zone of Sri Lanka. *International Journal of Primatology,* **33**(6): 1382-1405.

van Hooff JARAM. 2000. Relationships among non-human primate males: A deductive framework. *In*: Kappeler PM. Primate Males: Causes and Consequences of Variation in Group Composition. Cambridge: Cambridge University Press, 183-191.

van Schaik CP, van Hooff JARAM. 1983. On the ultimate causes of primate social systems. *Behaviour,* **85**(1): 91-117.

van Schaik CP, Hőrstermann M. 1994. Predation risk and the number of adult males in a primate group: a comparative test. *Behavioral Ecology and Sociobiology,* **35**(4): 261-272.

van Schaik CP, Kappeler PM. 1997. Infanticide risk and the evolution of male–female association in primates. *Proceedings of the Royal Society of London. Series B: Biological Sciences,* **264**(1388): 1687-1694.

Workman C. 2010. The Foraging Ecology of the Delacour's Langur (*Trachypithecus delacouri*) in Van Long Nature Reserve, Vietnam. Ph. D. Dissertation, Duke University.

Wrangham RW. 1980. An ecological model of female-bonded primate groups. *Behaviour*, **75**(3): 262-300.

Wroughton RC. 1915. Bombay Natural History Society's Mammal Survey of India, Burma and Ceylon. Report No. 16. Dry Zone, central Burma and Mt. Popa. *Journal of the Bombay Natural History Society.* **23**: 460-480

Zheng XJ. 1993. A primary study on the ecology of *Presbytis phayrei shanicus. In*: Ye ZZ. Langur Biology. Kunming: Yunnan Science and Technology Press, 52-69. (in Chinese)

Zhou QH, Huang CM, Li M, Wei FW. 2009. Sleeping site use by *Trachypithecus francoisi* at Nonggang Nature Reserve, China. *International Journal of Primatology,* **30**(2): 353-365.

Establishment of HIV-1 model cell line GHOST(3) with stable DRiP78 and NHERF1 knockdown

Lin ZHANG[1,†], Xu-He HUANG[2,†], Ping-Ping ZHOU[2], Guo-Long YU[2], Jin YAN[2], Bing QIN[2], Xin-Ge YAN[2], Li-Mei DIAO[2], Peng LIN[2], Yi-Qun KUANG[1,2,*]

[1] *Center for Translational Medicine*, *Huaihe Clinical Institute*, *Henan University*, *Kaifeng* 475000, *China*

[2] *Guangdong Institute of Public Health and Institute of AIDS Control and Prevention*, *Guangdong Center for Disease Control and Prevention*, *Guangzhou* 510433, *China*

ABSTRACT

Chemokine receptors CXCR4 and CCR5 are indispensable co-receptors for HIV-1 entry into host cells. In our previous study, we identified that dopamine receptor-interacting protein 78 (DRiP78) and Na^+-H^+ exchanger regulatory factor 1 (NHERF1) are the CXCR4 and CCR5 homo- or hetero-dimer-interacting proteins. DRiP78 and NHERF1 are able to influence the co-receptor internalization and intracellular trafficking. Over-expression of NHERF1 affects the ligands or HIV-1 gp120-induced CCR5 internalization and HIV-1 production. It is reasonable to speculate that DRiP78 and NHERF1, as well as the signaling pathways involved in viral replication, would probably affect HIV-1 replication through regulating the co-receptors. In this present study, we designed two short hairpin RNAs (shRNAs) targeting the DRiP78 and NHERF1, respectively, and constructed the pLenti6/BLOCK-iT-DEST lentiviral plasmids expressing DRiP78 or NHERF1 shRNA. The packaged lentiviruses were used to transduce the widely-applied HIV-1 model cell line GHOST(3). Then, cells with stable knockdown were established through selecting transduced cells with Blasticidin. This study, for the first time, reported the establishment of the GHOST(3) with DRiP78 and NHERF1 knockdown, which is the first stable cell line with HIV-1 co-receptor-interacting molecular defects.

Keywords: HIV-1; DRiP78; NHERF1; shRNA; GHOST(3) cells

INTRODUCTION

Human immunodeficiency virus type 1 (HIV-1) is the etiological agent of human acquired immunodeficiency syndrome (AIDS) that severely threats human health worldwide during the past three decades. The chemokine receptors CXCR4 and CCR5 are co-receptors for HIV-1 entry into host $CD4^+$ cells. Their ligands can strongly inhibit the replication of HIV-1 (Deng et al, 1996; Feng et al, 1996). Previous studies showed that after infection, CXCR4- and CCR5-tropic HIV-1 could activate different signaling pathways and thereafter result in different gene expression profiles (Cicala et al, 2006), suggesting that these two receptors can mediate different internalization and intracellular transport pathways to complete the infection and replication of the virus into host cells. Dopamine receptor-interacting protein 78 (DRiP78), also known as DnaJC14, Jiv or HDJ3, is a member of the heat shock proteins of the Hsp40 family (Kelley, 1998). Proteins of this family contain a J model domain composed of 70 amino acids, which plays an important role in raising the Hsp70 family membership and stimulating ATP hydrolysis during chaperone processing. DRiP78 is a molecular chaperone binds to endoplasmic reticulum and is involved in the regulations of a variety of Guanosine-binding protein coupled receptors (GPCR), including D1 dopamine receptor, M2 muscarinic receptor, AT1 angiotensin II receptor, adenosine receptor and the β2 adrenergic receptor of cell membrane transport (Bermak et al, 2001; Dupré et al, 2007; Leclerc et al, 2002; Málaga-Diéguez et al, 2010). Meanwhile, DRiP78 is also involved in the regulations of $G_{\beta\gamma}$ subunit of G protein assembly (Dupré et al, 2007).

Na^+-H^+ exchanger regulatory factor 1 (NHERF1) is an adaptor protein binds to a variety of GPCR. NHERF1, also called Ezrin-Radixin-Moesin binding phosphate phosphoprotein 50 (EBP50), is consisted with three functional domains,

Received: 21 January 2015; Accepted: 20 March 2015

Foundation items: This study was supported by the Science and Technology Planning Project of Guangdong Province of China (2012B031800267); the Natural Science Foundation of Guangdong Province of China (S2013010011860) and the National Natural Science Foundation of China (31200130 and 81371812)

†Authors contributed equally to this work

*Corresponding author, E-mail: yqkuang@henu.edu.cn

including two N-terminal tandem PDZ domains and one C-end Ezrin-Radixin-Moesin (ERM) domain (Hung & Sheng, 2002). NHERF1 is an important factor of protein kinase in inhibiting Na^+/H^+ exchange isoform 3 (NHE-3) and was initially identified in 1987 (Weinman et al, 1995). Studies showed that NHERF1 is involved in lots of events related with GPCR, ion channels, as well as transporter recycling and sorting (Cao et al, 1999; Lazar et al, 2004; Li et al, 2002; Wang et al, 2007).

Our previous studies showed that DRiP78 and NHERF1 were interacting proteins of HIV-1's co-receptors, CXCR4 and CCR5, but their recognition specificities were different (Hammad et al, 2010; Kuang et al, 2012a). DRiP78 recognizes and binds to the homologous dimers of CXCR4 and CCR5, but not the heterologous dimers of CXCR4-CCR5, whereas, NHERF1 binds to the homologous dimers of CCR5, but not the homologous dimers of CXCR4 nor heterologous dimers of CXCR4/CCR5.

DRiP78 promotes the formation of homologous dimers complex and the signal assembly of G protein subunit and CCR5, but cannot affect the assembly of heterologous dimers (Kuang et al, 2012a). DRiP78 regulates the signal complex of co-receptors CXCR4/CCR5, specifically, and influences the migration of receptor-mediated downstream biological function entry into immune cells (Kuang et al, 2012a). The molecular chaperone, DRiP78, may represent a novel class of target, which regulates the expression levels of receptors in the cytoplasm, and finally affects their binding on the cell surface of chemokine and related viruses, such as HIV-1. However, the effects of DRiP78 on HIV-1 entry and replication and the underlying mechanisms are still unclear. Therefore, the establishment of HIV-1 model cell line GHOST(3) with stable silencing of DRiP78 and NHERF1 is critical in understanding the roles of DRiP78 and NHERF1 play in the entry and replication of HIV-1 and the mechanisms involved.

MATERIALS AND METHODS

shRNA design and lentiviral plasmid construction

The nucleic acid sequences for RNA interference with human DRiP78 and NHERF1 were as follow: human DRiP78: 5′-CCG AGG AAC UAU GUC AAC UUG GAC A-3′ and human NHERF1: 5′-CAG AAG GAG AAC AGT CGT GAA-3′, respectively. The shRNA oligos of interest were synthesized by Invitrogen, China (Table 1).

The construction of shRNA-expressing lentiviral vector was outlined in Figure 1. The synthesized complementary oligo DNA was annealed and ligated with linear pENTR/U6-EGFP plasmid. The ligated product was transformed into DH5α competent cells and plated on LB plates containing 50 μg/mL Kanamycin, and then incubated inverted at 37 °C overnight. Three clonies were picked up from each plates and shaked at 37 °C overnight. The successful plasmids were named pENTR/U6-EGFP-shDRiP78 and pENTR/U6-EGFP-shNHERF1, respectively. Finally the plasmids were verified by sequencing.

Lentiviral interference vectors were constructed by LR clonase II recombining plasmid with the target vector pLenti6/BLOCK-iT-DEST, and ligated the target gene with the destination vector plasmid. These two recombinant plasmids were named pLenti6/BLOCK-iT-DEST-shDRiP78 and pLenti6/BLOCK-iT-DEST-shNHERF1, respectively. They were transformed into Stbl3 competent cells and plated on LB plates containing 100 μg/mL of Ampicillin. The plates were screened and monoclonies were picked up and were amplified in LB liquid medium containing 100 μg/mL Ampicillin. The plasmid was extracted using Axygen plasmid DNA kit and verified by direct sequencing.

Lentiviral package and preparation

The HEK293T cells on logarithmic phase were counted at the density of 6×10^6 cells/10 cm culture dish, and then were incubated at 37 °C, 5% CO_2, overnight. Before transfection, culture medium was replaced with 5 mL Opti-MEM medium (Invitrogen). Packaging mix (9 μg, Invitrogen) and lentiviral expression plasmid (3 μg) were added into 1.5 mL Opti-MEM and were mixed gently. Lipofectamine 2000 (36 μL, Invitrogen) was added into 1.5 mL Opti-MEM and was mixed gently, and then incubated at room temperature for 5 min. The diluted plasmid solution and diluted Lipofectamine 2000 were mix gently and were incubated at room temperature for 20 min. Plasmid-liposome complex (3 mL) was added carefully into the cells and was mixed gently, then incubated 6 hour in a 37 °C, 5% CO_2 incubator. Then, the medium was replaced with DMEM complete medium containing 10% fetal bovine serum (FBS). Fourty-eight hour later, the cell culture supernatants were collected, and were centrifuged at 3 000 g for 10 min to remove cells and debris, and then were filtered with a 0.45 μm filter. The clear viral supernatant was concentrated by ultracentrifugation at 50 000 g for 2 hour. The supernatant was removed, and the viral particles were resuspended in Opti-MEM. The viral stock was titrated and alliquoted into tubules for storage at -80 °C for later use. The produced shRNA-expressing lentiviral particles were designated as Lenti-shDRiP78 and Lenti-shNHERF1, respective.

Table 1 Target shRNA sequences and primers of human DRiP78 and NHERF1

Oligo type	Oligo DNA (5′-3′)
Human DRiP78 target sequence	CCGAGGAACUAUGUCAACUUGGACA
shRNA-U6-DRiP78-1F primer	CACCGCCGAGGAACTATGTCAACTTGGACACGAATGTCCAAGTTGACATAGTTCCTCGG
shRNA-U6-DRiP78-1R primer	AAAACCGAGGAACTATGTCAACTTGGACATTCGTGTCCAAGTTGACATAGTTCCTCGGC
Human NHERF1 target sequence	CAGAAGGAGAACAGUCGUGAA
shRNA-U6-NHERF1-2F primer	CACCGCAGAAGGAGAACAGTCGTGAACGAATTCACGACTGTTCTCCTTCTG
shRNA-U6-NHERF1-2R primer	AAAACAGAAGGAGAACAGTCGTGAATTCGTTCACGACTGTTCTCCTTCTGC

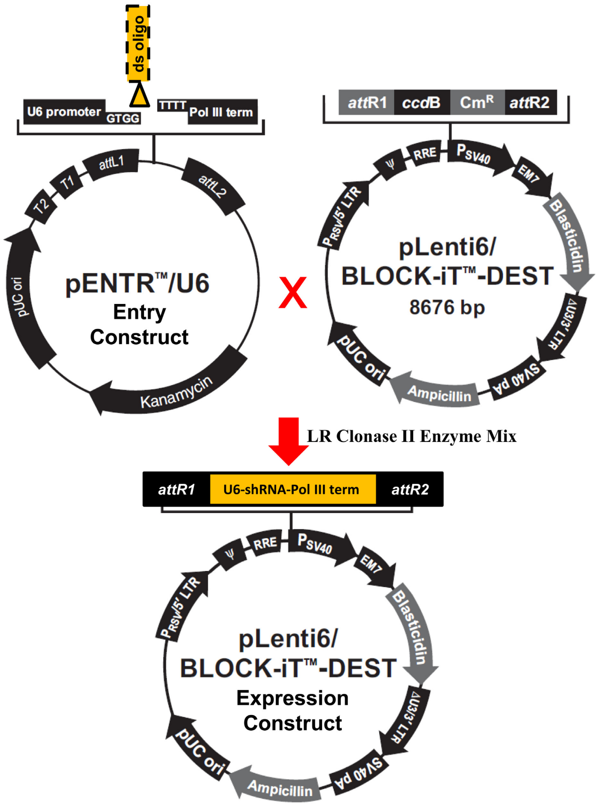

Figure 1 Construction of the shRNA-expressing lentiviral vector

The synthesized complementary oligos (shRNA of target gene) were annealed to produce the double strand oligo (ds oligo, highlighted in yellow). The ds oligo was inserted into the pENTR/U6 vector to generate the pENTR/U6-shRNA construct. The pENTR/U6-shRNA was recombined with the destination vector pLenti6/BLOCK-iT-DEST to finally generate the pLenti6/BLOCK-iT-DEST-shRNA lentiviral expression construct.

Cell culture

HEK293T cells were cultured in DMEM complete medium with 10% FBS, 100 mg/mL Penicillin and 100 U Streptomycin, at 37 °C, 5% CO_2. The GHOST(3)-CXCR4 and GHOST(3)-CCR5 were obtained from Dr. Vineet N. KewalRamani and Dr. Dan R. Littman through the NIH AIDS Research and Reference Reagent Program, Division of AIDS, NIAID, NIH (Mörner et al, 1999). The GHOST(3) cells were cultured in DMEM complete medium, supplemented with 500 μg/mL G418 (CalBiochem), 100 μg/mL Hygromycin (CalBiochem) and 1 μg/mL Puromycin (CalBiochem) in a 37 °C, 5% CO_2 incubator.

Blasticidin killing assay

GHOST(3)-CXCR4 and GHOST(3)-CCR5 cells at log state were collected and plated at 3×10^4 cells/well in 24-well plate with 2 mL DMEM complete medium. Cells were allowed to adhere overnight and were at approximately 25% confluence. A series concentration of Blasticidin (0, 2, 4, 6, 8, and 10 μg /mL) was added and cells were incubated at 37 °C, 5% CO_2. The selective media was replenished every 3-4 days, and the percentage of surviving cells was observed. Two weeks later, the viability of cells were observed under microscope to determine the sensible concentration of GHOST(3) cells to Blasticidin.

Lentiviral infection and stable cell selection

GHOST-CXCR4 and GHOST-CCR5 cells were seeded in 1 mL of 12 culture plates, 37 °C, 5% CO_2 overnight, to make sure the cell confluence is around 50%. The medium was changed with DMEM with 5 μg /mL of Polybrene (Santa Cruz) 24 hour later. Lenti-shDRiP78 and Lenti-shNHERF1 and control lentiviral supernatants were thawed in room-temperature water-bath, and then were added into cells; mixed well and incubated at 37 °C, 5% CO_2. Twenty-four hour later, passaged cells at the ratio of 1:5 were cultured overnight. The DMEM medium was changed with sensitive Blasticidin on the next day; and with fresh selection medium on the third day. Two weeks later, cell clones were collected for knockdown efficiency analysis by measuring protein expression levels.

Western Blot

Expression and knockdown efficiency of DRiP78 and NHERF1in GHOST(3) cells was detected by Western Blot. The stable-knockdown GHOST(3)-CXCR4 and GHOST(3)-CCR5 cells were collected and centrifuged, and then the supernatants were dispersed; RIPA lysis buffer (with EDTA-free protease inhibitor cocktail and PhosSTOP) was added, mixed well and set on ice for 30 min, mixed every 5 min; centrifuged at 12 000 g, 4 °C for 10 min. Cell lysates were transferred to a new tube, and protein concentrations were measured by the Bradford Reagent Ready-to-use Protein Measurement Kit (Kangcheng). Equal amount of proteins were separated in 10% SDS-PAGE, and then proteins were transferred to PVDF membrane (Millipore) via Semi-Dry electronic transfer. The membranes were blocked in 5% fat-skim milk for 2 hour at room temperature. The rabbit anti-DRiP78 polyclonal (Sigma-Aldrich) and rabbit anti-NHERF1 monoclonal (Cell Signaling) were incubated with the membrane overnight at 4 °C. The mouse anti-GAPDH monoclonal (Kangcheng) was used as a loading control. On the second day, membranes were washed in 0.05% Tween-20-TBST for 3 times, 5 min each. The HRP-conjugated goat anti-rabbit and anti-mouse second antibodies were then incubated with the PVDF membranes for 1 hour at room temperature. The membranes were washed and developed with the Western Lighting Plus ECL reagent (Perkin-Elmer). ImageJ v1.48 software (National Institutes of Health, USA) was used for densitometric quantitation of western blots.

RESULTS

Construction of lentiviral expression vectors and package of lentiviral particles

The constructed lentiviral expression vectors were sequenced and were aligned with the target gene sequences to verify the direction and shRNA sequences in the constructs. The

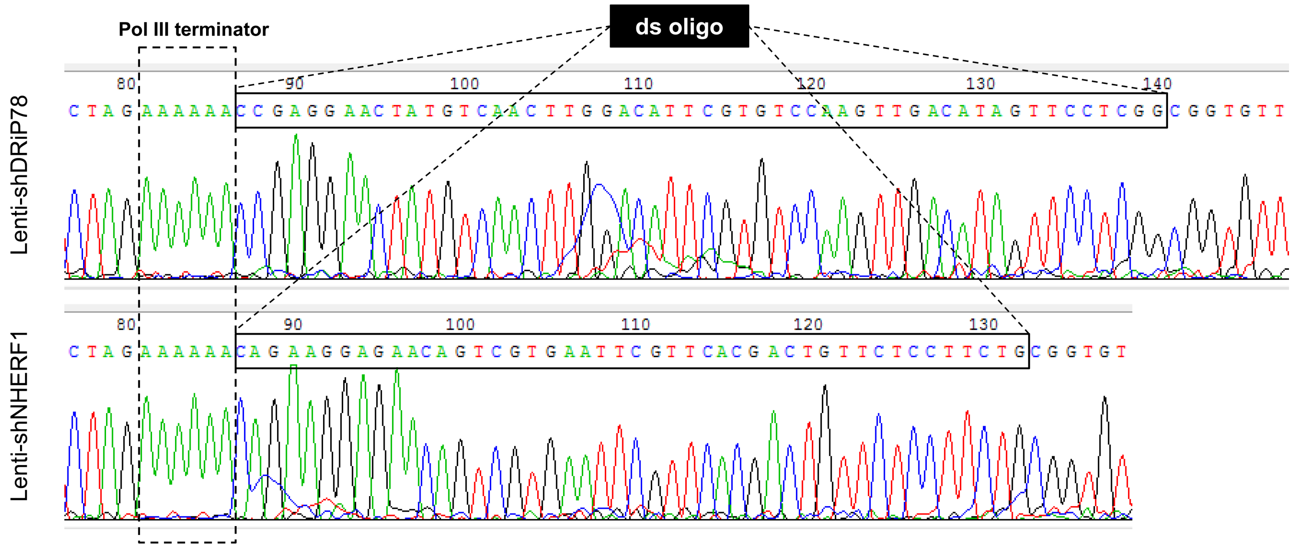

Figure 2 Sequences of inserted shRNA of target genes

The sequences of inserted DRiP78 shRNA (upper panel) and NHERF1 shRNA (lower panel) are shown. The dotted box indicates the Pol III terminator; the boxes indicate the shRNA sequences of DRiP78 (upper) and NHERF1 (lower).

sequencing data showed that the shRNA oligos in the vectors were correct and in the right directions.

Blasticidin sensitivity assay

The sensitive concentrations of HIV-1 susceptible model cell lines GHOST(3)-CXCR4 and GHOST(3)-CCR5 to Blasticidin were determined via killing assay. Cells were plated at approximately 25% confluence and cultured in DMEM complete medium containing 0, 2, 4, 6, 8, and 10 μg/mL of Blasticidin. Selective media were replenished every 3-4 days, and the percentage of survived cells was observed. Two weeks later, the sensitive concentrations of GHOST(3)-CXCR4 and GHOST(3)-CCR5 were determined according to the observations of viable cells in Blasticidin. The microscopic graphs showed that both cell lines were insensitive to the selection media containing 0, 2 and 4 μg/mL of Blasticidin on day 14 post the addition of Blasticidin (Figure 3). The cells were inviable in the selection medium containing 6 μg/mL of Blasticidin. When the selection concentration reached 8 and 10 μg/mL, almost all of the cells were killed.

DRiP78 and NHERF1 expression knockdown in GHOST(3)

The lentivrial particles expressing DRiP78 or NHERF1 shRNA challenged GHOST(3)-CXCR4 and GHOST(3)-CCR5 cells were selected in the selection medium with their sensitive concentrations of Blasticidin. GHOST(3) cells stably knocked down with DRiP78 and NHERF1 were collected and used for protein expression measurement by western blot. In both selected GHOST(3)-CXCR4 and GHOST(3)-CCR5 cell lines, remarkably low expression levels of DRiP78 and NHERF1 were observed (Figure 4). The relative density quantitation of blots showed that in GHOST(3)-CXCR4 cells, the DRiP78 and NHERF1 expressions were decreased by 89.75% and 79.69%, respectively, compared with the control cells (Figure 4),whereas, in the selected GHOST(3)-CCR5 cells, those of DRiP78 and NHERF1 decreased by 78.29% and 74.55%, respectively (Figure 4).

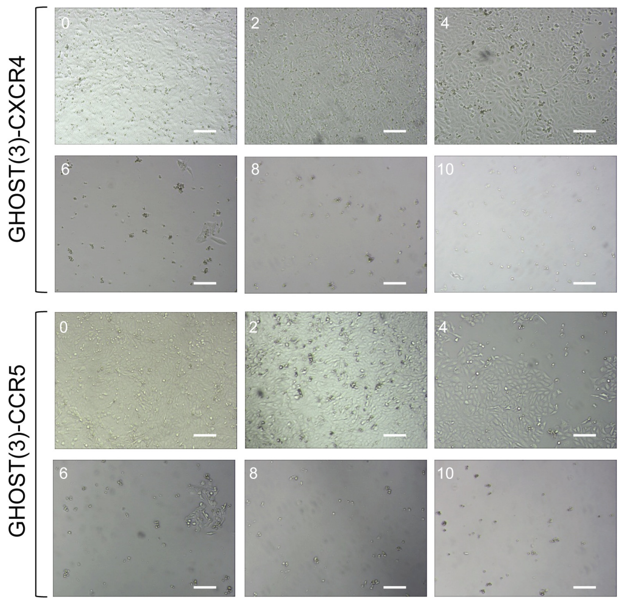

Figure 3 Sensitive concentrations of GHOST(3) cells to Blasticidin

The growth status of GHOST(3)-CXCR4 (upper panel) and GHOST(3)-CCR5 (lower panel) were imaged under microscope on the day 14 post the addition of Blasticidin; The number on the images represents the antibiotic concentration (0, 2, 4, 6, 8, and 10 μg /mL respectively); The magnification of microscope is 10×10; Results were shown of representative data from at least three independent trials; Scale bars=50 μm.

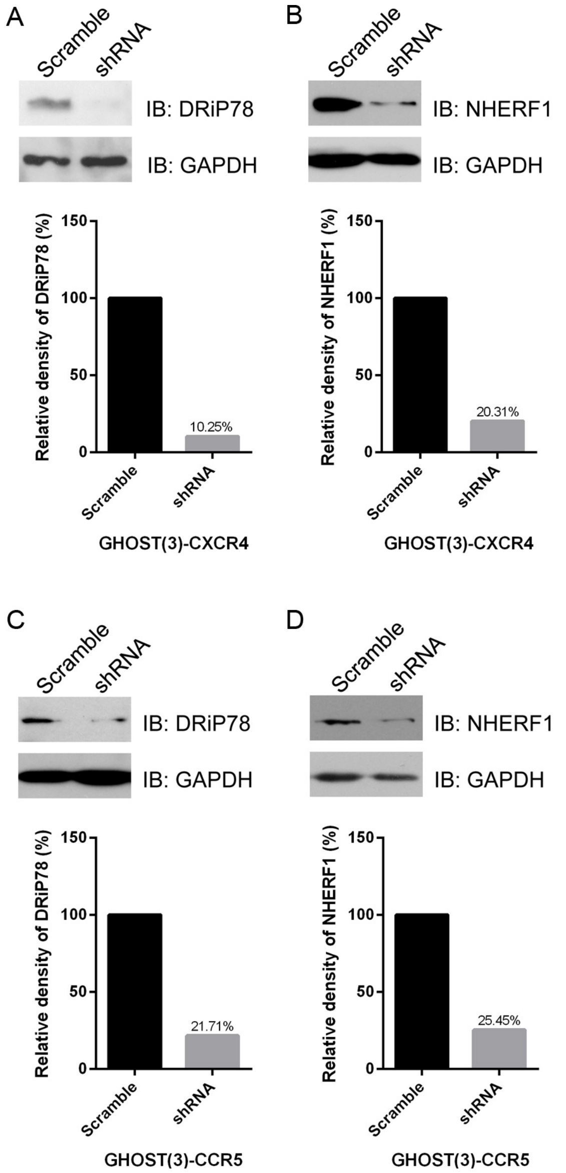

Figure 4 Target protein expressions in stable knocked down GHOST(3) cells

Expression levels of DRiP78 (A) and NHERF1(B) in GHOST(3)-CXCR4 cells and those of DRiP78 (C) and NHERF1 (D) in GHOST(3)-CCR5 cells were detected by western blot; The Scramble and shRNA indicate the control GFP shRNA-transduced cells and target genes (DRiP78 or NHERF1), shRNA-transduced GHOST(3) cells, respectively; The housekeeping GAPDH was used as a loading control; The relative densitometric ratios of each protein to β-tubulin were shown below each panel; Representative data from 3-4 independent trials were shown.

DISCUSSION

Susceptibility of HIV-1 infection, both *in vitro* and *in vivo*, requires interactions between the envelope glycoprotein gp120 and the primary receptor CD4 (Dalgleish et al, 1984; Klatzmann et al, 1984), as well as the co-receptors, either CCR5 or CXCR4, the members of the chemokine receptor family. CCR5-dependent viruses are predominantly responsible for the early stages of infection, such as the inter-individual transmission and the the viral pandemics sustaining. However, the CXCR4-dependent viruses, as well as the dual tropic R5X4, emerge in individuals only at the late, immunologically suppressed stages of diseases (Tsibris & Kuritzkes, 2007). These epidemiological observations imply that the co-receptor-mediated signaling affects the replication efficiency of the virus to its target cells. The identifications of HIV-1 co-receptor-interacting molecules are important in understanding the viral entry and post-entry viral replication proceedings. Our previous studies indicate that NHERF1 interacts with CCR5 via its PDZ2 domain (Hammad et al, 2010; Kuang et al, 2012b). DRiP78 can bind with both CXCR4 and CCR5 (Kuang et al, 2012a).

GHOST(3) cells are derived from human osteo sarcoma (HOS) cells that are stably transduced with MV7neo-T4 (CD4) retroviral vector (Mörner et al, 1999). These cells also contain the gene of green fluorescent protein (GFP) driven by the HIV-2_{ROD} LTR. GHOST(3) cells stably express CD4, as well as CXCR4 and / or CCR5, which are required for infection, through antibiotic resistant selections. The high levels of antibiotics ensure the stability and expressions of both CD4 and its co-receptors. Viral entry activates Tat and the subsequent transcription drives the GFP expression after infection. The ease to use and quick evaluation are the main advantages of the GHOST(3) cell assay. These cells can be used to titer viruses, to determine phenotypic properties, and to evaluate drug sensitivities and antibody neutralizations. In this present study, we used the widely-applied BLOCK-iT Lentiviral RNAi Expression system to silence DRiP78 and NHERF1. Blasticidin-selective GHOST(3) cells showed optimal selections at the concentration of 8 µg/mL. The stable GHOST(3) cells selected in Blasticidin medium were morphologically normal compared with cells without transduction (data not shown), suggesting that the expression of shRNA was not detrimental to the GHOST(3) cells. The results of western blot showed that the shRNA sequences used in this work were not off-targeted, and the efficiency in silencing DRiP78 and NHERF1 genes was comparable with the siRNA transfection assay applied in previous studies (Hammad et al, 2010; Kuang et al, 2012a, b; Yi et al, 2011). These findings indicate that the lentiviral RNAi expression system carrying an effective shRNA is an optimal method to silence a target gene, and the shRNA sequences for human DRiP78 and NHERF1 used in this present study can be applied in future works.

In conclusion, here, we have for the first time successfully established the HIV-1 susceptible model GHOST(3) cells expressing receptor CD4 and its co-receptor CXCR4 or CCR5 with stable DRiP78 or NHERF1 knockdown. The establishment of this stable cell line is critical in developing novel anti-viral drugs in the future.

ACKNOWLEDGEMENTS

We thank the NIH AIDS Research and Reference Reagent Program, Division of AIDS, NIAID, NIH for providing the GHOST(3) cell lines.

REFERENCES

Bermak JC, Li M, Bullock C, Zhou QY. 2001. Regulation of transport of the dopamine D1 receptor by a new membrane-associated ER protein. *Nature Cell Biology,* **3**(5): 492-498.

Cao TT, Deacon HW, Reczek D, Bretscher A, von Zastrow M. 1999. A kinase-regulated PDZ-domain interaction controls endocytic sorting of the β2-adrenergic receptor. *Nature,* **401**(6750): 286-290.

Cicala C, Arthos J, Martinelli E, Censoplano N, Cruz CC, Chung E, Selig SM, Van Ryk D, Yang J, Jagannatha S, Chun TW, Ren P, Lempicki RA, Fauci AS. 2006. R5 and X4 HIV envelopes induce distinct gene expression profiles in primary peripheral blood mononuclear cells. *Proceedings of the National Academy of Sciences of the United States of America,* **103**(10): 3746-3751.

Dalgleish AG, Beverley PC, Clapham PR, Crawford DH, Greaves MF, Weiss RA. 1984. The CD4 (T4) antigen is an essential component of the receptor for the AIDS retrovirus. *Nature,* **312**(5996): 763-767.

Deng H, Liu R, Ellmeier W, Choe S, Unutmaz D, Burkhart M, Di Marzio P, Marmon S, Sutton RE, Hill CM, Davis CB, Peiper SC, Schall TJ, Littman DR, Landau NR. 1996. Identification of a major co-receptor for primary isolates of HIV-1. *Nature,* **381**(6584): 661-666.

Dupré DJ, Robitaille M, Richer M, Ethier N, Mamarbachi AM, Hébert TE. 2007. Dopamine receptor-interacting protein 78 acts as a molecular chaperone for Gγ subunits before assembly with Gβ. *Journal of Biological Chemistry,* **282**(18): 13703-13715.

Feng Y, Broder CC, Kennedy PE, Berger EA. 1996. HIV-1 entry cofactor: functional cDNA cloning of a seven-transmembrane, G protein-coupled receptor. *Science,* **272**(5263): 872-877.

Hammad MM, Kuang YQ, Yan R, Allen H, Dupré DJ. 2010. Na^+/H^+ exchanger regulatory factor-1 is involved in chemokine receptor homodimer CCR5 internalization and signal transduction but does not affect CXCR4 homodimer or CXCR4-CCR5 heterodimer. *Journal of Biological Chemistry,* **285**(45): 34653-34664.

Hung AY, Sheng M. 2002. PDZ domains: structural modules for protein complex assembly. *Journal of Biological Chemistry,* **277**(8): 5699-5702.

Kelley WL. 1998. The J-domain family and the recruitment of chaperone power. *Trends in Biochemical Sciences,* **23**(6): 222-227.

Klatzmann D, Champagne E, Chamaret S, Gruest J, Guetard D, Hercend T, Gluckman JC, Montagnier L. 1984. T-lymphocyte T4 molecule behaves as the receptor for human retrovirus LAV. *Nature,* **312**(5996): 767-768.

Kuang YQ, Charette N, Frazer J, Holland PJ, Attwood KM, Dellaire G, Dupré DJ. 2012a. Dopamine receptor-interacting protein 78 acts as a molecular chaperone for CCR5 chemokine receptor signaling complex organization. *PLoS One,* **7**(7): e40522.

Kuang YQ, Pang W, Zheng YT, Dupré DJ. 2012b. NHERF1 regulates gp120-induced internalization and signaling by CCR5, and HIV-1 production. *European Journal of Immunology,* **42**(2): 299-310.

Lazar CS, Cresson CM, Lauffenburger DA, Gill GN. 2004. The Na^+/H^+ exchanger regulatory factor stabilizes epidermal growth factor receptors at the cell surface. *Molecular Biology of the Cell,* **15**(12): 5470-5480.

Leclerc PC, Auger-Messier M, Lanctot PM, Escher E, Leduc R, Guillemette G. 2002. A polyaromatic caveolin-binding-like motif in the cytoplasmic tail of the type 1 receptor for angiotensin II plays an important role in receptor trafficking and signaling. *Endocrinology,* **143**(12): 4702-4710.

Li JG, Chen C, Liu-Chen LY. 2002. Ezrin-radixin-moesin-binding phosphoprotein-50/Na^+/H^+ exchanger regulatory factor (EBP50/NHERF) blocks U50, 488H-induced down-regulation of the human κ opioid receptor by enhancing its recycling rate. *Journal of Biological Chemistry,* **277**(30): 27545-27552.

Málaga-Diéguez L, Yang Q, Bauer J, Pankevych H, Freissmuth M, Nanoff C. 2010. Pharmacochaperoning of the A1 adenosine receptor is contingent on the endoplasmic reticulum. *Molecular Pharmacology,* **77**(6): 940-952.

Mörner A, Björndal A, Albert J, Kewalramani VN, Littman DR, Inoue R, Thorstensson R, Fenyö EM, Björling E. 1999. Primary human immunodeficiency virus type 2 (HIV-2) isolates, like HIV-1 isolates, frequently use CCR5 but show promiscuity in coreceptor usage. *Journal of Virology,* **73**(3): 2343-2349.

Tsibris AM, Kuritzkes DR. 2007. Chemokine antagonists as therapeutics: focus on HIV-1. *Annual Review of Medicine*, **58**: 445-459.

Wang B, Bisello A, Yang Y, Romero GG, Friedman PA. 2007. NHERF1 regulates parathyroid hormone receptor membrane retention without affecting recycling. *Journal of Biological Chemistry,* **282**(50): 36214-36222.

Weinman EJ, Steplock D, Wang Y, Shenolikar S. 1995. Characterization of a protein cofactor that mediates protein kinase A regulation of the renal brush border membrane Na^+-H^+ exchanger. *The Journal of Clinical Investigation,* **95**(5): 2143-2149.

Yi Z, Sperzel L, Nürnberger C, Bredenbeek PJ, Lubick KJ, Best SM, Stoyanov CT, Law LM, Yuan Z, Rice CM, MacDonald MR. 2011. Identification and characterization of the host protein DNAJC14 as a broadly active flavivirus replication modulator. *PLoS Pathogens,* **7**(1): e1001255.

Autophagy prevents autophagic cell death in *Tetrahymena* in response to oxidative stress

Si-Wei ZHANG, Jiang-Nan FENG, Yi CAO, Li-Ping MENG, Shu-Lin WANG*

State Key Laboratory of Genetic Engineering, *Institute of Genetics*, *School of Life Sciences, Fudan University*, *Shanghai* 200433, *China*

ABSTRACT

Autophagy is a major cellular pathway used to degrade long-lived proteins or organelles that may be damaged due to increased reactive oxygen species (ROS) generated by cellular stress. Autophagy typically enhances cell survival, but it may also act to promote cell death under certain conditions. The mechanism underlying this paradox, however, remains unclear. We showed that *Tetrahymena* cells exerted increased membrane-bound vacuoles characteristic of autophagy followed by autophagic cell death (referred to as cell death with autophagy) after exposure to hydrogen peroxide. Inhibition of autophagy by chloroquine or 3-methyladenine significantly augmented autophagic cell death induced by hydrogen peroxide. Blockage of the mitochondrial electron transport chain or starvation triggered activation of autophagy followed by cell death by inducing the production of ROS due to the loss of mitochondrial membrane potential. This indicated a regulatory role of mitochondrial ROS in programming autophagy and autophagic cell death in *Tetrahymena*. Importantly, suppression of autophagy enhanced autophagic cell death in *Tetrahymena* in response to elevated ROS production from starvation, and this was reversed by antioxidants. Therefore, our results suggest that autophagy was activated upon oxidative stress to prevent the initiation of autophagic cell death in *Tetrahymena* until the accumulation of ROS passed the point of no return, leading to delayed cell death in *Tetrahymena*.

Keywords: Autophagy; Autophagic cell death; Lysosome; Mitochondria; Reactive oxygen species; *Tetrahymena*

Abbreviations used: ROS: reactive oxygen species; ATG: autophagy-related genes; PND: programmed nuclear degradation; CQ: chloroquine; 3MA: 3-methyladenine; PI3K: phosphatidylinositol-3 kinase; MOMP: mitochondrial membrane potential.

INTRODUCTION

Autophagy is a well-conserved catabolic process used to degrade long-lived proteins and cytoplasmic organelles damaged by cellular stresses, such as reactive oxygen species (ROS), and involves the formation of double-membrane vesicles called autophagosomes by sequestering cytoplasmic materials and subsequently fusing with lysosomes for degradation (Levine & Klionsky, 2004). It is well accepted that autophagy plays dual roles in controlling the fate of cells (Maiuri et al, 2007). The pro-survival characteristic of autophagy is to maintain tissue homeostasis and sustain cell viability under conditions of nutrient deprivation, growth factor withdrawal or pathogen infection by recycling damaged proteins or organelles to generate anti-apoptotic ATP. Successful removal of damaged proteins or organelles followed by repair and adaption increases cell survival. Paradoxically, when failing to restore homeostasis, autophagy executes its death-promoting characteristic and facilitates cell death through the autophagic cell death (ACD) pathway (Kroemer et al, 2009; Levine & Kroemer, 2008). Apoptosis involves the activation of catabolic enzymes, especially caspases, in the signaling cascades, which leads to the rapid demolition of apoptotic cells. ACD is morphologically defined by the presence of autophagosomes and autolysosomes in dying cells and is referred to as cell death with autophagy (Kroemer & Levine, 2008). However, in contrast to autophagy, which is well characterized and requires nearly 30 autophagy-related genes (ATG) (Levine & Klionsky, 2004), little is known about the mechanisms that regulate autophagic cell death.

ROS play an important part in regulating autophagy and cell death in yeast, nematodes and higher eukaryotes. ROS can effectively serve as signaling molecules that induce adaptive response autophagy by degrading impaired cellular components to promote cell survival. In other cellular settings, however, autophagy induction has been shown to enhance cell death in yeast and mammalian cells in response to oxidative stress (Kang et al, 2007; Scherz-Shouval & Elazar, 2007). Our

Received: 16 March 2015; Accepted: 07 May 2015

*Corresponding author, E-mail: shulinwang@fudan.edu.cn

previous studies demonstrated that the unicellular eukaryotic protozoan *Tetrahymena* is a good model to study the signal transduction pathway under cellular stresses such as cold, osmotic or oxidative stress (Li et al, 2009; Nakashima et al, 1999; Wang et al, 1998; Wang et al, 1999). Although a set of ATG genes and their homologues were discovered in yeast and mammalian cells (Klionsky, 2007), their counterparts in *Tetrahymena* are largely unknown. *Tetrahymena* is an organism with two distinct types of nuclei within the same cytoplasm. *Tetrahymena* enters a unique programmed nuclear degradation (PND) during conjugation, in which the parental macronucleus is eliminated from the progeny cytoplasm while other nuclei, such as new micro- and macro-nuclei, remain unaffected. PND triggers the destruction of macronuclei through an apoptosis-like autophagic degradation (Ejercito & Wolfe, 2003; Endoh & Kobayashi, 2006; Kobayashi & Endoh, 2003; Lu & Wolf, 2001). However, the mechanisms that regulate autophagy and the cellular self-decomposition of *Tetrahymena* under normal conditions or cellular stress, such as oxidative stress, have not yet been studied.

Here, we determined the effect of oxidative stress on cell death in *Tetrahymena* and the modulation of autophagy in the self-destruction of *Tetrahymena*. We found that *Tetrahymena* cells displayed increased double-membrane vesicles characteristic of autophagosomes and underwent autophagic cell death after exposure to hydrogen peroxide. Moreover, our data showed that starvation or blockage of the mitochondrial respiratory chain induced accumulation of ROS and activation of autophagy, followed by autophagic cell death, which was reversed by antioxidant treatment. Thus, our results indicated that mitochondrial ROS might play a pivotal role in regulating autophagy and autophagic cell death of *Tetrahymena*. Importantly, we found that treatment of cells with autophagy inhibitor resulted in a parallel suppression of autophagy associated with augmented autophagic cell death in response to oxidative stress. Taken together, our results suggest that autophagy was activated under oxidative stress to inhibit the initiation of autophagic cell death in *Tetrahymena* until increased ROS production surfeited the threshold to delayed cell death.

MATERIALS AND METHODS

Cell culture

Tetrahymena thermophila cells were kindly provided by Dr. Osamu Numata at the University of Tsukuba, Japan. Cells were grown in stock medium (2% polypeptone, autoclaved) at 28 °C, and were subcultured every week. Cells for experiments were grown in PYG medium (1% polypeptone, 0.5% yeast extract and 0.87% glucose, autoclaved) at 34 °C, as described previously (Nakashima et al, 1999; Wang et al, 1998; Wang et al, 1999).

Induction of ROS and antioxidant treatment

Tetrahymena cells were treated with 1 mmol/L, 10 mmol/L or 20 mmol/L hydrogen peroxide, respectively, by direct addition to 1 mL cell cultures. To induce the accumulation of ROS by starvation, *Tetrahymena* cells were concentrated and resuspended in sterilized phosphate buffer solution (PBS, pH 7.0) and cultured for the indicated durations. We used 40 μg/mL oligomycin (Sigma, USA), a pharmaceutical inhibitor for mitochondrial electron transport chain, or 50 μmol/L menadione/vitamin K3 (Sigma, USA) to induce oxidative stress, respectively. To determine the effect of antioxidants on ROS production, cells were pretreated with 2 mmol/L N-acetyl-L-cysteine (NAC) (Sigma, USA) for 2 h or 0.5 mmol/L catalase (Sigma, USA) for 10 min, respectively.

Inhibitors for autophagy

To suppress autophagy, cells were treated with 10 mmol/L 3-methyladenine (Sigma, USA), 100 μmol/L LY294002 (Cell Signaling, USA) or 250 nmol/L wortmannin (Cell Signaling), which are inhibitors for phosphatidylinositol-3 kinase (PI3K) required for autophagosome formation. Alternatively, *Tetrahymena* cells were treated with 500 nmol/L chloroquine (Sigma, USA), a lysosomotropic alkaline, to suppress the function of autophagy.

Fluorescent microscopy

The lysosomal bodies and nuclear degradation were visualized in *Tetrahymena* by staining with apofluor, a dye mixed with two parts 100 μg/mL acridine orange (Sigma, USA) and one part 1 mg/mL Hoechst 33342 (Sigma, USA) (Lu & Wolf, 2001). Cells were concentrated by centrifugation at 5 000 r/min for 5 min and then fixed with 2% formalin (37% formaldehyde). Cells were observed with an Olympus IX-71 fluorescence microscope (Japan) using the filter for blue light with an exposure time of 1/1.5 or 1/2.0 s. Photos were taken automatically and analyzed with DP controller software (Japan)

Transmission electron microscopy

Nuclear structures, lysosome aggregation and autophagosome formation were observed by transmission electron microscopy (TEM). Treated cells were concentrated and fixed with 2.5% glutaraldehyde at 4 °C for 2 h. TEM was performed with a Philips CM120 electron microscope (German) following the procedure at the electron microscope laboratory of Fudan University School of Medicine in Shanghai, China.

Flow cytometric analysis

Variations in *Tetrahymena* cells with degraded DNA were determined by flow cytometry combined with propidium iodide labeling (Sigma, USA). *Tetrahymena* cells were permeated with 0.03% Triton 100× (Sigma, USA) in PBS. After washing with PBS, cells were resuspended in PBS with PI, and incubated for 30 min at room temperature. Cells were sorted and analyzed using a FACS Calibur (Becton Dickinson, USA) from collections of $2×10^4$ cells.

The percentage of cells with degraded DNA and ROS accumulation were determined by flow cytometry. Cells were stained with propidium iodide (Sigma, USA) and 2',7'-dichlorofluorescescin diacetate (DCF-DA) (Sigma, USA) at 37 °C for 30 min. Cells were sorted and quadrant diagrams were analyzed using a FACS Calibur (Becton Dickinson, USA) from

collections of 2×10^4 cells.

Mitochondrial membrane potential assay

A JC-1 Detection Kit (KeyGEN, China) was used to determine changes in mitochondrial membrane potential. *Tetrahymena* cells were incubated with 5 μg/mL JC-1 (5, 5', 6, 6'-tetrachloro-1, 1', 3, 3'-tetraethylbenzimidazolcarbocyanine) at 34 °C for 30 min, and then washed and resuspended with the kit buffer. Cells were sorted under wavelengths of 488 nm and 530 nm simultaneously by a FACS Calibur (Becton Dickinson, USA) from collections of 2×10^4 cells.

RESULTS AND DISCUSSION

Induction of autophagy in *Tetrahymena* cells after exposure to hydrogen peroxide.

Autophagy occurs at low basal levels in all cells and involves the delivery of damaged organelles or proteins sequestered inside double-membrane vesicles to lysosomes for degradation in order to maintain tissue homeostasis. Autophagy is rapidly activated as an adaptive catabolic process when cells need to generate energy in response to different forms of metabolic stress, including growth factor deprivation and nutrient shortages (Shintani & Klionsky, 2004). In mammalian cells and plants, ROS act as signaling molecules in various intracellular processes and play a regulatory role in autophagy leading to, under certain circumstances, cell survival or cell death (Baehrecke, 2005; Klionsky, 2007).

To study the effect of oxidative stress on autophagy in *Tetrahymena* cells, we used apofluor staining to specifically stain the acid vesicles incorporated into lysosomes acridine orange so as to visualize the lysosome-containing vesicles characteristic of autophagy (Lu & Wolf, 2001). Our results indicated that lysosome-containing vesicles located at the posterior end of the cells under normal conditions tended to be aggregated and clustered near the macronucleus 10 min after exposure to 1 mmol/L H_2O_2, and reached maximal accumulation 30 min after treatment (Figure 1A). Apofluor staining showed that the nucleus color gradually turned into a combination of blue and orange, indicating that it became acidified and gradually underwent degradation after treatment with 1 mmol/L H_2O_2 (Figure 1A). To substantiate this observation,

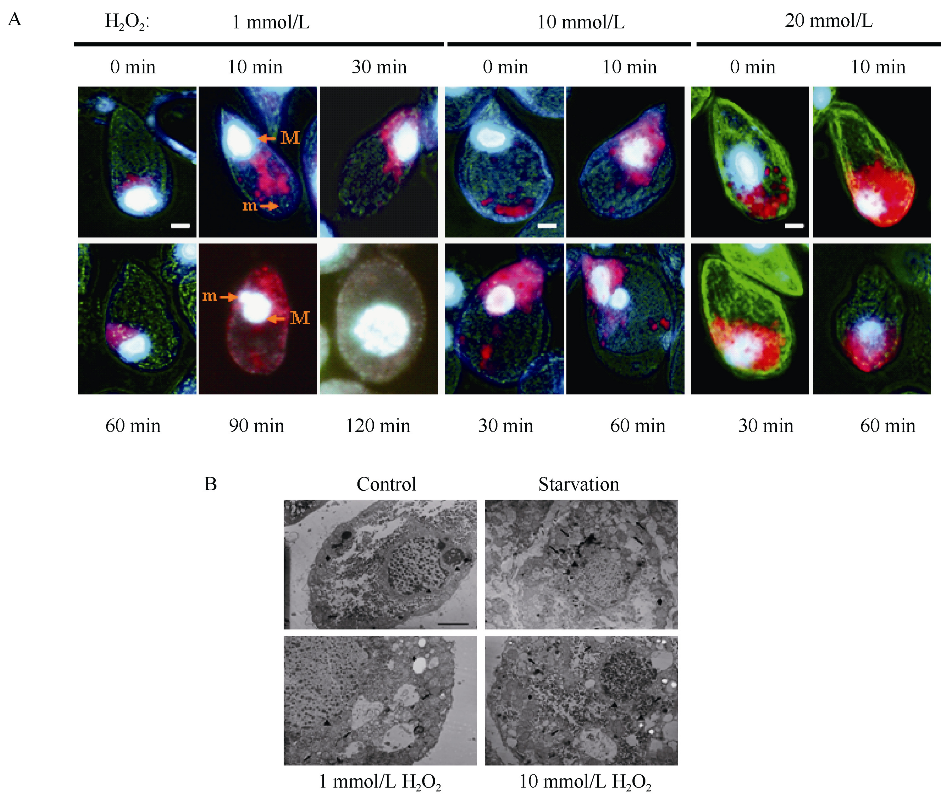

Figure 1 Autophagy activated in *Tetrahymena* upon exposure to hydrogen peroxide

A: *Tetrahymena* cells were treated with 1 mmol/L or 20 mmol/L H_2O_2, respectively, and harvested at the indicated time points for apofluor staining. The micronucleus (m) and macronucleus (M) are blue, and lysosome-containing vesicles are stained orange red. B: *Tetrahymena* cells were treated as indicated and subjected to transmission electron microscopic analysis. Arrows indicate double-membrane autophagosome-like vesicles. M represents macronucleus of *Tetrahymena*. Scale bars (1 μm) are shown.

we determined the induction of autophagy by TEM. The results revealed that *Tetrahymena* cells displayed intact mitochondria and endoplasmic reticula, condensed cytoplasm, and importantly increased large cytoplasmic inclusions, which were the membrane-bound vacuoles characteristic of autophagy (Figure 1B). The consistent results obtained by apofluor staining and TEM analysis suggest that autophagy was activated in *Tetrahymena* cells in response to hydrogen peroxide treatment.

Induction of autophagy preceded autophagic cell death in *Tetrahymena* after exposure to hydrogen peroxide

The crosstalk between autophagy and cell death is complicated in the sense that, in several scenarios, autophagy constitutes a stress adaptation to promote cell survival, whereas under other cellular settings, autophagy follows an alternative pathway leading to cell death (Baehrecke, 2005; Klionsky, 2007). In higher eukaryotes, autophagy serves as a double-edged sword in the cellular response to oxidative stress. High levels of ROS oxidize cell components, such as lipids, proteins and DNA, and thus cause cell death. Various defense mechanisms have been developed to protect cells from oxidative stress through the removal of damaged proteins or organelles by autophagy. When survival mechanisms fail, however, death programs are activated in response to oxidative stress and thus contribute to autophagic cell death (Scherz-Shouval & Elazar, 2007). To study the effect of hydrogen peroxide treatment on *Tetrahymena* cell death and its association with autophagy, we used flow cytometry combined with PI staining to determine variations in cells with degraded DNA after exposure to H_2O_2. Our results indicated that *Tetrahymena* cells undergo cell death accompanied by an accumulation of double-membrane vacuoles in the cytoplasm, and that cell death increased in a time-dependent fashion after H_2O_2 treatment (Figure 1, 2). Using the unified criteria on the definition of cell death proposed by the Nomenclature Committee on Cell Death, that is, autophagic cell death occurs together with the appearance of autophagy (Kroemer et al, 2009; Kroemer & Levine, 2008), we defined cell death with autophagic vacuolization in *Tetrahymena* as autophagic cell death induced by oxidative stress. Importantly, a time course analysis comparing the results in Figure 1 revealed that the increased autophagic vacuolization in the cytoplasm occurred before *Tetrahymena* underwent cellular self-destruction, suggesting that activation of autophagy preceded the initiation of autophagic cell death in *Tetrahymena* after exposure to H_2O_2.

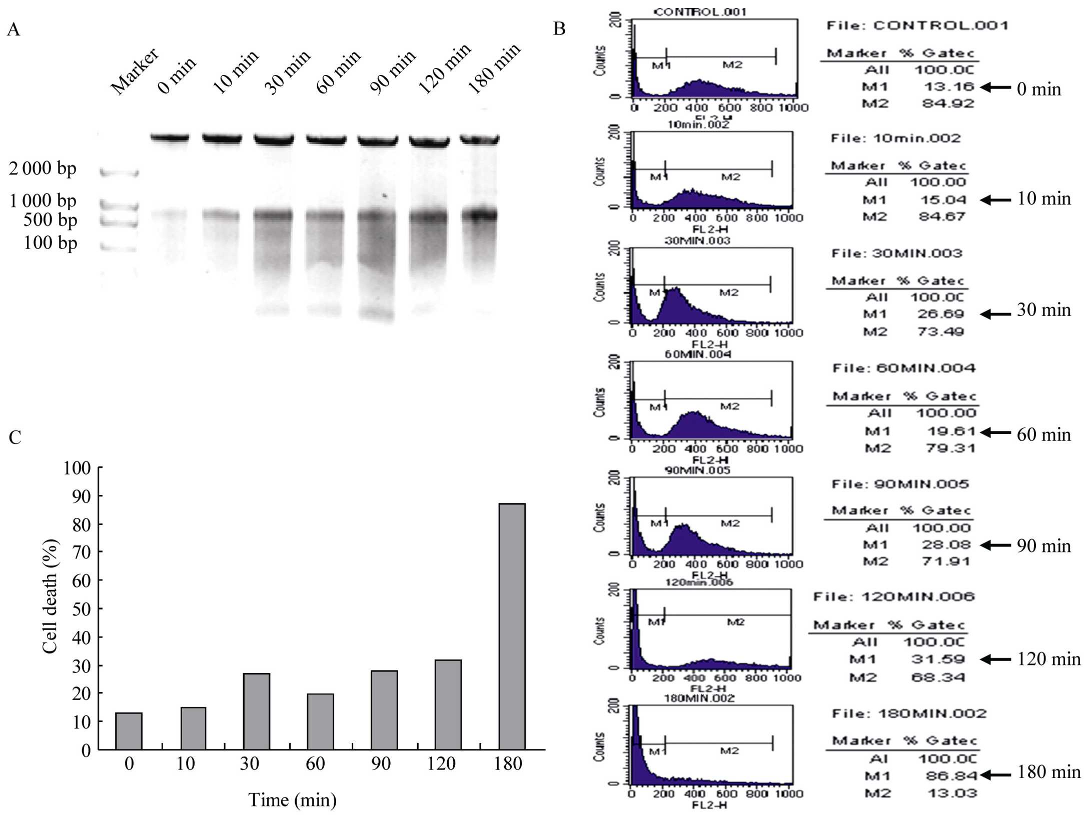

Figure 2 Autophagy occurred prior to autophagic cell death of *Tetrahymena* after hydrogen peroxide treatment

Tetrahymena cells were treated with 1 mmol/L H_2O_2 for the indicated time periods. DNA fragmentation (A) and percentages of cells with degraded DNA determined by flow cytometry combined with PI staining are shown (B and C).

Inhibition of autophagy potentiated the hydrogen peroxide-induced autophagic cell death of *Tetrahymena*

We found that the accumulation and clustering of double-membrane vacuoles around the macronucleus occurred prior to the self-decomposition of *Tetrahymena* after H_2O_2 treatment (Figure 1). This interesting observation drove us to determine the role of autophagy in H_2O_2-induced autophagic cell death. Chloroquine (CQ), a specific inhibitor for autophagy, effectively impairs lysosomal acidification and autophagic protein degradation (Poole & Ohkuma, 1981). By blocking the final step of the autophagy pathway, CQ treatment can lead to the accumulation of ineffective autophagosomes and increased death in cells reliant on autophagy for survival (Amaravadi et al, 2007; Maclean et al, 2008; Lum et al, 2005). To study the effect of autophagy inhibition and its modulation on *Tetrahymena* cell death, we pretreated cells with CQ or inhibitors for PI3K required for autophagy (Lu & Wolf, 2001), followed by H_2O_2 treatment. We found that CQ, 3-MA, LY294002 and wortmannin pretreatment, which block the function of autophagy, significantly increased autophagic cell death in *Tetrahymena* after H_2O_2 exposure (Figure 3A, B). Our results suggest, therefore, that autophagy inhibition augmented H_2O_2-induced autophagic cell death in *Tetrahymena* and that autophagy was activated to act as a "guardian" (colorful "clouds" around nucleus in Figure 1) for the *Tetrahymena* genome upon H_2O_2 treatment and protect the cells from further oxidative injury.

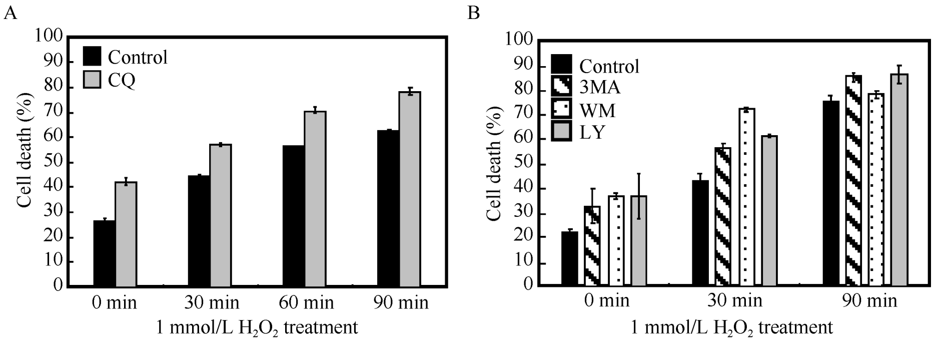

Figure 3 Autophagy inhibition led to augmented autophagic cell death in *Tetrahymena* in response to hydrogen peroxide treatment

A: *Tetrahymena* cells were pretreated with 500 nmol/L chloroquine for 18 h followed by 1 mmol/L H_2O_2 for the indicated time periods. B: *Tetrahymena* cells were pretreated with 10 mmol/L 3-methyladenine for 24 h, 100 μmol/L LY294002 for 1 h or 250 nmol/L wortmannin for 14 h, respectively, and then treated with 1 mmol/L H_2O_2 for the indicated time periods. Cell death was analyzed by flow cytometry combined with PI staining. Data are from three independent experiments and presented as mean±*SD*.

ROS formation in mitochondria was a regulatory event in autophagy and autophagic cell death in *Tetrahymena*

The mitochondrial respiratory chain, which comprises four enzymes complexes, transfers electrons from NADH to molecular oxygen to generate ATP and H_2O (Bedard & Krause, 2007; Lambeth, 2004). However, partial one-electron reduction occurring primarily at complexes 1 and 3 results in the accumulation of ROS and oxidative stress, which can be detoxified by anti-oxidizing agents (Lambeth, 2004). To study the effect of mitochondrial ROS on autophagy induction and cell death in our system, we examined the effect of starvation on ROS production and cell viability in *Tetrahymena* by flow cytometry combined with PI and DCF-DA staining. We observed that *Tetrahymena* cells swam slower, experienced shrinkage and finally underwent decomposition during starvation. Furthermore, we found that ROS were accumulated in *Tetrahymena* cells during starvation in a time-dependent manner and the elevated ROS production resulted in a time-dependent increase in cell death (Figure 4A). Importantly, TEM analysis revealed an increased amount of vacuoles characteristic of autophagosomes in *Tetrahymena* after 24 h starvation (Figure 1B), supporting the notion that autophagy was activated before the initiation of autophagic cell death in starved *Tetrahymena* cells. We also used oligomycin treatment to disrupt the mitochondrial respiratory chain to induce oxidative stress, which resulted in the accumulation of ROS and loss of mitochondrial membrane potential in *Tetrahymena* cells (Figure 4B). Oligomycin treatment also significantly increased autophagic cell death in *Tetrahymena* (Figure 4C). In addition, analyses of cells treated with vitamin K3, a free radical generator, showed consistent results that autophagic cell death was significantly induced in *Tetrahymena* (Figure 4D). Our results indicated that CQ treatment enhanced autophagic cell death in *Tetrahymena* induced by oligomycin and vitamin K3 treatment (Figure 4C, D). To further examine the effect of mitochondrial ROS in regulating autophagy and cell death, we pretreated cells with antioxidants in the presence or absence of CQ during starvation. Our results showed that pretreatment with antioxidants, specifically N-acetyl-L-cysteine (NAC) or catalase, partially reversed the accumulation of ROS and loss of mitochondrial membrane potential during starvation (Figure 5A, B). Importantly, we found that autophagy inhibition increased autophagic cell death in *Tetrahymena* in response to the elevated ROS production from starvation, which was reversed by antioxidant treatment (Figure 5B). These results suggest, therefore, that ROS production in the mitochondria plays an important role in modulating the induction of autophagy and autophagic cell death in *Tetrahymena*.

Taken together, our current study revealed that autophagy was dramatically induced following oxidative stress. Interestingly,

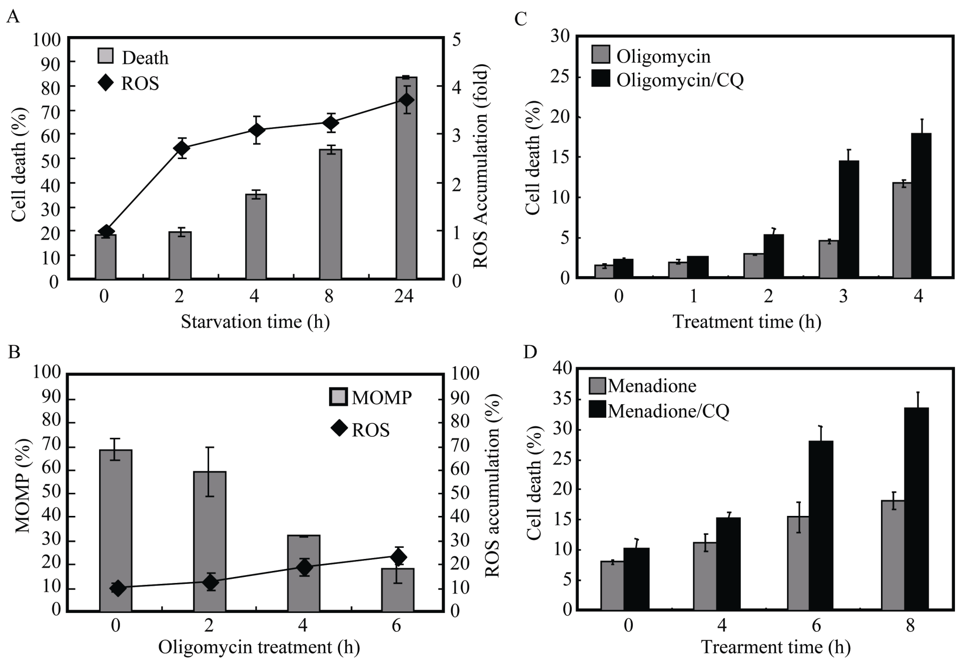

Figure 4 Mitochondrial ROS modulated autophagy and autophagic cell death in *Tetrahymena* during starvation or in response to oligomycin or vitamin K3 treatment

A: Cells grown at the mid-log phase were concentrated and resuspended in sterilized phosphate buffer solution (PBS, pH 7.0). Starved cells were harvested at the indicated time points. Cell death and ROS accumulation was determined by flow cytometry combined with PI and DCF-DA staining. B: *Tetrahymena* cells were treated with 40 μg/mL oligomycin at the indicated time periods. Treated cells were stained with JC-1 as described in the MATERIALS AND METHODS, and MOMP was determined by flow cytometry. C: *Tetrahymena* cells were pretreated with 500 nmol/L chloroquine for 18 h followed by 50 μmol/L menadione treatment at the indicated time periods. D: *Tetrahymena* cells were pretreated with 500 nmol/L chloroquine for 18 h followed by 40 μmol/L oligomycin treatment at the indicated time points. Cell death and ROS production were determined by flow cytometry combined with PI and DCF-DA staining. Data are from three independent experiments and presented as mean±*SD*.

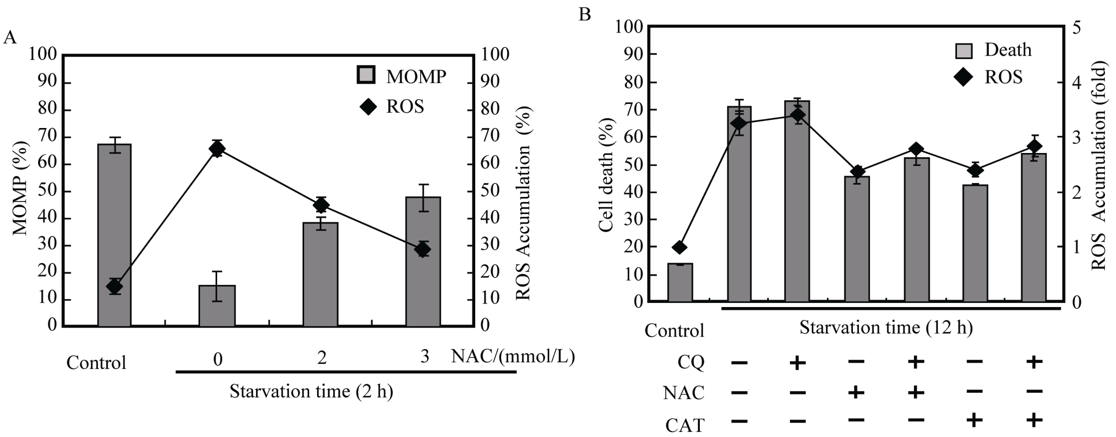

Figure5 Antioxidant reversed ROS accumulation and CQ-induced cell death in *Tetrahymena* during starvation.

A: Cells were grown in the presence or absence of 2 mmol/L or 3 mmol/L N-acetyl-L-cysteine for 2 h, respectively, and subjected to starvation for 2 h. Mitochondrial membrane potential and ROS production were measured as described in the MATERIALS AND METHODS. B: *Tetrahymena* cells were pretreated in the presence or absence of 500 nmol/L chloroquine for 18 h, 2 mmol/L N-acetyl-L-cysteine for 2 h or 0.5 mmol/L catalase for 10 min, respectively, and then subjected to starvation for 12 h. Cell death and ROS production were determined by flow cytometry combined with PI and DCF-DA staining. Data are from three independent experiments and presented as mean±*SD*.

suppression of autophagy enhanced autophagic cell death in *Tetrahymena* in response to ROS accumulation resulting from starvation or blockage of mitochondrial electron transport, suggesting that autophagy might prevent the initiation of

autophagic cell death in *Tetrahymena* until the accumulation of ROS switches autophagy into an alternative process, leading to delayed cell death. However, the molecular basis that regulates autophagic cell death, especially the genes responsible for autophagy in unicellular eukaryotic protozoans such as *Tetrahymena* has not been identified. Further studies are needed to investigate the mechanisms underlying the paradox that autophagy promotes cell survival in some instances but can lead to cell death under other cellular settings.

ACKNOWLEDGEMENTS

We appreciate Dr. Wei MIAO at the Institute of Hydro-Biology, Chinese Academy of Sciences, for providing *Tetrahymena* strains and technical help. We also thank Dr. Shu-Qin SHEN at Fudan University for her expertise on flow cytometry analysis.

REFERENCES

Amaravadi RK, Yu DN, Lum JJ, Bui T, Christophorou MA, Evan GI, Thomas-Tikhonenko A, Thompson CB. 2007. Autophagy inhibition enhances therapy-induced apoptosis in a Myc-induced model of lymphoma. *Journal of Clinical Investigation,* **117**(2): 326-336.

Baehrecke EH. 2005. Autophagy: Dual roles in life and death?. *Nature Reviews Molecular Cell Biology,* **6**(6): 505-510.

Bedard K, Krause KH. 2007. The NOX family of ROS-generating NADPH oxidases: Physiology and pathophysiology. *Physiological Reviews,* **87**(1): 245-313.

Ejercito M, Wolfe J. 2003. Caspase-like activity is required for programmed nuclear elimination during conjugation in *Tetrahymena*. *Journal of Eukaryotic Microbiology,* **50**(6): 427-429.

Endoh H, Kobayashi T. 2006. Death harmony played by nucleus and mitochondria: nuclear apoptosis during conjugation of *Tetrahymena*. *Autophagy,* **2**(2): 129-131.

Kang C, You YJ, Avery L. 2007. Dual roles of autophagy in the survival of *Caenorhabditis elegans* during starvation. *Genes & Development,* **21**(17): 2161-2171.

Klionsky DJ. 2007. Autophagy: from phenomenology to molecular understanding in less than a decade. *Nature Reviews Molecular Cell Biology,* **8**(11): 931-937.

Kobayashi T, Endoh H. 2003. Caspase-like activity in programmed nuclear death during conjugation of *Tetrahymena thermophila*. *Cell Death and Differentiation,* **10**(6)**:** 634-640.

Kroemer G, Levine B. 2008. Autophagic cell death: the story of a misnomer. *Nature Reviews Molecular Cell Biology,* **9**(12): 1004-1010.

Kroemer G, Galluzzi L, Vandenabeele P, Abrams J, Alnemri ES, Baehrecke EH, Blagosklonny MV, El-Deiry WS, Golstein P, Green DR, Hengartner M, Knight RA, Kumar S, Lipton SA, Malorni W, Nuñez G, Peter ME, Tschopp J, Yuan J, Piacentini M, Zhivotovsky B, Melino G. 2009. Classification of cell death: recommendations of the Nomenclature Committee on Cell Death 2009. *Cell Death and Differentiation,* **16**(1): 3-11.

Lambeth JD. 2004. NOX enzymes and the biology of reactive oxygen. *Nature Reviews Immunology,* **4**(3): 181-189.

Levine B, Klionsky DJ. 2004. Development by self-digestion: Molecular mechanisms and biological functions of autophagy. *Developmental Cell,* **6**(4): 463-477.

Levine B, Kroemer G. 2008. Autophagy in the pathogenesis of disease. *Cell,* **132**(1): 27-42.

Li WZ, Zhang SW, Numata O, Nozawa Y, Wang SL. 2009. *TpMRK* regulates cell division of *Tetrahymena* in response to oxidative stress. *Cell Biochemistry and Function,* **27**(6): 364-369.

Lu E, Wolfe J. 2001. Lysosomal enzymes in the macronucleus of *Tetrahymena* during its apoptosis-like degradation. *Cell Death and Differentiation,* **8**(3): 289-297.

Lum JJ, Bauer DE, Kong M, Harris MH, Li C, Lindsten T, Thompson CB. 2005. Growth factor regulation of autophagy and cell survival in the absence of apoptosis. *Cell,* **120**(2): 237-248.

Maclean KH, Dorsey FC, Cleveland JL, Kastan MB. 2008. Targeting lysosomal degradation induces p53-dependent cell death and prevents cancer in mouse models of lymphomagenesis. *Journal of Clinical Investigation,* **118**(1): 79-88.

Maiuri MC, Zalckvar E, Kimchi A, Kroemer G. 2007. Self-eating and self-killing: crosstalk between autophagy and apoptosis. *Nature Reviews Molecular Cell Biology,* **8**(9): 741-752.

Nakashima S, Wang SL, Hisamoto N, Sakai H, Andoh M, Matsumoto K, Nozawa Y. 1999. Molecular cloning and expression of a stress-responsive mitogen-activated protein kinase-related kinase from *Tetrahymena* cells. *Journal of Biological Chemistry,* **274**(15): 9976-9983.

Poole B, Ohkuma S. 1981. Effect of weak bases on the intralysosomal ph in mouse peritoneal macrophages. *The Journal of Cell Biology,* **90**(3): 665-669.

Scherz-Shouval R, Elazar Z. 2007. ROS, mitochondria and the regulation of autophagy. *Trends in Cell Biology,* **17**(9): 422-427.

Shintani T, Klionsky DJ. 2004. Autophagy in health and disease: A double-edged sword. *Science,* **306**(5698): 990-995.

Wang SL, Nakashima S, Numata O, Fujiu K, Nozawa Y. 1999. Molecular cloning and cell-cycle-dependent expression of the acetyl-CoA synthetase gene in *Tetrahymena* cells. *Biochemical Journal,* **343**(2): 479-485.

Wang S, Nakashima S, Sakai H, Numata O, Fujiu K, Nozawa Y. 1998. Molecular cloning and cell-cycle-dependent expression of a novel NIMA (never-in-mitosis in *Aspergillus nidulans*)-related protein kinase (TpNrk) in *Tetrahymena* cells. *The Biochemical Journal,* **334**: 197-203.

Purification and characterization of cholecystokinin from the skin of salamander *Tylototriton verrucosus*

Wen-Bin JIANG[1,†], Ma HAKIM[2,†], Lei LUO[2], Bo-Wen LI[2], Shi-Long YANG[2], Yu-Zhu SONG[1,*], Ren LAI[2], Qiu-Min LU[2,*]

[1] *Faculty of Life Science and Technology*, *Kunming University of Science and Technology*, *Kunming Yunnan* 650500, *China*

[2] *Key Laboratory of Animal Models and Human Disease Mechanisms of Chinese Academy of Sciences & Yunnan Province*, *Kunming Institute of Zoology*, *Kunming Yunnan* 650223, *China*

ABSTRACT

As a group of intestinal hormones and neurotransmitters, cholecystokinins (CCKs) regulate and affect pancreatic enzyme secretion, gastrointestinal motility, pain hypersensitivity, digestion and satiety, and generally contain a DYMGWMDFG sequence at the C-terminus. Many CCKs have been reported in mammals. However, only a few have been reported in amphibians, such as *Hyla nigrovittata*, *Xenopus laevis*, and *Rana catesbeiana*, with none reported in urodele amphibians like newts and salamanders. Here, a CCK called CCK-TV was identified and characterized from the skin of the salamander *Tylototriton verrucosus*. This CCK contained an amino acid sequence of DYMGWMDF-NH_2 as seen in other CCKs. A cDNA encoding the CCK precursor containing 129 amino acid residues was cloned from the cDNA library of *T. verrucosus* skin. The CCK-TV had the potential to induce the contraction of smooth muscle strips isolated from porcine gallbladder, eliciting contraction at a concentration of 5.0×10^{-11} mol/L and inducing maximal contraction at a concentration of 2.0×10^{-6} mol/L. The EC_{50} was 13.6 nmol/L. To the best of our knowledge, this is the first report to identify the presence of a CCK in an urodele amphibian.

Keywords: Cholecystokinin; Salamander; Skin; Amphibian

INTRODUCTION

Amphibian skins contain numerous bioactive compounds. Many bioactive peptides exerting defensive and regulatory or hormonal functions have been identified and characterized from amphibian secretions (Lu et al, 2010; Xu & Lai, 2015; Zhang, 2006). Recently, a few neurotoxins acting on ion channels, which also possibly play defensive roles, have been found in amphibian skins (Wu et al, 2011; You et al, 2009). Amphibian peptides with regulatory or hormonal functions are analogs of mammalian hormones and neurotransmitters such as bombesin, gastrin-releasing peptide, bradykinin, caerulein and cholecystokinin (CCK) (Bevins & Zasloff, 1990; Johnsen & Rehfeld, 1992; Lai et al, 2001, 2002; Wakabayashi et al, 1985).

CCKs are important intestinal hormones and neurotransmitters, and play major roles in the physiological regulation of pancreatic enzyme secretion and gastrointestinal (GI) motility (Rourke et al, 1997). Most amphibian CCKs are found in the brain and gastrointestinal tract of animals. Two CCK groups have been identified from the brain and small intestine of the bullfrog *Rana catesbeiana* using antiserum specific for the common C-terminus of mammalian gastrin and CCK (Rourke et al, 1997). The group of small peptides contains CCK-7 and CCK-8 and another group contains CCK-69 and CCK-70, which are identical to each other and to mammalian CCKs. For example, both CCK-69 and CCK-70 contain the monobasic and dibasic cleavage sites that give rise to CCK-33, CCK-39 and CCK-58 in mammals (Johnsen & Rehfeld, 1992; Johnsen, 1994). Recently, we identified a CCK from the frog skin of *Rana nigrovittata* (Liu et al, 2007). To date, however, all known amphibian CCKs have been identified in anuran amphibians only, with no CCK yet reported in urodele amphibians. To investigate whether amphibian CCKs are expressed in urodele amphibians, we purified a CCK and cloned cDNA encoding CCK precursors from *Tylototriton verrucosus* skin.

Received: 16 March 2015; Accepted: 09 April 2015

Foundation items: This work was supported by the National Basic Research Program of China (973 Program) (2013CB911300), National Natural Science Foundation of China (U1132601) and the Chinese Academy of Sciences (SAJC201308)

[*]Corresponding authors, E-mails: lvqm@mail.kiz.ac.cn; yuzhusong@kmust.edu.cn

[†]These authors contributed equally to this paper

MATERIALS AND METHODS

Tylototriton verrucosus sample

As per our previous report, adult *T. verrucosus* (either sex, 20±5 g) were collected from the Yunnan province in China (Mu et al, 2014). They were anesthetized using 2.5% vaporized inhaled isoflurane and the dorsal skin was removed after cleansing with distilled water. The skin was homogenized by a tissue homogenizer with 0.1 mol/L phosphate buffer, pH 6.0 (PBS) (containing 1% (v/v) protease inhibitor cocktail, Sigma, USA, P8340-5). The skin homogenate solutions were quickly centrifuged (10 000 g for 10 min) at 4 ˚C and the supernatants were lyophilized. All experiments were approved by the Kunming Institute of Zoology, Chinese Academy of Sciences.

Peptide purification

An aliquot (1 g) of the lyophilized skin homogenate supernatant was dissolved in 10 mL PBS and centrifuged at 5 000 g for 10 min at 4 ˚C. The supernatant was applied to a Sephadex G-50 (Superfine, Amersham Biosciences, Sweden, 2.6 cm diameter, 100 cm length) gel filtration column equilibrated with 0.1 mol/L PBS for preliminary separation. Elution was performed with the same buffer, collecting fractions of 3.0 mL. The eluted fractions were monitored at 280 nm. The fraction containing smooth muscle contraction-inducing activity was further purified by a C_{18} reversed-phase high performance liquid chromatography column (RP-HPLC, Gemini C_{18} column, Phenomenex, USA, 5 μm particle size, 110 Å pore size, 250 mm length, 4.6 mm diameter,). Elution was performed using a linear gradient of 0–80% acetonitrile containing 0.1% (v/v) trifluoroacetic acid in 0.1% (v/v) trifluoroacetic acid/water over 60 min. UV-absorbing peaks were collected and lyophilized. Each purification step was traced by assaying for contraction of smooth muscle strips isolated from porcine gallbladder, as described below.

Primary structure analysis

Peptide sequencing was performed by automated Edman degradation analysis on a pulsed liquid-phase Shimadzu protein sequencer (PPSQ-31A, Shimadzu, Japan) according to the manufacturer's instructions. Mass spectrometry (MS) was undertaken on an UltraFlex I mass spectrometer (Bruker Daltonics, Germany) by spotting the tested sample (0.5 μL) in 0.1% (v/v) trifluoroacetic acid/water onto a matrix-assisted laser desorption ionization time-of-flight (MALDI-TOF) plate with a 0.5 μL α-cyano-4-hydroxycinnamic acid matrix (10 mg/mL in 60% acetonitrile). The MS analysis was run in positive ion mode.

Construction and screening of cDNA library

A cDNA library was constructed according to previous research (Mu et al, 2014) using a SMART™ cDNA Library Construction Kit (Clontech, USA/Canada). The synthesized cDNA was used as a template for PCR to screen the cDNAs encoding the CCK. Two pairs of oligonucleotide primers, (S1: 5'-GA(T/C)TA(C/T)ATGGG(A/T/C/G)TGGATGGA(T/C)TT(T/C)-3', according to the sequence determined by Edman degradation, in the antisense direction, and primer II A: 5′-AAGCAG TGGTATCAACGCAGAGT-3; S2: 5'-ATGGAGCTATGCCTC ATACTCAC-3′ and primer II A) were used in PCR reactions. The PCR conditions were: 2 min at 95 °C, and 30 cycles of 10 sec at 92 °C, 30 sec at 50 °C, 40 sec at 72 °C followed by a 10 min extension at 72 °C. The PCR products were cloned into a pGEM®-T Easy vector (Promega, Madison, WI, USA). DNA sequencing was performed on a model ABI PRISM 377 DNA sequencer (Applied Biosystems, USA).

Contraction of smooth muscle strips isolated from porcine gallbladder

Preparation of porcine gallbladder muscle strips was according to Nielsen et al (1998). Immediately after removal, the gallbladders were rinsed of bile with Krebs bicarbonate buffer of the following composition, in mmol/L: NaCl, 120.0; KCl, 5.9; $MgCl_2$, 1.2; $CaCl_2$, 2.5; NaH_2PO_4, 1.4; $NaHCO_3$, 14.9; and glucose, 11.5. The medium was maintained at 37°C and constantly bubbled with a mixture of 95% O_2 and 5% CO_2, resulting in a pH of 7.4. The gallbladders were dissected free from serosa. Strips (2×10 mm) were cut in the longitudinal direction from the midregion of the gallbladder corpus. They were left for 1 h in Krebs medium, before being attached to strain gauge transducers with a force of 10 mN. After an equilibration period of 45 min, the experiments were performed with cumulative concentrations of CCK-TV peptide.

Synthetic peptide

CCK (DYMGWMDF-NH_2, Phe in C-terminus was amidated) was synthesized by GL Biochem Ltd. (Shanghai, China) and analyzed by HPLC and mass spectrometry to confirm purity greater than 98%. The smooth muscle contraction-inducing activity of the synthesized peptide was confirmed to be the same as the natural peptide.

Statistics

All data in this paper are presented as means±*SD* and were analyzed by Student's *t*-tests following parametric one-way analysis of variance.

RESULTS

Purification of CCK-TV

As reported in our previous work (Mu et al, 2014), the skin homogenate supernatant of *T. verrucosus* was divided into six fractions after Sephadex G-50 gel filtration. The fraction (Fraction VI) containing activity to induce the contraction of smooth muscle strips isolated from porcine gallbladder was pooled and subjected to a C_{18} RP-HPLC column for further purification (Figure 1). The purified peptide was named CCK-TV (marked by an arrow).

Structural characterization

The complete amino acid sequence of purified CCK-TV was determined as DYMGWMDF by Edman degradation. CCK-TV was composed of eight amino acid residues. MALDI-TOF-MS gave an observed mass of 1063.1, well-matched to the theoretical molecular weight (1063.2) of CCK-TV containing an amidated C-terminus Phe as seen in other CCKs. The

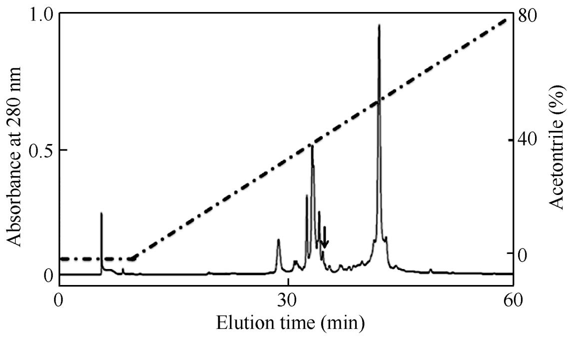

Figure 1 Purification of CCK-TV from salamander *Tylototriton verrucosus* by C_{18} reversed-phase high performance liquid chromatography

Peptide purification from the lyophilized skin homogenate supernatant of the salamander was as per our previous method using Sephadex G-50 gel filtration followed by C_{18} reversed-phase high performance liquid chromatography (RP-HPLC). Each purification step was traced by assaying for contraction of smooth muscle strips isolated from porcine gallbladder. The purified peptide is marked by an arrow.

presence of an amidated C-terminus Phe in native CCK-TV was further confirmed by the synthesized peptide, which had the same observed mass and RP-HPLC elution manner as that of the native CCK-TV.

cDNA cloning

The nucleotide sequence encoding the CCK-TV precursor and the encoded amino acid sequence are shown in Figure 2. The sequence contained a coding region of 387 nucleotides and the encoded amino acid sequence corresponded to a polypeptide of 129 amino acids, including mature CCK-TV. A BLAST search indicated that the precursor was a member of the CCK family and contained a conserved DYMGWMDFG domain.

```
atgtacagaggaatctgtgtttgtgtgttacttgctgtgctctccatgagttcttctgga  60
 M  Y  R  G  I  C  V  C  V  L  L  A  V  L  S  M  S  S  S  G   20
cagcagacagcaaggtctaattatggggaccaagttgcagctgaaattgagaaaagcctg 120
 Q  Q  T  A  R  S  N  Y  G  D  Q  V  A  A  E  I  E  K  S  L   40
acagaccaccaccggcccgtccgcatgccctcgtcttcaggtcagctgaaaccctttcag 180
 T  D  H  H  R  P  V  R  M  P  S  S  S  G  Q  L  K  P  F  Q   60
agaatggatagaagcattgaccaaaaggccaacgttcaggctttaatggccaaatacctg 240
 R  M  D  R  S  I  D  Q  K  A  N  V  Q  A  L  M  A  K  Y  L   80
cagcagaggaaaggtggcccatctggcagatatgcaattgtgcaaaaccggcctatcatc 300
 Q  Q  R  K  G  G  P  S  G  R  Y  A  I  V  Q  N  R  P  I  I  100
gaccccacccaccggataaatgacagagattacatgggctggatggattttggacgccgc 360
 D  P  T  H  R  I  N  D  R [D  Y  M  G  W  M  D  F] G  R  R  120
agtgccgaagaatatgaatactcctcgtagcct                            393
 S  A  E  E  Y  E  Y  S  S  *                                129
```

Figure 2 Nucleotide sequence encoding CCK-TV from salamander skin and the amino acid sequence of the precursor polypeptide

The mature CCK-TV peptide sequence is boxed. *: Stop codon.

Induction of bladder smooth muscle contraction

Concentration–response experiments were performed with the CCK-TV. The peptide induced contractions in a concentration-dependent manner (Figure 3). CCK-TV elicited a contraction at a concentration of 5.0×10^{-11} mol/L and induced maximal contraction at a concentration of 2.0×10^{-6} mol/L. The EC_{50} value, expressed as –log(mol/L), was 7.87±0.21 (*n*=5), which corresponded to 13.6 nmol/L.

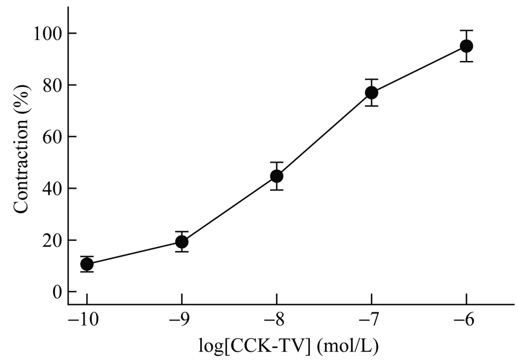

Figure 3 Contraction of porcine gallbladder strips by CCK-TV

Each gallbladder strip was stimulated with cumulative increases of CCK-TV in alternated order. Responses are expressed as percentages of the maximal contraction induced by CCK-TV. Values represent mean±*SE* (*n*=5).

DISCUSSION

CCKs are important intestinal hormones and neurotransmitters that regulate or affect pancreatic enzyme secretion, gastrointestinal motility, pain hypersensitivity, and digestion and satiety. CCKs, which generally contain DYMGWMDFG at the C-terminus, have been extensively reported in mammals and in some anuran amphibians, including *H. nigrovittata*, *X. laevis*, and *R. catesbeiana* (Xu & Lai, 2015). To date, however, no CCKs have been reported in urodele amphibians. In this study, an amphibian CCK was purified from the skin of *Tylototriton verrucosus*, which is the first report of a CCK from salamander skin. To confirm the presence of CCK in the salamander skin, cDNA clones encoding CCKs were screened from the skin cDNA library of *Tylototriton verrucosus*. Results indicated that CCKs could be expressed in the skins of urodele amphibians like salamanders, as other amphibian skin–gut–brain triangle peptides (Erspamer et al, 1981).

The diversion of the CCK/gastrin family can be dated early in vertebrate history (Oliver & Vigna, 1996). The CCK/gastrin family may join the increasing number of peptide families that showed early expansion during vertebrate evolution, although the gap between amphibia and the most "original" vertebrates still needs to be filled. However, the existence of CCKs in urodele salamanders may help fill this gap.

The C-terminal of salamander CCK-TV and frog CCK-8 were identical (Figure 4). As expected for a mammalian system, CCK-TV stimulated porcine gallbladder contraction (Figure 3). The EC_{50} of CCK-TV on porcine gallbladder contraction was 13.6 nmol/L, which was higher than that of CCK-8 (7.2 nmol/L) (Nielsen et al, 1998). This difference may result from the different modification of the peptides, since the Tyr of the CCK-8 sample was O-sulfated. Amphibian CCKs and gastrin were only distinguished by the substitution of Ala for Met in position six

CCK-TV			D	Y	M	G	W	M	D	F·NH_2
CCK-8			D	Y	M	G	W	M	D	F·NH_2
Frog gastrin-8			D	Y	A	G	W	M	D	F·NH_2
Chicken gastrin-8			F	Y	P	S	W	M	D	F·NH_2
Turtle/alligator gastrin-8			D	Y	P	G	W	M	D	F·NH_2
Caerulein	E	E	D	Y	S	G	W	M	D	F·NH_2
Mammalian gastrin			A	Y	–	G	W	M	D	F·NH_2

Figure 4 Sequence alignment of CCK/gastrin peptides
Conserved amino acid residues in all sequences are boxed. Gaps are added to acquire maximum identity.

from the C-terminus (Figure 4). Chicken gastrin exhibits clear gastrin properties in both birds and mammals lack of CCK-like properties (Dimaline & Lee, 1990). This was attributed to steric effects of proline residue in position six from the C-terminus (Figure 4). Also, the alligator contains two distinct receptors that discriminate between CCK and gastrin (Oliver & Vigna, 1997). In mammals, the Tyr residue shifted to position six from the C-terminus (Figure 4), which induces a major change in binding to the CCK-A receptor (Oliver & Vigna, 1997). We did not identify gastrin peptide in *Tylototriton verrucosus*. Further work is needed to clarify whether gastrin peptides exist in salamander and their interactions with the receptors.

REFERENCES

Bevins CL, Zasloff M. 1990. Peptides from frog skin. *Annual Review of Biochemistry,* **59**: 395-414.

Dimaline R, Lee CM. 1990. Chicken gastrin: A member of the gastrin/CCK family with novel structure-activity relationships. *The American Journal of Physiology,* **259**(5 Pt 1): G882-G888.

Erspamer V, Melchiorri P, Broccardo M, Erspamer GF, Falaschi P, Improta G, Negri L, Renda T. 1981. The brain–gut–skin triangle: new peptides. *Peptides,* **2**(Suppl. 2): 7-16.

Johnsen AH, Rehfeld JF. 1992. Identification of cholecystokinin/gastrin peptides in frog and turtle. Evidence that cholecystokinin is phylogenetically older than gastrin. *European Journal of Biochemistry,* **207**(2): 419-428.

Johnsen AH. 1994. Identification of cholecystokinin from frog and turtle. Divergence of cholecystokinin and gastrin occurred before the evolution of amphibia. *European Journal of Biochemistry,* **224**(2): 691-702.

Lai R, Liu H, Lee W H, Zhang Y. 2001. A novel bradykinin related peptide from skin secretions of toad *Bombina maxima* and its precursor containing six identical copies of the final product. *Biochemical and Biophysical Research Communications,* **286**(2): 259-263.

Lai R, Liu H, Lee WH, Zhang Y. 2002. A novel proline rich bombesin-related peptide (PR-bombesin) from toad *Bombina maxima*. *Peptides,* **23**(3): 437-442.

Liu X H, Wang Y P, Cheng L H, Song Y Z, Lai R. 2007. Isolation and cDNA cloning of cholecystokinin from the skin of *Rana nigrovittata*. *Peptides,* **28**(8): 1540-1544.

Mu L, Tang J, Liu H, Shen C, Rong M, Zhang Z, Lai R. 2014. A potential wound-healing-promoting peptide from salamander skin. *The FASEB Journal*, 2014, 28(9): 3919-3929.

Lu QM, Lai R, Zhang Y. 2010. Animal toxins and human disease: from single component to venomics, from biochemical characterization to disease Mechanisms, from crude venom utilization to rational drug design. *Zoological Research,* **31**(1): 2-16. (in Chinese)

Nielsen KG, Bomgren P, Holmgren S, Johnsen AH. 1998. Gastrin and cholecystokinin of the bullfrog, *Rana catesbeiana*, have distinct effects on gallbladder motility and gastric acid secretion in *vitro*. *General and Comparative Endocrinology,* **112**(2): 247-254.

Oliver AS, Vigna SR. 1996. CCK-X receptors in the endothermic mako shark (*Isurus oxyrinchus*). *General and Comparative Endocrinology,* **102**(1): 61-73.

Oliver AS, Vigna SR. 1997. CCK-A- and CCK-B-like receptors in the gallbladder and stomach of the alligator (*Alligator mississippiensis*). *General and Comparative Endocrinology,* **105**(1): 91-101.

Rourke IJ, Rehfeld JF, Møller M, Johnsen AH. 1997. Characterization of the cholecystokinin and gastrin genes from the bullfrog, *Rana catesbeiana:* evolutionary conservation of primary and secondary sites of gene expression. *Endocrinology,* **138**(4): 1719-1727.

Wakabayashi T, Kato H, Tachibana S. 1985. Complete nucleotide sequence of mRNA for caerulein precursor from *Xenopus* skin: the mRNA contains an unusual repetitive structure. *Nucleic Acids Research,* **13**(6): 1817-1828.

Wu J, Liu H, Yang H L, Yu H N, You D W, Ma Y F, Ye H H, Lai R. 2011. Proteomic analysis of skin defensive factors of tree frog *Hyla simplex*. *Journal of Proteome Research,* **10**(9): 4230-4240.

Xu X Q, Lai R. 2015. The chemistry and biological activities of peptides from amphibian skin secretions. *Chemical Reviews,* **115**(4): 1760-1846.

You D W, Hong J, Rong M Q, Yu H N, Liang S P, Ma Y F, Yang H L, Wu J, Lin D H, Lai R. 2009. The first gene-encoded amphibian neurotoxin. *The Journal of Biological Chemistry,* **284**(33): 22079-22086.

Zhang Y. 2006. Amphibian skin secretions and bio-adaptive significance — Implications from *Bombina maxima* skin secretion proteome. *Zoological Research,* **27**(1): 101-112. (in Chinese)

New Record of *Lycodon liuchengchaoi* in Anhui

Liang ZHANG [1,2,†], Li-Fang PENG[3,4,†], Lei YU[5], Zheng-Ping WANG[4], Li-Qun HUANG[6], Song HUANG [4,*]

[1] *Guangdong Entomological Institute*, *Guangzhou* 510260, *China*

[2] *Guangdong Public Laboratory of Wild Animal Conservation and Utilization*, *Guangzhou* 510260, *China*

[3] *College of Biology and Environment*, *Graduate School*, *Nanjing Forestry University*, *Nanjing* 210037, *China*

[4] *Huangshan University*, *Huangshan* 245041, *China*

[5] *Anhui Bird Watching Society*, *Hefei* 230601, *China*

[6] *Bureau of Parks*, *Huangshan Management Committee*, *Huangshan Tourism Development Co.*, *Ltd*, *Huangshan* 245000, *China*

ABSTRACT

One juvenile and one adult female wolf snake (Colubridae: *Lycodon*) were sampled at Yixian and Fuxi, Huangshan, Anhui, China in the summer of 2011 and 2012, respectively. The two specimens were identified as *Lycodon liuchengchaoi* based on external morphology and molecular data. This is a new reptile record in Anhui Province. In our laboratory, four eggs were laid and three neonates were hatched successfully. This is the first record of the laying and incubation of *L. liuchengchaoi* eggs. The five specimens were deposited at the Museum of Huangshan University (HUM20140001) and Guangdong Entomological Institute (HB-lcfsp12613, HB-lcfsp-ch1~3).

Keywords: Reptile; *Lycodon liuchengchaoi*; Incubation; New record

In our routine summer ecological investigations of amphibians and reptiles in Huangshan of Anhui Province, a juvenile wolf snake (Collection number: HUM20140001, Figure 1) was sampled at Yixian (E117°9.112′, N29°9.248′) on June 24, 2011, and a female adult wolf snake (Collection number: HB-lcfsp12613, Figure 2) was collected at Fuxi (E118°8.191′, N30°5.439′; 700 m a.s.l.) on June 3, 2012. The two specimens were identified as *L. liuchengchaoi* (Zhang et al, 2011a). This is the first time that *L. liuchengchaoi* has been found in Anhui, China (Chen et al, 1991; Zhao et al, 1998; Zhao, 2006; Zhang et al, 2011a).

Figure 1 Juvenile *Lycodon liuchengchaoi* (HUM20140001) sampled at Yixian, Huangshan

A: Dorsal; B: Ventral. Photo by Li-Fang PENG.

Figure 2 Adult female *Lycodon liuchengchaoi* (HB-lcfsp12613) sampled at Fuxi, Huangshan

A: Dorsal; B: Ventral. Photo by Liang ZHANG.

EXTERNAL MORPHOLOGY

External morphological examination of the two specimens showed elongated and subcylindrical bodies; head distinct from neck, distinctly flattened; snout projected beyond lower jaw; vertebral ridge poorly developed. When different from HS12088, the features of HB-lcfsp12613 follow in parentheses. HS12088 juvenile (adult female) with snout-vent length: 126 mm (316 mm), tail length: 36 mm (104 mm), tail length/total length: 0.222 (0.248); dorsal scale rows 17-17-15; dorsal scales small and feebly keeled in median several rows close with the ridge (invisible on neck); ventrals 190 (228), angulated weakly; anal entire; subcaudals 75.

Rostral large, triangular, about 1.5 times as broad as deep; nasal divided, nostril in the anterior nasal; internasals subtriangular and slightly broader than long; laterally in contact with nasal; loreals rectangular, contacting orbit; pupil elliptical; preocular 1/1, upward; postoculars 2/2; temporals 2+3/2+3; supralabials 8 (2+3+3)/8 (2+3+3), first supralabial in contact

Received: 12 March 2015; Accepted: 24 April 2015

Foundation items: This project was funded by the National Natural Science Foundation of China (NSFC 31071891, 31471968)

*Corresponding author, E-mail: snakeman@hsu.edu.cn

† Authors contributed equally to this work

with rostral and nasal, second supralabial in contact with nasal and loreal, third, fourth and fifth entering eye, sixth in contact with postocular and anterior temporal, seventh in contact with lower anterior and lower posterior temporal, eighth in contact with posterior temporal; infralabial 8/8. Prefrontals not in contact with orbit but with loreal; prefrontal suture obviously longer than internasal suture; frontal subtriangular, long and wide slightly equal; parietals longer than broad, parietal suture obviously longer than frontal suture.

Body ground color black; crown largely black, except for a yellow crossband across the occipital, faint or incomplete along the midline; 25 (33) jagged-edged, brownish-yellow rings on the body, and 8 (12) on the tail. The width of all rings are 2 to 3 dorsal scales. The yellow rings extend across the belly as wide as 2 to 4 ventral plates. The above-mentioned data are listed in Table 1 and are compared with those of the type specimen (Zhang et al, 2011a) and Shaanxi specimen (Peng et al, 2014). They agreed in characteristics of scales and colored patches.

Uncorrected *P*-distance of partial cytochrome *b*

Total genomic DNA was extracted according to the phenol/chloroform extraction procedure (Sambrook et al, 1989). One mitochondrial DNA segment (cytochrome *b*, 832 bp) of the two specimens was obtained by polymerase chain reaction (PCR) and direct sequencing using the primers and methods described in Burbrink et al (2000). The two sequences shared one haplotype (GenBank accession number: KP898899). The uncorrected *P*-distance was 0.8% between this haplotype and *L. liuchengchaoi* (GenBank accession number: Kf732928; Lei et al, 2014). Genetically, they were identified as *L. liuchengchaoi.*

Laying and incubation of eggs

All measurements and observations were conducted on live snakes, and the description of the eggs was taken at 90% humidity.

Wolf snakes are oviparous. The adult female snake (HB-lcfsp12613) laid four eggs (Figure 3) in our laboratory on June 11, 2012. The eggs were white, smooth-shelled and non-adhesive. Egg weight was 0.77-0.84 g (average 0.805 g), long diameter was 24.8-25.0 mm (24.9 mm) and short diameter was 7.0-7.3 mm (7.2 mm). The ratio of long diameter to short diameter was 3.46.

Figure 3 Four eggs from female *Lycodon liuchengchaoi* (HB-lcfsp12613) (Photo by Liang ZHANG)

The four eggs were incubated in our laboratory at room temperature. The temperature ranged from 24 °C to 35 °C in June and July, 2012, at Guangzhou. The eggs were buried in the substrate at near half the volume. Water was sprayed on the substrate once a day to maintain proper humidity. Figure 4 shows the four incubated eggs on the seventh day. On July 28, three neonate snakes were hatched successfully (Figure 5). The period of incubation lasted 48 days. On August 7, all three neonates sloughed their skin (intact) for the first time. Total length of the three neonates was 134.51-147.64 mm (average 141.65 mm), tail length was 32.44-35.94 mm (34.25 mm), tail length/total length was 0.242, and head length was 6.98-8.19 mm (7.68 mm).

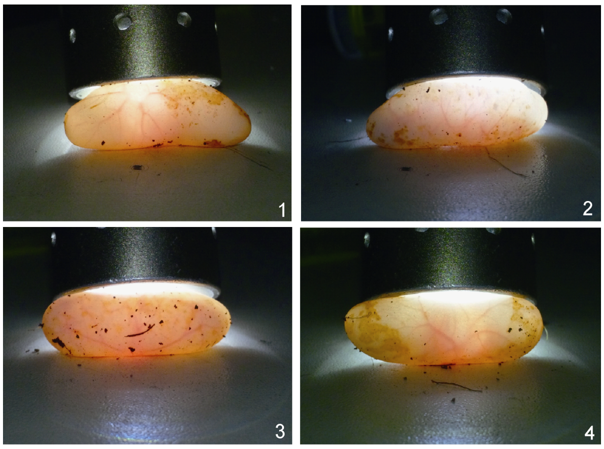

Figure 4 Four eggs on the seventh day of incubation (Photo by Liang ZHANG)

DISCUSSION

Huangshan lies in the southern part of Anhui Province. Seventy-eight percent of this region is forested and the level of snake diversity is highest. Among the 51 snake species found in Anhui, 49 species are found in Huangshan, including the newly discovered species described in this paper. (Chen et al, 1991; Chen et al, 2013; Huang, 1990; Huang et al, 2007; Peng & Huang, 2015; Zhao, 2006).

Lycodon liuchengchaoi was initially described based on three specimens from Tangjiahe and Monping (Hengduan Mountains) in Sichuan in 2011 (Zhang et al, 2011a). Peng et al (2014) found one female adult *L. liuchengchaoi* from Ningshan (Qinling Mountains) in Shaanxi. The new record sites (Huangshan Mountains, this paper) are nearly 2 000 km from the known distribution localities. There are many suitable habitats available between these sites, and this species might also occur in Henan (Funiushan Mountains) and Hubei (Dabieshan Mountains). As we only compared the cytochrome b fragments between our samples and the reported *L. liuchengchaoi*, and observed few differences, it might be desirable to collect more specimens of this species and perform phylogenetic analysis of related species within the same genus. It would also be appropriate to use other DNA markers with a high mutation rate to determine intraspecies genetic diversity, and reconstruct the potential migration route.

Figure 5 Neonate emerging from its shell (1-6) (Photo by Liang ZHANG)

In recent years, a growing number of small-sized snakes have been found in the field (Chen et al, 2013; Li et al, 2012; Peng & Huang, 2015; Sun et al, 2013; Wang et al, 2015; Zhang et al, 2011b). One possible reason might be the decline of natural small snake predators. For example, some large-sized snakes, which naturally feed on small snakes, have been overhunted in recent years, e.g., *Elaphe carinata*, *Ptyas dhumnades*, *Orthriophis taeniurus*, *Naja atra* and *Bungarus multicinctus*.

ACKNOWLEDGMENTS

We thank Dr. Hui-Jian HU (Guangdong Entomological Institute), Yong ZHANG, Yu-Sheng SU and Su-Ping ZOU (Huangshan University) for their help with counting scales.

REFERENCES

Burbrink FT, Lawson R, Slowinski JB. 2000. Mitochondrial DNA phylogeography of the polytypic North American rat snake (*Elaphe obsoleta*): a critique of the subspecies concept. *Evolution,* **54**(6): 2107-2118.

Chen BH, Sun YL, Liang RJ, Wang YQ, Li BH, Dong YW, Wang AT, Yuan XB. 1991. The amphibian and reptilian fauna of Anhui. Hefei, China: Anhui Sciences and Technology Publishing House, 235-361. (in Chinese)

Chen JM, Tang XS, Huang S. 2013. *Sinomicrurus kelloggi* firstly found in Anhui province, China. *Chinese Journal of Zoology,* **48**(1): 134-135. (in Chinese)

Huang JT. 1990. *Azemiops feae*: A new record of snake from Anhui Province, China. *Sichuan Journal of Zoology,* **9**(2): 30. (in Chinese)

Huang S, He SP, Peng ZG, Zhao K, Zhao EM. 2007. Molecular phylogeography of endangered sharp-snouted pitviper (*Deinagkistrodon acutus*; Reptilia, Viperidae) in Mainland China. *Molecular Phylogenetics and Evolution,* **44**(3): 942-952.

Lei J, Sun XY, Jiang K, Vogel G, Booth DT, Ding L. 2014. Multilocus phylogeny of *Lycodon* and the taxonomic revision of *Oligodon multizonatum*. *Asian Herpetological Research,* **5**(1): 26-37.

Li ZY, Luo J, Wei QL, Yu BC, Zhang L. 2012. Lycodon fasciatus: A snake new record to Guangdong Province, China. *Chinese Journal of Zoology,* **47**(1): 116-118. (in Chinese)

Peng LF, Huang S. 2015. *Achalinus rufescens* was found in Anhui Province, China. *Chinese Journal of Zoology,* **50**(1): 159. (in Chinese)

Peng LF, Zhu YW, Huang S. 2014. *Lycodon liuchengchaoi* was found in Shaanxi Province, China. *Chinese Journal of Zoology,* **49**(6): 952. (in Chinese)

Sambrook J, Fritsch EF, Maniatis T. 1989. Molecular Cloning: A Laboratory Manual. 2nd ed. New York: Cold Spring Harbor Laboratory Press.

Sun XY, Lei J, Ding L. 2013. *Sibynophis chinensis* firstly found in Hebei Province, China. *Chinese Journal of Zoology,* **48**(1): 139-140. (in Chinese)

Wang DQ, Yang DC, Peng LF, Cheng ZW, Xu JC, Hu XQ, Huang S. 2015. *Sinomicrurus kelloggi* was Found in Yunnan Province, China. *Sichuan Journal of Zoology*, **34**(2): 314. (in Chinese)

Zhang J, Jiang K, Vogel G, Rao DQ. 2011a. A new species of the genus *Lycodon* (Squamata, Colubridae) from Sichuan Province, China. *Zootaxa*, **2982**: 59-68.

Zhang L, Jiang K, Hu P, Yu BC, Peng BY, Tang XP, Hu HJ. 2011b. *Lycodon futsingensis*: a new snake record in Guangdong Province, China. *Chinese Journal of Zoology,* **46**(1): 128-130. (in Chinese)

Zhao EM. 2006. Snakes of China. Hefei, China: Anhui Sciences and Technology Publishing House, 215-219. (in Chinese)

Zhao EM, Huang MH, Zong Y. 1998. Fauna Sinica: Reptilia, Vol. 3. Squamata, Serpentes. Beijing: Science Press, 570 pp. (in Chinese)

ZOOLOGICAL RESEARCH

动物学研究 DONGWUXUE YANJIU

Bimonthly, Since 1980

中国精品科技期刊 中国科技核心期刊 动物学类核心期刊

Editor-in-Chief: Yong-Gang YAO

Executive Editor-in-Chief: Yun ZHANG

Editors: Su-Qing LIU Long NIE Andrew Willden

Edited by Editorial Office of Zoological Research

(Kunming Institute of Zoology, Chinese Academy of Sciences, 32 Jiaochang Donglu, Kunming, Yunnan, Post Code: 650223 Tel: +86 871 65199026 E-mail: zoores@mail.kiz.ac.cn

Sponsored by Kunming Institute of Zoology, Chinese Academy of Sciences; China Zoological Society©

Supervised by Chinese Academy of Sciences

Published by Science Press (16 Donghuangchenggen Beijie, Beijing 100717, China)

Printed by Kunming Xiaosong Plate Making & Printing Co, Ltd

Domestic distribution by Yunnan Post and all local post offices in China

International distribution by China International Book Trading Corporation (Guoji Shudian) P.O.BOX 399, Beijing 100044, China

Advertising Business License 广告经营许可证：滇工商广字66号

Domestic Postal Issue No.: 64-20

Price: 10.00 USD/60.00 CNY Post No.: BM358

ISSN 2095-8137